



1300-1-015PCTUS

IN THE UNITED STATES PATENT AND TRADEMARK OFFICE

APPLICANT: Nicola Anne Burgess EXAMINER: Anne M. Gussow, Ph.D.
SERIAL NO : 10/575,311 ART UNIT: 1643
FILED : April 11, 2006
FOR : PROTEIN INVOLVED IN OVARIAN CANCER

DECLARATION UNDER 37 C.F.R. 1.132

I, SEAN MASON, as evidenced by my signature below, declare the following:

1. I am a Molecular Biologist, having received my Ph.D. degree in 1993, after which I was a postdoctoral fellow with the ICRF (now CRUK) at the Molecular Oncology Unit, Hammersmith Hospital, London. Following this, I was a Senior Scientist at Acambis in Cambridge, UK before joining Oxford Glycosciences and becoming Group Leader in the Therapeutic Antibody Dept. I am currently employed as a Senior Group Leader in the Oncology Biology Dept of UCB, Slough, Berks, UK.

2. My curriculum vitae is attached hereto as Exhibit A.

3. My principal area of research is the characterization, validation and pre-clinical evaluation of therapeutic antibodies for human cancer.

4. I am not an inventor of subject matter claimed in the above-referenced patent application.

**Statements Regarding Adequacy of the Disclosure
to Enable Practice of the Invention**

5. I have read and am familiar with the Official Action dated August 24, 2007, received in connection with United States Serial No. 10/575,311 (hereinafter “the ‘311 Application”). I understand the nature of the rejections made by the Examiner concerning adequacy of the disclosure to enable one skilled in the art to practice the invention.

Responsive to the Examiner’s statements pertaining to the potential for an anti-CDCP1 antibody to provide therapy through recruitment of immune effector mechanisms, modulation of CDCP1 function or via a toxin conjugated antibody, I offer the following experimental evidence. In short, the experimental data demonstrate that binding and/or internalization of the antibody/polypeptide complex leads to cell death. Moreover, the results presented herein are fully supportive of the ability of unconjugated anti-CDCP1 antibody to be effective as an ovarian cancer therapy.

6. ***In vitro and in vivo antibody-mediated lysis of cell lines expressing CDCP1.*** Antibodies specific for the extracellular domain (ECD) of CDCP1 and the fluorescent molecule fluorescein isothiocyanate (FITC) were derived from a phage display library. The CDCP1-specific antibody is designated Ab 002-G07, whereas the control antibody is referred to as the anti-FITC isotype control Ab. Both the CDCP1-specific and isotype control antibodies were comprised of human variable regions fused to a human IgG1 constant region. These antibodies were used in the antibody-dependent cellular cytotoxicity (ADCC) assay described below.

ADCC assays performed using these antibodies revealed that the human ovarian tumour cell line SKOV-3, is lysed in the presence of the CDCP1-specific antibody (Ab 002-G07) in an antibody dose-dependent manner. The anti-FITC isotype control Ab has essentially no effect in this assay. Data from an example of such an assay are shown in Fig. 1 (Appendix B). The methodological details are set forth briefly as follows: monolayer SKOV-3 target cells (TC),

maintained in growth medium (McCoys5A /10%FBS /2mM glutamine), were harvested from culture flasks, washed and incubated with the labeling reagent BATDA (Perkin Elmer Life and Analytical Sciences, Inc, MA, USA) for 25 minutes at 37°C in a humidified, 5% CO₂ incubator. The cells were washed five times in growth medium and distributed in 100µl aliquots, each comprising 10,000 cells, into wells of a 96 well tissue culture plate. After adhering for approximately 1 hour at 37°C, the medium was replaced by growth medium (100µl) containing the test antibody where appropriate.

Peripheral blood mononuclear cells (PBMC) from freshly-harvested human blood were isolated by density centrifugation using Ficoll-Paque and comprised the effector cells (EC). Following isolation, the EC were resuspended in growth medium at 5×10^6 cells/ml and 100µl aliquots were transferred to the labeled target cells. The plates were incubated at 37°C in a humidified, 5% CO₂ incubator for 2 hours before being centrifuged for 5 minutes at 250 x g. 20µl supernatant was transferred to a 96 well assay plate to which 200µl of DELFIA® Europium solution (Perkin Elmer Life and Analytical Sciences, Inc, MA, USA) was added. The plate was incubated for 15 minutes at room temperature before being read in a time-resolved fluorimeter. Fluorescence signal is proportional to the quantity of labeling reagent released from TC and hence to cell lysis.

A number of control wells were included to enable accurate assessment of antibody-dependent lysis. Spontaneous release of labeling reagent from TC was determined by incubating 100µl TC with 100µl of assay medium without addition of EC or antibody. Maximum lysis was determined by incubating 100µl TC with 100µl assay medium supplemented with lysis buffer (10% final concentration, Lysis buffer supplied with the DELFIA® EuTDA Cytotoxicity Assay Kit, Perkin Elmer Life and Analytical Sciences, Inc, MA, USA), without addition of EC or antibody. Control wells comprising 100µl TC and antibody and 100µl assay medium without addition of EC permitted the detection of effects of antibody treatment alone. Specific lysis was calculated using the formula:

$$((\text{Experimental release} - \text{Spontaneous release}) / (\text{Maximum release} - \text{Spontaneous release})) \times 100.$$

Further to the *in vitro* ADCC assays, the efficacy of the CDCP1-specific antibody (002-G07) was examined in an experimental metastasis model using B16 F10 murine melanoma cells in athymic nude mice where the site of the metastatic tumour is in the lung. Development of metastases in the lung resulting from the inoculation of murine B16 F10 melanoma cells into the tail vein of mice is a well-established model where treatment with the TA-99 Ab (specific for the gp75 melanoma antigen present on the surface of the B16 F10 cells) has been extensively shown to reduce drastically the number of metastases which form in the lung (Hara, I. et al, J Exp Med. 1995, 182: 1609-1614; Takechi, H. et al, Clin Canc Res. 1996, 2: 1837-42; Clynes, R. et al, PNAS 1998, 95 652-6; Clynes, R. and Ravetch, J. Nat Med. 2000 6(4): 443-6; Nimerjahn, F. and Ravetch, J. Science 2005, 310: 1510-1512; van Spriel, A. et al, Blood 2003, 101(1): 253-8; Bevaart, L. et al Canc Res. 2006, 66(3): 1261-4). A variant of the B16 F10 cell line, B16F10-Luc, engineered to stably express luciferase, has been developed by Xenogen (Caliper Life Sciences, Mountain View, CA). Administration of luciferin to B16 F10-Luc tumour-bearing mice permits the *in situ*-quantitation of tumour growth by detection of a bioluminescent signal using imaging technology (*e.g.* IVIS® imaging systems, Xenogen/Caliper Life Sciences). The existence of such a system has permitted the development of a universal model of tumour growth in mice. Therefore, the expression of a desired antigen on B16 F10 cells which can then be targeted by an antibody specific for that antigen allows the assessment of the efficacy of antibodies in the treatment of a cancer expressing that antigen. For example, Lutterbuese *et al* (Cancer Immunol Immunother. 2007;56(4):459-68) have generated a B16 F10 cell line that stably expresses the antigen EpCAM, a pan-carcinoma antigen, and utilized this clone in the above-described metastasis model format. In this system, administration of an anti-EpCAM antibody was shown to decrease significantly the number of metastases in the lung as compared to an isotype control antibody suggesting that antibodies targeted against EpCAM may be useful in the treatment of carcinoma. Antibodies directed toward EpCAM have been the subject of trials for prostate cancer (Oberneder et al. 2007, Eur. J. Cancer. 42:2530-2538), metastatic breast cancer (Adecatumumab, from Micromet) and colorectal cancer (Edrecolomab, from Centocor).

In light of its proven utility, the B16 F10 model system described above has been developed with respect to CDCP1 to enable monitoring of *in vivo* studies through the use of bioluminescent imaging technology. Thus, B16 F10-Luc cells were stably transfected to express human CDCP1 and a clonal cell line (clone O) was selected that expresses CDCP1 (Fig. 2a, Appendix C) and maintains expression of gp75 (Fig. 2b, Appendix C) and luciferase (Fig. 2c, Appendix C). *In vitro* ADCC assays revealed that this clone is susceptible to lysis mediated by Ab 002-G07 (Fig. 2d, Appendix C). Moreover, *in vivo* experiments demonstrated the ability of clone O cells to establish metastases expressing CDCP1 in the lung that could be detected and quantitated by bioluminescence imaging.

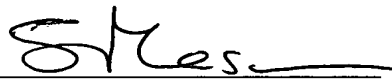
The efficacy of Ab 002-G07 was examined in an *in vivo* study utilizing the above model system. Groups of 9 nude mice were injected *via* the tail vein with 5×10^5 clone O cells on day 0 and treated with 100 μ g of either anti-CDCP1 Ab 002-G07, anti-FITC isotype control Ab, anti-gp75 TA-99 Ab or 100 μ l vehicle (PBS) on days 0, 2, 5, 7, 9, 12 and 14. The CDCP1 and isotype control Abs comprise human sequence variable regions fused to murine IgG2a constant regions, whilst TA-99 is a fully murine IgG2a Ab. *In vivo* imaging of the injected cells was carried out at several time points during the course of the study. Luciferin (Caliper Life Sciences) was injected intraperitoneally (4.5mg in PBS), the animals anaesthetised and the bioluminescent signal quantitated using an IVIS® Imaging System 200 Series imager. Animals were sacrificed on day 17, lungs harvested and the metastatic lesions counted under a dissecting microscope.

A dramatic reduction in the bioluminescent signal was observed in mice treated with the anti-CDCP1 antibody 002-G07, or TA-99, as compared to both the isotype control and PBS groups, indicating a decreased tumour burden in the lung (Fig. 3a, Appendix D). Manual quantitation of tumour metastases in the lung *post mortem* confirmed these findings. Analysis using ANOVA followed by Dunnet's post-test revealed the statistical significance of these data ($p \leq 0.05$ for 002-G07 Ab compared to isotype control or vehicle control groups) (Fig. 3b, Appendix D). Hence, the two methods for analyzing tumour burden are in good agreement.

The data presented in this Declaration, therefore, show that a CDCP1-specific antibody is able to mediate the lysis of ovarian cancer cells *in vitro* and drastically decrease tumour growth and/or establishment *in vivo* of cells that express CDCP1. In turn, this suggests that an antibody able to bind CDCP1 could target tumours that express this antigen and provide a therapy through recruitment of immune effector mechanisms, modulation of CDCP1 function, or a combination of both processes.

7. All statements made herein of my own knowledge are true and all statements made on information and belief are believed to be true; and further these statements were made with the knowledge that willful false statements and the like so made are punishable by fine or imprisonment, or both, under Section 1001 of Title 18 of the United States Code; and that such willful false statements may jeopardize the validity of the application, or any patent issuing thereon.

- 14th November 2007
DATE


Sean Mason

APPENDIX A

EXHIBIT A**CURRICULUM VITAE**
Sean Mason**PROFILE**

I am a molecular/cell biologist with 11 years experience in the biotechnology industry in the fields of oncology and allergy. The allergy research focused upon IgE and the development of a potential active vaccine to combat this disease. My current responsibilities are focused on the identification, validation and pre-clinical progression of candidate therapeutic antibodies specific for tumour-associated antigens. Validation of putative tumour antigens as viable targets also forms part of the research effort of my group. I am currently leading a collaboration with an antibody based company.

EMPLOYMENT

July 2001 – present UCB, 216 Bath Road, Slough, BERKS. SL1 4EN

Position: Senior Group Leader Oncology Biology

Responsibilities: Research group of 6: 2 Senior Scientists (PhD),
4 Scientists (Graduate)

- Joined OGS in 2001 (OGS acquired by Celltech in 2003; UCB acquired Celltech in 2004).
- Responsible for directing, organising and prioritising the research activities of the Group. This includes: identification, selection and characterisation of candidate therapeutic antibodies to a number of tumour antigens. Progression of Abs to pre-clinical proof of efficacy studies.
- Responsible for development of Group members.
- Project Leader for 2 projects – includes co-ordinating research activities across several departments.
- Lead the collaboration with BioInvent. Played a lead role in establishing the working relationship with BI. Previously (during OGS employment) involved extensively in Medarex collaboration. Represent research at quarterly Joint Steering Committee meetings.
- Identified and progressed lead candidate in first therapeutic antibody project at OGS to IND submission stage: *in vitro* assays, *in vivo* xenograft models, selection of toxicity study species, development of lot release and PK assays for lead mAb.
- Group research activities include antibody selection screens, functional cell based assays, IHC, *in vitro* assays, *in vivo* model development.

1300-1-015PCTUS

June 1996 – July 2001 Acambis plc, Peterhouse Technology Park, 100 Fulbourn Rd, Cambridge. CB1 9PT.

Position: Senior Scientist

- Main project involved development of an active vaccine to combat allergy. Initial responsibilities included reagent production (recombinant proteins) and assay development (*in vitro* and cell line based) to enable characterisation of key mAbs and polyclonal sera.
- Epitope identification and subsequent mimotope development for several mAbs. The epitopes/mimotopes were expressed in a biological display system for candidate vaccine identification and development.
- Introduced a structural biology focus to the project that led to the identification of the lead vaccine candidate.
- In addition to practical work, I was involved in directing project strategy and liaising with our collaborators with whom I worked closely in the production of two patents. Patents currently continued.
- Co-ordinated final research phase of project.
- Supervisory duties across several projects
- Final project aimed to express heterologous antigens in *Salmonella*.

Jan 1993 – June 1996 Imperial Cancer Research Fund Molecular Oncology Laboratory, Hammersmith Hospital, London. W12 ONN.
Head of laboratory: Prof W J Gullick

Position: Postdoctoral Research Fellow

- Cloning, expression and characterisation of a single-chain antibody fragment (scFv) to the epidermal growth factor receptor for the purpose of tumour imaging. Large scale production of this scFv was being developed at the Hybridoma/Service department of the ICRF in preparation for a small scale trial to image bladder tumours. Tumour targeting studies *in vivo* (mouse model) formed part of the research.
- Generation of scFv-fusion proteins for potential therapeutic purposes.
- Inhibition of dimerisation of the *neu* oncogene product by the expression of targeted peptides.

EDUCATION

Oct 1987 – Mar 1992 University of Warwick, Coventry, West Midlands
 PhD “Mapping the Cell Binding Domain of the σ 1 Protein of Reovirus”
 Supervisor: Prof M A McCrae

1984 – 1987 University of Sussex, Falmer, Brighton
 BSc (Hons) Biochemistry (2.1)

APPENDIX**Publications**

McKenzie E, Young K, Hircock M, Bennett J, Bhaman M, Felix R, Turner P, Stamps A, McMillan D, Saville G, Ng S, **Mason S**, Snell D, Schofield D, Gong H, Townsend R, Gallagher J, Page M, Parekh R, Stubberfield C. (2003) Biochemical characterisation of the active heterodimer form of Human Heparanase (Hpa1) protein expressed in insect cells. *Biochem J.* **373** (2), 423-35.

Fletcher G, **Mason S**, Terrett J, Soloviev M. (2003) Self-assembly of proteins and their nucleic acids. *J Nanobiotechnology.* Jan 28;1(1):1.

Lohmeyer, M; **Mason, S** and Gullick WJ. (1997) Characterization of chimeric proteins constructed from human epidermal growth factor (EGF) and the *Drosophila* EGF-receptor antagonist *argos*. *Int J Oncology* 10, 677-682.

Jannot, CB; Beerli, RR; **Mason, S**; Gullick, WJ and Hynes, NE. (1996) Intracellular expression of a scFv directed to the EGFR leads to growth inhibition of tumour cells. *Oncogene* **13** 275-282.

Mason, S and Gullick, WJ. (1995) The Type 1 Growth Factor Receptors: an Overview of Recent Developments. *The Breast* **4**, 11-18.

Patents

Epitopes or mimotopes derived from the c-epsilon-2 domain of IgE, antagonists thereof, and their therapeutic uses (WO 00/50460)

Epitopes or mimotopes derived from the c-epsilon-3 or c-epsilon-4 domains of IgE, antagonists thereof, and their therapeutic uses (WO 00/50461)

Human monoclonal antibodies to heparanase. Filed Nov 2002 (Patent no. WO2004043989)

APPENDIX B

APPENDIX B

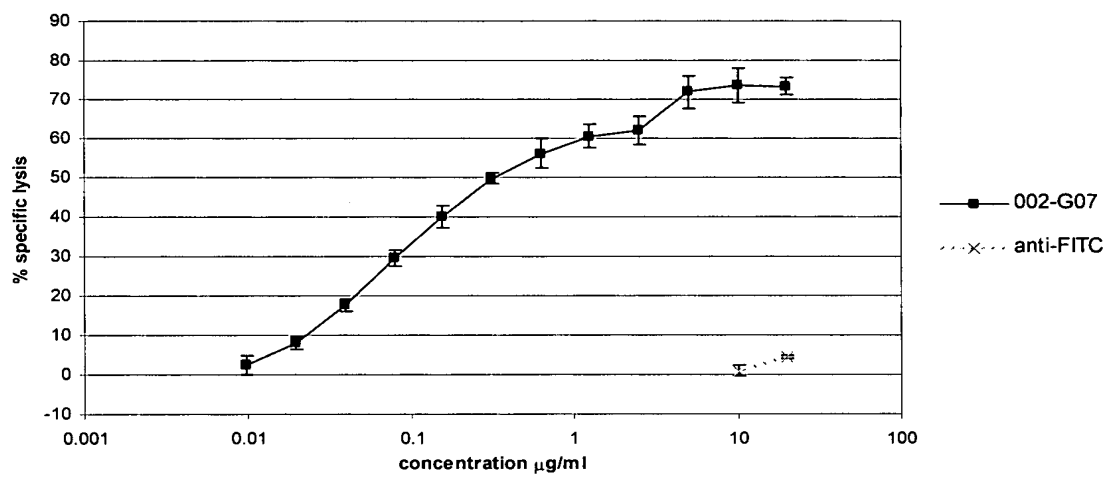


Figure 1: ADCC of SKOV-3 cells mediated by CDCP1-specific Ab 002-G07

Antibody 002-G07 shows a dose-dependent effect in an *in vitro* ADCC assay utilising SKOV-3 target cells and human PBMC as effector cells. Effector:target cell ratio was 50:1. No specific lysis was observed with the isotype control antibody at either 50 or 10 µg/ml.

APPENDIX C

APPENDIX C

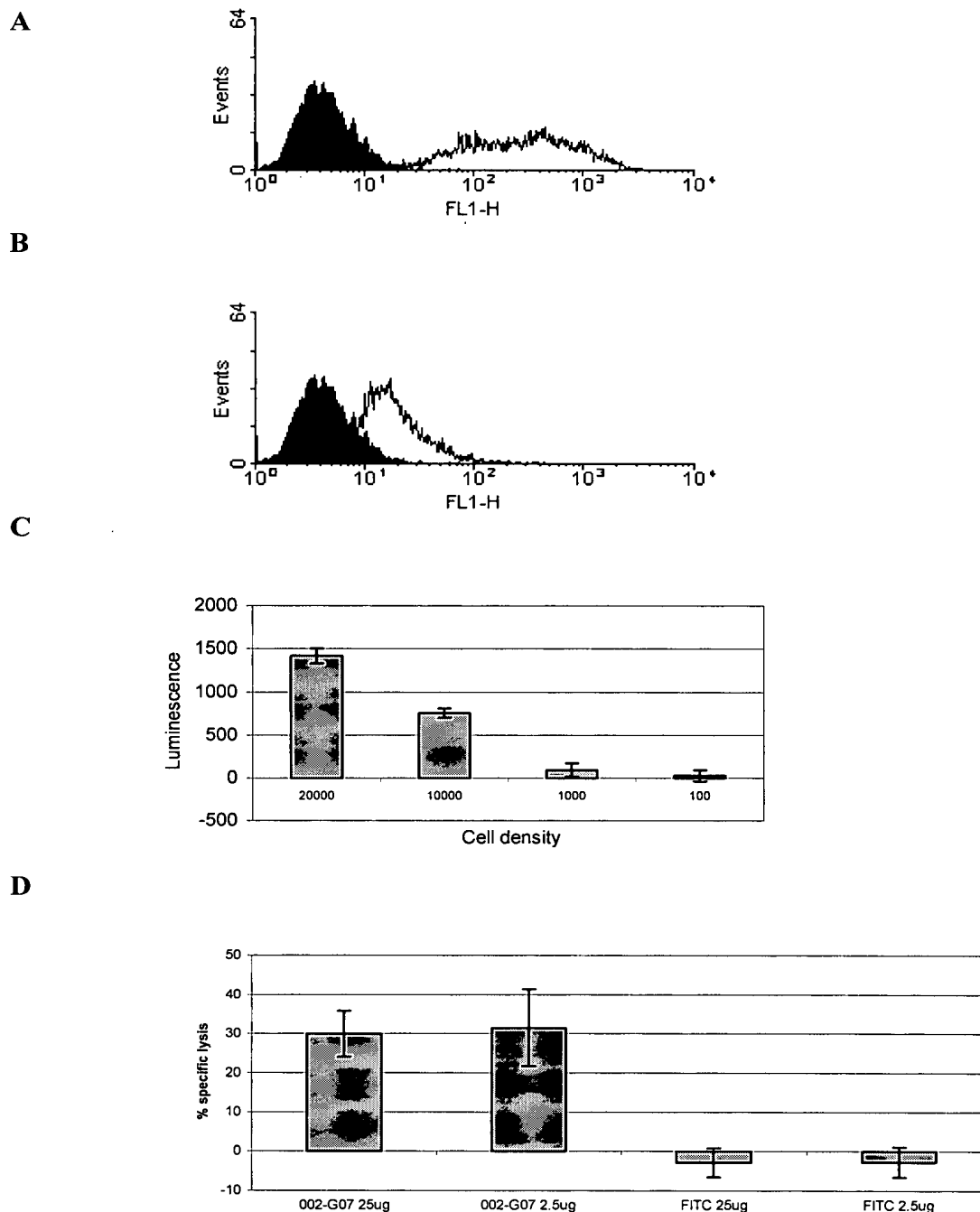


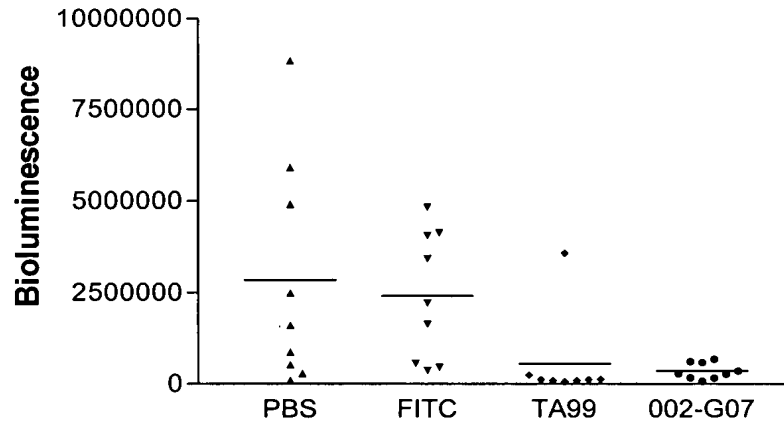
Figure 2: Characterisation of the clonal B16F10-Luc Clone O cell line.

A: To confirm expression of CDCP1, Clone O cells were labelled with 10 μ g/ml CDCP1-specific Ab 002-G07 (white) or FITC-specific isotype control (black). Antibody binding was detected using an Alexa488 fluorophore-conjugated secondary antibody and flow cytometry. **B:** To confirm expression of gp75, Clone O cells were stained in a similar manner using the gp75-specific Ab TA99 (White) or FITC-specific isotype control (black). **C:** To confirm expression of luciferase, Clone O cells were seeded at various densities in a 96 well plate format and luminescence measured using Steady-Glo Luciferase Assay System, according to the manufacturer's instructions (Promega). **D:** To confirm the susceptibility of clone O cells to ADCC, BATDA-labelled cells were exposed to Abs in the presence of human PBMC effector cells and % specific cell lysis determined as described in this declaration.

APPENDIX D

APPENDIX D

A



B

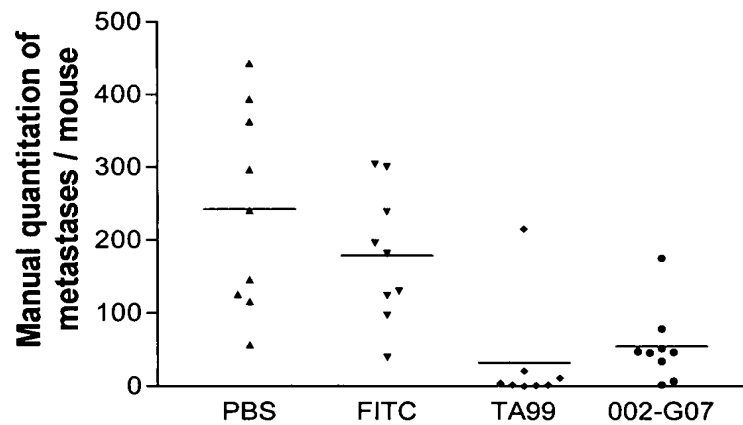


Figure 3: CDCP1-specific Ab 002-G07 inhibits growth of B16F10Luc Clone O cells in mice

Mice were injected with cells *via* the tail vein and treatment with 100ug of 002-G07, TA-99 or isotype control antibody or PBS. Treatment was continued three times per week for 15 days. **A:** Lung tumour growth was quantitated by bioluminescence detection or **B:** by manual quantitation *post mortem*. CDCP1-specific antibody 002-G07 or TA-99 significantly reduced tumour burden compared to isotype control- or PBS-treated mice ($p < 0.05$ One-way ANOVA with Dunnett's post-test).

APPENDIX E

Implicating a Role for Immune Recognition of Self in Tumor Rejection: Passive Immunization against the Brown Locus Protein

By Isao Hara, Yoshizumi Takechi, and Alan N. Houghton

From the Memorial Sloan-Kettering Cancer Center, New York 10021

Summary

The immune system can recognize differentiation antigens that are selectively expressed on malignant cells and their normal cell counterparts. However, it is uncertain whether immunity to differentiation antigens can effectively lead to tumor rejection. The mouse *brown* locus protein, gp75 or tyrosinase-related protein 1, is a melanocyte differentiation antigen expressed by melanomas and normal melanocytes. The gp75 antigen is recognized by autoantibodies and autoreactive T cells in persons with melanoma. To model autoimmunity against a melanocyte differentiation antigen, mouse antibodies against gp75 were passively transferred into tumor-bearing mice. Passive immunization with a mouse monoclonal antibody against gp75 induced protection and rejection of both subcutaneous tumors and lung metastases in syngeneic C57BL/6 mice, including established tumors. Passive immunity produced coat color alterations but only in regenerating hairs. This system provides a model for autoimmune vitiligo and shows that immune responses to melanocyte differentiation antigens can influence mouse coat color. Immune recognition of a melanocyte differentiation antigen can reject tumors, providing a basis for targeting tissue autoantigens expressed on cancer.

Experimental evidence shows that the immune system can recognize antigens expressed by cancer cells. Recently, the isolation of genes encoding cancer antigens has led to the identification of these molecules (1–3). From these studies, a paradigm emerges in which the immune repertoire recognizes a set of self-antigens, termed differentiation antigens, expressed by malignant cells but also by their normal cell counterparts (3–5).

The immune response to melanoma has been studied more extensively than that to any other human cancer. Dissection of the immune response to melanoma has shown that differentiation antigens expressed by normal melanocytes and related neuroectoderm-derived cells are dominant antigens recognized by the immune system (3, 5–16). Among the best-characterized melanoma autoantigens are proteins of the tyrosinase family. Tyrosinase (the product of the *albino* locus) is the prototype molecule, and other members include gp75 or tyrosinase-related protein 1 (the product of the *brown* locus) and gp100 (the presumed product of the *silver* locus) (17–19). These molecules, plus the MelanA/MART-1 antigen, are all melanocyte-specific molecules recognized by the immune system of melanoma patients (8, 9, 11–16). The question of whether immune recognition of self (differentiation antigens) can lead to tumor rejection arises. In particular, we considered whether immunity to melanocytes can actually lead to rejection of melanoma, and whether there are sequelae in normal tissues that contain melanocytes.

Materials and Methods

Mice and Tumors. C57BL/6 (6–8 wk-old females) were obtained from The Jackson Laboratory (Bar Harbor, ME). B16F10 is a mouse melanoma cell line of C57BL/6 origin kindly provided by Dr. Isaiah Fidler (M.D. Anderson Cancer Center, Houston, TX) (20). B78H.1 is a variant of B16 melanoma that does not express the gp75 antigen. JBRH is a melanoma from C57BL/6 provided by Dr. P. Livingston (Memorial Sloan-Kettering, NY). Other tumors derived from C57BL/6 mice include the RMA and EL-4 lymphomas, Lewis lung carcinoma, and MC58 sarcoma (from Dr. J. Nicolic-Zugic, Memorial Sloan-Kettering, NY). All animal experiments and care were in accordance with institutional guidelines.

For subcutaneous tumors, tumor cells were injected subcutaneously in the mouse flank. B16F10 melanoma cells (5×10^4 cells), B78H.1, RMA, EL-4, JBRH, and Lewis lung carcinoma (10^4 – 10^6 cells) were injected subcutaneously in 0.1 ml normal saline into the flank of syngeneic C57BL/6 mice. Tumors were checked at least four times per week by palpation and inspection. For each tumor type, palpable tumors formed in 10–21 d. For B16F10 melanoma lung metastases, C57BL/6 mice were injected intravenously through the tail vein with 1×10^5 B16F10 melanoma cells in sterile saline. For depilation experiments, C57BL/6 mice were depilated on the day before starting treatment over the posterior flank and observed for coat color. The same results were observed if the coat was plucked manually under anesthesia or depilated with hair remover (JMC, Inc., Tokyo).

Mice were treated intraperitoneally with mAb TA99 or control mouse IgG2a mAb UPC10 diluted in 0.3–0.4 ml of normal saline. TA99 mAb was purified from mouse ascites by protein A

affinity column. $F(ab')_2$ fragments of mAb TA99 were produced by digestion with pepsin and purification over protein A Sepharose (Pharmacia Biotech, Inc., Piscataway, NJ). Control IgG2a mAb UPC10 was from Sigma Chemical Co. (St. Louis, MO). Injection with control mAb UPC10 did not induce any difference in growth of B16F10 melanoma compared with untreated control mice. For subcutaneous tumor measurements, the longest surface length (a) and its perpendicular width (b) were measured, and tumor size reported as $a \times b$. For lung metastases, at 16–20 d after tumor challenge, mice were killed and surface lung metastases were scored and counted as black nodules under a dissecting microscope. Surface lung metastases were detected by day 4–7 under a dissecting microscope and by day 7–10 by eye. For histologic evaluation, tissues and tumors were fixed in formalin solution, blocked in paraffin, sectioned every 4 μ m, and stained with hematoxylin and eosin. Statistical analysis of tumor growth was performed using the Student's t test or Bonferroni two-sided t test, a conservative analysis to allow for multiple comparisons.

Antibody Treatments In Vivo. Depletion of T cells in vivo was accomplished by intraperitoneal administration of rat mAb GK1.5 (anti-CD4; IgG2b) and mAb 2.43 (anti-CD8; IgG2b), and Thy1.2⁺ cells by mAb 30-H12 (produced by hybridomas from the American Type Culture Collection, Rockville, MD). These mAbs were used as ascites fluids (titer $>1:10,000$ by staining of mouse thymocytes by flow cytometry). mAb preparations (0.2 ml) were injected intraperitoneally at day -3 and every 7 d thereafter. Throughout experiments, these treatments depleted respective T cell subpopulations and Thy-1⁺ populations $>97\%$ as determined by indirect immunofluorescence staining and cytofluorometric analysis of lymph nodes and thymocytes with mAbs GK1.5 (CD4), 2.43 (CD8), or 30-H12 (Thy1.2). Natural killer (NK) cell depletion was performed using mAb PK136 (anti-NK-1.1) (American Type Culture Collection). Antibody (0.2 ml) was injected intraperitoneally at day -3 and every 7 d thereafter. Depletion of NK cells was assessed by 4-h ^{51}Cr -release assays with 5,000 YAC cells as targets and spleen cells as effector cells at effector-to-target ratios of 100:1, 50:1, and 25:1, and depletion was shown to abrogate completely detectable NK activity. For depletion of complement, mice were injected intraperitoneally with 10 U cobra venom factor (Diamedix Corp., Miami, FL) on day -1 and every 4 d. Depletion of complement in sera of treated mice was verified using lysis of sensitized rabbit RBC (21).

Expression of gp75 Antigen on B16F10 Melanoma. Intracellular expression of gp75 was determined using mAb TA99 in indirect immunofluorescence assays against B16F10 melanoma cells fixed and permeabilized in methanol/acetone (1:1) at 4°C for 15 min. Intracellular expression was confirmed by immunoelectron microscopy using protein A-labeled colloidal gold particles as described (22). Cell-surface expression was shown by binding of mAb TA99 to intact, live B16F10 cells by enzyme-linked immunosorbent assay (titer $>1/10,000$) and by protein A-mixed hemadsorption assay (titer $>1/5,000$) (5, 22).

Results and Discussion

Syngeneic mouse tumor models were established to examine whether immunity against antigens expressed on normal melanocytes and melanoma can lead to tumor rejection. The *brown* locus product, gp75, was the target antigen in these models. The gp75 autoantigen is relevant because it is potentially immunogenic in persons with melanoma,

recognized on melanomas by both autoantibodies and autoreactive T cells (8, 9). The mouse mAb TA99 binds to both human and mouse gp75 and reacts with normal melanocytes and melanoma but does not react with other tissues (22). TA99 mAb has been shown to localize efficiently to melanoma xenografts in mice (tumor/normal tissue ratios $>100:1$ to $10^5:1$), showing that systemic administration of antibody against gp75 can specifically localize to tumor sites (23).

The gp75⁺ B16F10 melanoma is a spontaneously arising tumor that is very weakly immunogenic in syngeneic C57BL/6 mice. B16F10 cells from fresh tumors express gp75 in melanosomes within the cell and on the cell surface (see Materials and Methods). Incubation of mAb TA99 (up to 600 μ g/ml for 7 d) with B16F10 melanoma cells in vitro did not affect the cell growth, morphology, or pigmentation. Mice were challenged subcutaneously with B16F10 melanoma and treated with either mAb TA99 or isotype-matched control mAb UPC10. With this tumor challenge, B16F10 uniformly forms palpable tumors in ~ 2 wk. Tumors were rejected in mice treated with mAb TA99 but not in control mice (Fig. 1). Protection against tumor growth was observed with doses of mAb TA99 as low as 37.5 μ g, but optimal protection was seen with doses of ≥ 150 μ g mAb TA99 (Fig. 2). Tumor protection was observed beyond 50–70 d.

This antitumor effect was specific for tumors that expressed gp75 antigen. Tumor protection was seen for the gp75⁺ JBRH melanoma after subcutaneous challenge in syngeneic C57BL/6 mice (time to median appearance of tumors delayed by >31 d). However, no antitumor effects were observed in syngeneic C57BL/6 mice with a gp75⁻ variant of the parental B16 melanoma (B78H.1 melanoma), nor with other subcutaneous gp75⁻ tumors, including EL4 lymphoma, RMA lymphoma, Lewis lung carcinoma, or MC58 sarcoma.

Intravenous injection of B16F10 leads reproducibly to lung metastases (20, 24). Treatment with mAb TA99 mark-

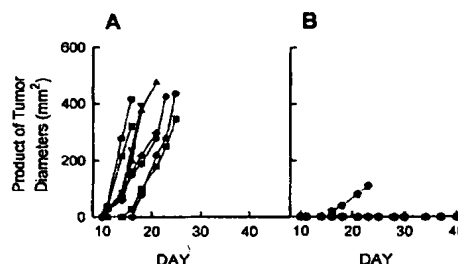


Figure 1. Protective immunity induced by mAb TA99 against B16F10 melanoma cells. Melanoma cells (5×10^4) were injected subcutaneously into the flank of C57BL/6 mice. Mice were treated intraperitoneally with (A) control mouse IgG2a mAb UPC10 or (B) mAb TA99, injected at a dose of 150 μ g (days 0, 2, 4, 7, 9, and 11). There were eight mice in each group. Treatment with mAb TA99 produced a significant increase ($P < 0.0001$, Bonferroni two-sided t test) in proportion of tumor-free mice. Each symbol in A represents an individual mouse. In group B, eight mice were treated with mAb TA99, and only one mouse developed palpable tumor (●).

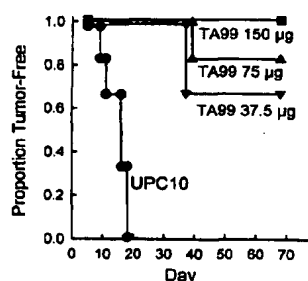


Figure 2. Protective immunity by different doses of mAb TA99 against B16F10 melanoma. Mice were treated with 150 µg of control mAb UPC10 (●) or mAb TA99 at 150 µg (■), 75 µg (▲), or 37.5 µg (▼) per dose as described in the legend of Fig. 1. There were six to eight mice in each group. Mice were scored as tumor free or tumor bearing, and the proportion of tumor-bearing mice (ratio of tumor-bearing/total number of mice per group) was calculated for each time point.

edly reduced the number of lung surface metastases even at individual doses as low as 50 µg (Fig. 3 A and data not shown). Injection of F(ab')₂ fragments of mAb TA99 did not have any effect on the number of B16F10 metastases, supporting a crucial role for the Fc portion of mAb TA99 in antitumor effects (data not shown).

We asked whether treatment with mAb TA99 would have antitumor effects in established metastases. Delaying treatment with mAb TA99 for 2–7 d after challenge with B16F10 still induced substantial protection against metastases but required higher doses of mAb TA99 ($P < 0.001$, paired Student's *t* test at 7 d) (Fig. 3 B). Effects of mAb TA99 were also observed on growth of subcutaneous B16F10 melanoma when treatment was delayed 4 d after tumor challenge (median time to appearance of tumor increased by 14 d), and slightly but reproducibly when treatment was delayed 7 d (median time to appearance of tumor increased 6 d).

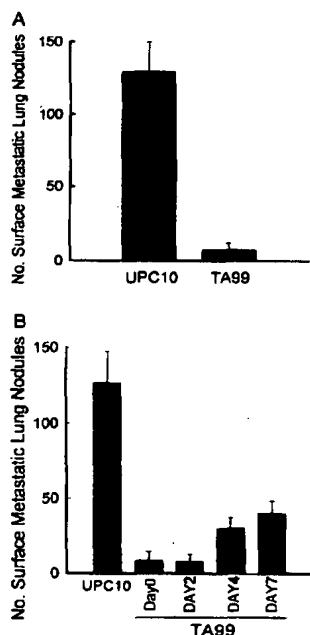


Figure 3. Antitumor effects of mAb TA99 on B16F10 lung metastases, including established metastases. Syngeneic C57BL/6 mice were injected intravenously through the tail vein with B16F10 melanoma cells. Mice were treated intraperitoneally with control mAb UPC10 or mAb TA99. 18 d after tumor challenge, mice were killed, and surface lung metastases were scored. There were eight to nine mice in each group. (A) mAb TA99 and control mAb UPC10 were administered at a 150-µg dose (days 0, 2, 4, 7, 9, and 11). (B) 600-µg doses of mAb TA99 were given three times per week for 2 wk starting on day 0 (6 h after tumor challenge), day 2, day 4, or day 7; a 600-µg dose of mAb UPC10 was given on days 0, 2, 4, 7, 9, and 11. Error bars represent 1 SD.

Histologic examination of residual B16F10 subcutaneous lesions and metastatic lung lesions in mice treated with mAb TA99 showed occasional infiltration of lymphocytes and macrophages, compared with no mononuclear or inflammatory infiltrates observed in control mice. To assess what components of the immune or inflammatory system might be involved in tumor rejection, T lymphocyte subsets, complement, or NK cell populations were depleted before challenge with tumor cells. Depletion of CD8⁺ T cells and complement did not alter tumor rejection mediated by mAb TA99 (Fig. 4 shows results for lung metastases; data not shown for subcutaneous tumors). Depletion of CD4⁺ cells partially decreased rejection of B16F10 lung metastases by mAb TA99 (Fig. 4) (depletion of CD4⁺ cells without mAb TA99 treatment did not affect the number of B16F10 metastases; data not shown) but did not affect growth of subcutaneous B16F10 tumors.

Depletion of an NK1.1⁺ cell population appeared to abrogate the protective effect of mAb TA99 in both metastatic B16F10 in the lung (Fig. 4) and subcutaneous B16F10 tumors (data not shown), supporting a role for NK cells in tumor rejection mediated by mAb TA99. NK1.1⁺ cells appear to provide natural immunity against B16F10 lung metastases (24). We further examined the role of NK1.1⁺ cells in the lung metastases model (using the same experimental design described in Fig. 5 with six to eight mice per group): (a) Depletion of NK1.1⁺ cells from C57BL/6 mice led to a significant increase in the number of metastases (mean 314 ± 58 metastases) compared with control undepleted mice (136 ± 25 metastases); (b) treatment with mAb TA99 markedly decreased metastases (12 ± 11 metastases); and (c) the number of lung metastases in mice treated with mAb TA99 and also depleted of NK1.1⁺ cells was significantly greater (mean 186 ± 42) than in mice treated with TA99 alone (12 ± 11), but not as great as the number of metastases in untreated NK1.1-depleted mice (314 ± 58). These results suggested that other components of the host in addition to NK cells, such as CD4⁺ cells (Fig. 4), partic-

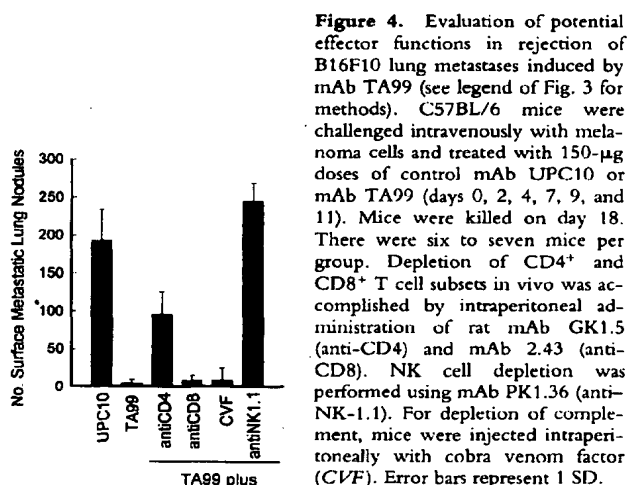


Figure 4. Evaluation of potential effector functions in rejection of B16F10 lung metastases induced by mAb TA99 (see legend of Fig. 3 for methods). C57BL/6 mice were challenged intravenously with melanoma cells and treated with 150-µg doses of control mAb UPC10 or mAb TA99 (days 0, 2, 4, 7, 9, and 11). Mice were killed on day 18. There were six to seven mice per group. Depletion of CD4⁺ and CD8⁺ T cell subsets in vivo was accomplished by intraperitoneal administration of rat mAb GK1.5 (anti-CD4) and mAb 2.43 (anti-CD8). NK cell depletion was performed using mAb PK1.36 (anti-NK1.1). For depletion of complement, mice were injected intraperitoneally with cobra venom factor (CVF). Error bars represent 1 SD.

ipated in rejection of lung metastases mediated by mAb TA99. It is possible that NK1.1⁺ cells binding mAb TA99 through Fc receptors secondarily activated CD4⁺ cells to participate in tumor rejection. Alternatively, CD4⁺ T cells might be activated by APC through internalization and presentation of antigen-antibody complexes.

Mice treated with mAb TA99 were examined for changes in pigmentation and other autoimmune-type manifestations. The coat of animals remained black unless animals were depilated to prepare skin sites for tumor injection. Pigmented melanocytes on the trunk of adult mice are found in hair bulbs. Regenerating hairs on the trunk were depigmented in 13 of 13 tumor-bearing mice treated with mAb TA99 at 300–900 μ g per dose (three times per week for 2 wk) but not in mice treated with control mAb UPC10 (0 of 36 mice) or untreated control mice (0 of 30 mice). Depigmentation was not related to injection of tumor cells; treatment of depilated C57BL/6 mice without injection of tumor cells still led to depigmentation in 12 of 12 mice treated with 300–1,000- μ g dose of mAb TA99 (Fig. 5). At TA99 doses \leq 150 μ g, depigmentation was not observed (0 of 54 mice). Thus, the threshold dose of mAb TA99 required for coat color changes was fivefold greater than the threshold required for antitumor effects in tumor protection experiments. Histologic sections of skin from mice treated with mAb TA99 showed depigmented hair follicles and regenerating hairs in previously depilated areas. The bulbs of white hairs did not contain pigment, and follicles lacked pigmented melanocytes. There were no signs of decrease in pigmentation or pigmented granules, inflammation, or changes in cellular morphologies or tissue architecture in the eyes (choroid and retina) of mice treated with mAb TA99. There were no detectable alterations in behavior or weights of mice during or after treatment. In vivo depletion with an mAb against Thy1.2 showed that Thy1⁺ cells were necessary for depigmentation, but NK1.1⁺ cells, complement, and the individual CD4⁺ or CD8⁺ T cell subsets were not necessary.

These findings suggest that autoimmunity directed against tyrosinase-related proteins and other antigens expressed by melanocytes can influence coat color in mice. This implies that coat color can be regulated at the level of a host response in addition to previously defined genetic controls at the cellular level. The induction of concomitant tumor rejection and autoimmunity recalls a relevant clinical observation in persons with metastatic melanoma who develop vitiligo. The spontaneous appearance of vitiligo has been associated with an improved prognosis in persons with metastatic melanoma (25, 26). A related observation is that the immune system of patients with vitiligo can recognize tyrosinase and other specific antigens expressed by melanocytes (27, 28). This mouse model has recapitulated an association between melanoma and vitiligo, showing that a



Figure 5. Alteration of coat color in C57BL/6 mice treated with mAb TA99. Mice were depilated on day -1 over the left posterior flank and abdomen. On day 0, mice started treatment with either mAb TA99 (left mouse) or mAb UPC10 (right mouse) three times per week for 2 wk (see schedule in Fig. 1) at individual daily doses of 300 μ g. The line demarcating the upper border of the shaved coat (dorsal trunk of the animal) can be seen in the control animal (right mouse). The coat of mice treated with mAb TA99 showed depigmentation in areas of regenerating hairs but not in the nondepilated coat, while no alteration in coat color was observed in mice treated with isotype control mAb UPC10.

biologic response to the tyrosinase family of proteins in melanocytes of the skin can mediate melanoma rejection.

In summary, an increasing body of data suggests that immune recognition of melanoma in humans is directed most frequently against molecules expressed by melanocytes or other neural crest-derived cell types (it should be pointed out that this perceived "immune repertoire" against melanoma can be biased by the use of selected in vitro assays and may not be a random sampling). These experiments suggest that the threshold for depigmentation, a potential autoimmune manifestation, can be greater than that for tumor protection, and that the biologic state of melanocytes may be important in the development of autoimmune signs. Passive transfer of mAb against gp75 was able to lead to rejection even of established B16F10 tumors in the lung (similar effects have been observed with mAb treatment against other antigens expressed by B16F10) (29). We have shown that passive immunity against melanocytes can lead to effective rejection of even established tumors. Melanoma is not the only tumor type where differentiation antigens are recognized by the immune system. Immune recognition of differentiation antigens has also been detected in patients with breast, colon, and pancreas carcinomas (30–32).

We thank Drs. H. Nyugen, S. Vijayasaradhi, P.B. Chapman, C. Naftzger, and P. Srivastava and Ms. Shakan-tula Tiwari for useful discussions and assistance with these studies.

This work was supported by grants from the National Cancer Institute (RO1 CA56821), Swim Across America, the Sutcliffe Foundation, and the Louis and Anne Abrons Foundation.

Address correspondence to Dr. Alan N. Houghton, Memorial Sloan-Kettering Cancer Center, 1275 York Avenue, New York, NY 10021.

Received for publication 24 May 1995.

References

1. Boon, T., A. Van Pel, E. De Plaen, P. Chomez, C. Lurquin, J.P. Szikora, C. Sibille, B. Mariame, B. Van den Eynde, B. Lethe, and V. Brichard. 1989. Genes coding for T-cell defined tum transplantation antigens: point mutations, antigenic peptides, and subgenic expression. *Cold Spring Harbor Symp. Quant. Biol.* 54:587-596.
2. Tsomides, T.J., and H.N. Eisen. 1994. T-cell antigens in cancer. *Proc. Natl. Acad. Sci. USA.* 91:3487-3489.
3. Houghton, A.N. 1994. Cancer antigens: immune recognition of self and altered self. *J. Exp. Med.* 180:1-4.
4. Boyse, E.A., and L.J. Old. 1969. Some aspects of normal and abnormal cell surface genetics. *Ann. Rev. Genet.* 3:269-285.
5. Houghton, A.N., M. Eisinger, A.P. Albino, J.C. Cairncross, and L.J. Old. 1982. Surface antigens of melanocytes and melanoma. Markers of melanocyte differentiation and melanoma subsets. *J. Exp. Med.* 156:1755-1766.
6. Irie, R.F., K. Irie, and D.L. Morton. 1976. A membrane antigen common to human cancer and fetal brain tissues. *Cancer Res.* 36:3510-3517.
7. Watanabe, T., C.S. Pukel, H. Takeyama, K.O. Lloyd, H. Shiku, L.T. Li, L.R. Travassos, H.F. Oettgen, and L.J. Old. 1984. Human melanoma antigen AH is an autoantigenic ganglioside related to GD2. *J. Exp. Med.* 156:1884-1889.
8. Vijayasarithi, S., B. Bouchard, and A.N. Houghton. 1990. The melanoma antigen gp75 is the human homologue of the mouse *b* (*brown*) locus gene product. *J. Exp. Med.* 171:1375-1380.
9. Wang, R.-F., P.F. Robbins, Y. Kawakami, X.-Q. Kang, and S.A. Rosenberg. 1995. Identification of a gene encoding a melanoma tumor antigen recognized by HLA-A31-restricted tumor-infiltrating lymphocytes. *J. Exp. Med.* 181:799-804.
10. Brichard, V., A. Van Pel, T. Wolfel, C. Wolfel, E. De Plaen, B. Lethe, P. Coulie, and T. Boon. 1993. The tyrosinase gene codes for an antigen recognized by autologous cytolytic T lymphocytes on HLA-A2 melanomas. *J. Exp. Med.* 178:489-495.
11. Bakker, A.B., M.W. Schreurs, A.J. de Boer, Y. Kawakami, S.A. Rosenberg, G.J. Adema, and C.J. Figdor. 1994. Melanocyte lineage-specific antigen gp100 is recognized by melanoma-derived tumor-infiltrating lymphocytes. *J. Exp. Med.* 179:1005-1009.
12. Cox, A.L., J. Skipper, Y. Chen, R.A. Henderson, T.L. Darrow, J. Shabanowitz, V.H. Engelhard, D.F. Hunt, and C.L. Slingluff. 1994. Identification of a peptide recognized by five melanoma-specific human cytotoxic T cell lines. *Science (Wash. DC)*. 264:716-719.
13. Coulie, P.G., V. Brichard, A. Van Pel, T. Wolfel, J. Schneider, C. Traversari, E. De Plaen, C. Lurquin, J.-P. Szikora, J.-C. Renauld, and T. Boon. 1994. A new gene coding for a differentiation antigen recognized by autologous cytolytic T lymphocytes on HLA-A2 melanomas. *J. Exp. Med.* 180:35-42.
14. Kawakami, Y., S. Eliyahu, C.H. Delgado, P.F. Robbins, K. Sakaguchi, E. Appella, J.R. Yannelli, G.J. Adema, T. Miki, and S.A. Rosenberg. 1994. Identification of a human melanoma antigen recognized by tumor-infiltrating lymphocytes associated with in vivo tumor rejection. *Proc. Natl. Acad. Sci. USA.* 91:6458-6462.
15. Kawakami, Y., S. Eliyahu, C.H. Delgado, P.F. Robbins, L. Rivoltini, S.L. Topalian, T. Miki, and S.A. Rosenberg. 1994. Cloning of the gene coding for a shared human melanoma antigen recognized by autologous T cells infiltrating into tumor. *Proc. Natl. Acad. Sci. USA.* 91:3515-3519.
16. Topalian, S.L., L. Rivoltini, M. Mancini, N.R. Markus, P.F. Robbins, Y. Kawakami, and S.A. Rosenberg. 1994. Melanoma-specific CD4⁺ T lymphocytes recognize human melanoma antigens processed and presented by Epstein-Barr virus-transformed B cells. *Int. J. Cancer.* 58:69-79.
17. Hearing, V.J., K. Tsukamoto, K. Urabe, K. Kameyama, P.M. Montague, and I.J. Jackson. 1992. Functional properties of cloned melanogenic proteins. *Pigm. Cell Res.* 5:264-270.
18. Jackson, I.J. 1988. A cDNA encoding tyrosinase-related protein maps to the brown locus in mouse. *Proc. Natl. Acad. Sci. USA.* 85:4392-4396.
19. Kwon, B.S., C. Chintamaneni, C.A. Kozak, N.G. Copeland, D.J. Gilbert, N. Jenkins, D. Barton, U. Francke, Y. Kobayashi, and K.K. Kim. 1991. A melanocyte-specific gene, *Pmel* 17, maps near the silver coat color locus on mouse chromosome 10 and is in a syntenic region on human chromosome 12. *Proc. Natl. Acad. Sci. USA.* 88:9228-9232.
20. Fidler, I.J. 1973. Selection of successive tumour lines for metastasis. *Nature (Lond.)*. 242:148-149.
21. Klerx, J.P.A.M., C.J. Beukelman, H. van Dijk, and J.M.N. Willers. 1983. Microassay for colorimetric estimation of complement activity in guinea pig, human and mouse serum. *J. Immunol. Methods.* 63:215-220.
22. Thomson, T.M., F.X. Real, S. Murakami, C. Cordon-Cardo, L.J. Old, and A.N. Houghton. 1988. Differentiation antigens of melanocytes and melanoma: analysis of melanosome and cell surface markers of human pigmented cells with monoclonal antibodies. *J. Invest. Dermatol.* 90:459-466.
23. Welt, S., M.J. Mattes, R. Grando, T.M. Thomson, R.W. Leonard, P.B. Zanzonico, R.E. Bigler, S. Yeh, H.F. Oettgen, and L.J. Old. 1987. Monoclonal antibody to an intracellular antigen images human melanoma transplants in nu/nu mice. *Proc. Natl. Acad. Sci. USA.* 84:4200-4204.
24. Zoller, M. 1988. IFN-treatment of B16-F1 versus B16-F10: relative impact on non-adaptive and T-cell-mediated immune defense in metastatic spread. *Clin. & Exp. Metastasis.* 6: 411-429.
25. Nordlund, J.J., J.M. Kirkwood, B.M. Forget, G. Milton, D.M. Albert, and A.B. Lerner. 1983. Vitiligo in patients with metastatic melanoma: a good prognostic sign. *J. Am. Acad. Derm.* 9:689-696.

26. Duhra, P., and A. Ilchyshyn. 1991. Prolonged survival in metastatic malignant melanoma associated with vitiligo. *Clin. Exp. Dermatol.* 16:303-305.
27. Song, Y.-H., E. Connor, Y. Li, B. Zorovich, P. Balducci, and N. Maclaren. 1994. The role of tyrosinase in autoimmune vitiligo. *Lancet.* 344:1049-1052.
28. Naughton, G.K., M. Eisinger, and J.C. Bystryn. 1983. Autoantibodies to normal human melanocytes in vitiligo. *J. Exp. Med.* 158:246-251.
29. Hearing, V.J., S.P. Leong, W.D. Vieira, and L.W. Law. 1991. Suppression of established pulmonary metastases by murine melanoma-specific monoclonal antibodies. *Int. J. Cancer.* 47:148-153.
30. Lloyd, K.O. 1991. Humoral immune responses to tumor-associated carbohydrate antigens. *Semin. Cancer Biol.* 2:421-438.
31. Disis, M.L., E. Calenoff, G. McLaughlin, A.E. Murphy, W. Chen, B. Groner, M. Jeschke, N. Lydon, E. McGlynn, R.B. Livingston, et al. 1994. Existent T-cell and antibody immunity to HER2/neu protein in patients with breast cancer. *Cancer Res.* 54:54-57.
32. Barnd, D.L., M.S. Lan, R.S. Metzgar, and O.J. Finn. 1989. Specific, major histocompatibility complex-unrestricted recognition to tumor-associated mucins by human cytotoxic T cells. *Proc. Natl. Acad. Sci. USA.* 86:7159-7163.

A Melanosomal Membrane Protein Is a Cell Surface Target for Melanoma Therapy¹

Yoshizumi Takechi, Isao Hara, Clarissa Naftzger, Yiqing Xu, and Alan N. Houghton²

The Swim Across America Laboratory, Memorial Sloan-Kettering Cancer Center [Y. T., I. H., C. N., Y. X., A. N. H.], and Cornell University Medical College, New York, NY 10021 [C. N., Y. X., A. N. H.]

ABSTRACT

Differentiation antigens on cancer cells are recognized by the immune system. A prototype set of these autoantigens in melanoma cells are the melanosomal glycoproteins, expressed in both melanomas and normal melanocytes. These are intracellular proteins that can be recognized by both antibodies and T lymphocytes. While one can understand how T cells can respond to intracellular proteins, based on cellular requirements for antigen processing and presentation, it is more difficult to understand how antibody responses to melanosomal proteins could lead to tumor rejection. We demonstrate that gp75 is expressed on the cell surface as well as intracellularly in human and mouse melanomas. The surface expression of gp75 can be augmented by IFN- γ and during tumor growth *in vivo*. Surface expression of gp75 on mouse melanoma cells correlates with the ability of a monoclonal antibody (mAb) against gp75 to reject melanomas in syngeneic mice. Antibody-mediated rejection seems to require the Fc portion of the antibody, suggesting a role for Fc receptor-positive effector cells such as natural killer cells. However, although NK1.1⁺ cells have been implicated in antibody-induced rejection *in vivo*, cell surface expression of gp75⁺ on melanoma does not lead to susceptibility to antibody-dependent cellular cytotoxicity *in vitro*. The mAb to gp75 induced tumor rejection in mice carrying both *scid* and *bg/bg* traits, showing that neither thymus-dependent T cells nor natural killer cytotoxic activity was required *in vivo*. Long-term treatment of mice with mAb led to patchy depigmentation in the coat. In summary, an intracellular organellar protein can be expressed at the cell surface and provide an antigenic target for antibody therapy and autoimmunity.

INTRODUCTION

Until recently, little was known about the structure of antigens recognized on cancer cells by the immune system. The

identification of a handful of potentially immunogenic tumor antigens has shown that these antigens are not typically foreign. Most of the central work in human cancer immunology has been done in melanoma. Surprisingly, studies of melanoma have shown that self molecules are typically recognized (1). A majority of melanoma antigens recognized by the immune system are expressed both on malignant cells and their normal cell counterparts (*e.g.*, melanocytes), defining them as differentiation antigens (2). Furthermore, autoantibodies against differentiation antigens predict a favorable outcome in patients with metastatic melanoma (3). Thus, studies point to differentiation antigens as one set of dominant antigens recognized on human cancer cells and suggest that immunity to differentiation antigens may alter the progression of melanoma.

Melanosomes are specialized cellular organelles. Melanosomal glycoproteins expressed specifically in melanocytes are among the best-characterized melanoma antigens (4-6). Three of these antigens are melanosomal membrane glycoproteins (tyrosinase, gp75/TRP-1,³ and the gp100 protein) that are recognized by T cells, and two of these antigens are recognized by autoantibodies (tyrosinase and gp75; Refs. 1, 4, 7-10). Because T cells recognize peptides that are processed and presented from intracellular compartments, it was predicted that melanosomal proteins could be recognized by T cells (4). However, it is unclear how melanosomal proteins might be recognized by antibodies in intact cells. Antibodies against the *brown* locus protein gp75 or gp75/TRP-1 have been shown to efficiently localize to human melanoma xenografts (11). Furthermore, a mouse mAb against gp75 can be used to treat mouse melanomas (12). One explanation has been that tumor necrosis can spill intracellular contents, allowing access to antibodies. However, tumors without any necrosis (*e.g.*, <1-2 mm in diameter) are rejected by antibodies against gp75. Here, we show that gp75 is expressed on the cell surface, allowing antibody-mediated tumor rejection. Cell-surface gp75 can be up-regulated by the host inflammatory cytokines, specifically IFN- γ . Finally, we characterize the antitumor effects and manifestations of autoimmunity mediated by antibodies against gp75.

MATERIALS AND METHODS

Mice and Tumors. C57BL/6 (6-8-week-old females) were obtained from The Jackson Laboratory (Bar Harbor, ME). CB-17 mice with either *scid/scid* or *scid/scid;bg/bg* traits were purchased from Taconic Farms, Inc. (Germantown, NY). B16F10 is a mouse melanoma cell line of C57BL/6 origin kindly provided by Dr. Isaiah Fidler (M. D. Anderson Cancer

Received 3/12/96; revised 8/5/96; accepted 8/19/96.

¹Supported by grants from the National Cancer Institute (RO1 CA56821), Swim Across America, the Sutcliffe Foundation, and the Louis and Anne Abrons Foundation.

²To whom requests for reprints should be addressed, at Memorial Sloan-Kettering Cancer Center, 1275 York Avenue, New York, NY 10021. Phone: (212) 639-7595; Fax: (212) 717-3036.

³The abbreviations used are: TRP-1, tyrosinase-related protein 1; mAb, monoclonal antibody; MHA, mixed hemadsorption; ADCC, antibody-dependent cellular cytotoxicity; IL-2, interleukin 2; NK, natural killer; conA, concanavalin A.

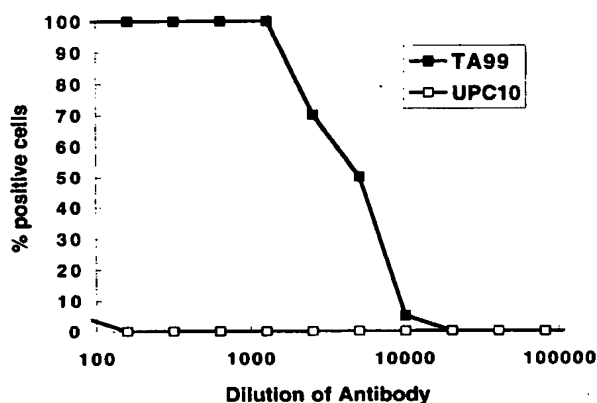


Fig. 1 The cell surface expression of gp75 was assessed in B16F10 melanoma cells by the MHA assay. Reactivity was scored according to the proportion of target melanoma cells covered by RBC rosettes. A test was read as negative when wells showed <10% rosetted target cells.

Center, Houston, TX). B78H.1 is a variant of B16 melanoma that does not express the gp75 antigen (12). B78H.1 cells were transfected with syngeneic gp75 cDNA expressed in the plasmid pcEXV-3 (13). Cell lines were tested routinely for mycoplasma contamination. Cell lines were grown in Eagle's MEM + 1% nonessential amino acids, 100 μ g/ml each of penicillin and streptomycin, and 2 mM glutamine (Life Technologies, Inc., Grand Island, NY) supplemented with 5% heat-inactivated fetal bovine serum (Sigma, St. Louis, MO). B16F10 melanoma cells were detached with 0.02% EDTA in PBS and were washed twice in PBS. Then 1×10^7 cells were injected s.c. into the flanks of mice. Two weeks later, mice that had s.c. B16F10 tumors were sacrificed. Tumor tissue was removed and minced between two frosted microscope slides (Fisher Scientific, Pittsburgh, PA) to disaggregate mechanically. A single-cell suspension from the tumor was obtained by passing tumor tissue through a cell strainer (Falcon, Lincoln Park, NJ), and cells were cultured short-term at 37°C at 5% CO₂ in a 37°C incubator. For B16F10 melanoma lung metastases, C57BL/6 mice were injected i.v. through the tail vein with 1×10^5 B16F10 melanoma cells in 0.2 ml of sterile PBS.

mAbs and Cytokine. The mouse mAb TA99 (IgG2a), which binds to the *brown* locus product gp75 or TRP-1, was purified from mouse ascites by protein A affinity column (Pharmacia LKB, Piscataway, NJ). TA99 F(ab')₂ fragments were constructed by using pepsin digestion. IgG2a mAb UPC10 (Sigma) was used as a control mAb. Mice were treated i.p. with mAb TA99, TA99 F(ab')₂, or control mouse IgG2a mAb UPC10 diluted in 0.3–0.4 ml of PBS three times/week. Recombinant mouse IFN- γ was from Genzyme Corp. (Cambridge, MA), and recombinant human IL-2 was from Chiron (Emeryville, CA). To make conA-activated supernatant, mouse spleen cells (1×10^6 cells/ml) were cultured for 48 h in RPMI 1640 (Life Technologies, Inc.), 50 μ M 2-mercaptoethanol (Sigma), and 10% fetal bovine serum in the presence of 5 μ g/ml conA (Boehringer Mannheim, Indianapolis, IN). Residual conA in the supernatant was removed by absorption with 10 mM methyl α -D-mannopyranoside (Sigma).

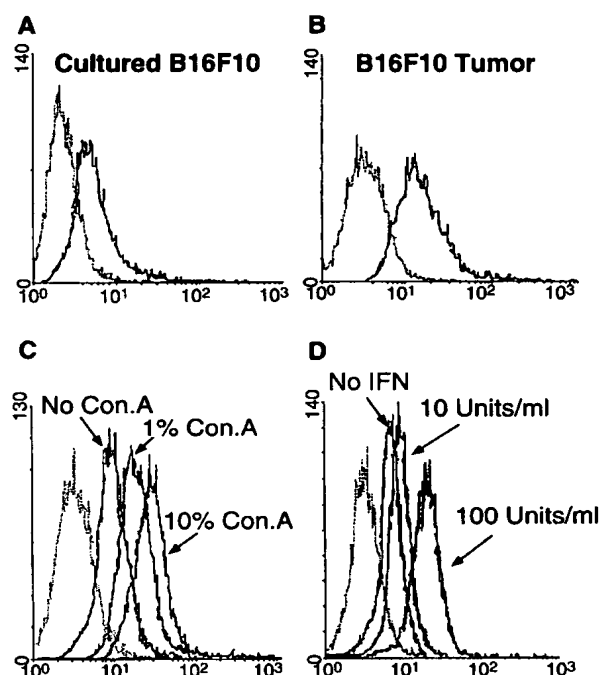


Fig. 2 A and B, cell surface expression of gp75 analyzed on B16F10 cells by flow cytometry. Cultured B16F10 cells (A) and primary explanted B16F10 lung metastases (B16F10 Tumor; B) were stained on ice with mAb TA99. Cells were evaluated by flow cytometry as described in "Material and Methods." Abscissa, fluorescence intensity; ordinate, relative cell number. The lighter line is a control representing the staining of B16F10 cells that were incubated with control mAb. C, induction of cell surface expression of gp75. B16F10 cells were cultured for 3 days with different amounts of supernatant from conA-stimulated syngeneic splenocytes (0, 1, or 10% v/v conA/medium). Cells were stained with mAb TA99 or control mAb and analyzed as described. The lighter line is a control representing the staining of B16F10 cells that were incubated with control mAb. D, induction of cell surface expression of gp75 analyzed on B16F10 cells by IFN- γ . B16F10 cells were cultured with different doses of recombinant mouse IFN- γ (0, 10, or 100 units/ml) for 3 days. Cells were stained with mAb. The lighter line is a control representing the staining of B16F10 cells that were incubated with control mAb.

Flow Cytometry Analysis. Cells were stained for 30 min on ice with saturating concentrations of mAbs and FITC-conjugated rabbit anti-mouse IgG (Accurate Chemicals, Westbury, NY). Cells were washed twice in PBS containing 1% BSA and 0.1% sodium azide after each incubation. The stained cells were analyzed on a FACScan (Becton Dickinson, Sunnyvale, CA). Routinely, 1×10^4 events were collected on a live gate.

MHA Rosetting Assay. Rabbit anti-mouse immunoglobulin MHA assay was used for the detection of cell surface antigens (14). B16F10 cells (2×10^3 cells/well) were seeded in Terasaki plates (Nunc, Naperville, IL) overnight. Wells were washed three times with PBS, and the plates were blotted with gauze. Diluted antibody was added to the wells and incubated for 1 h at room temperature. Plates were blotted, washed five times with PBS, and blotted again. Ten μ l of rabbit anti-mouse

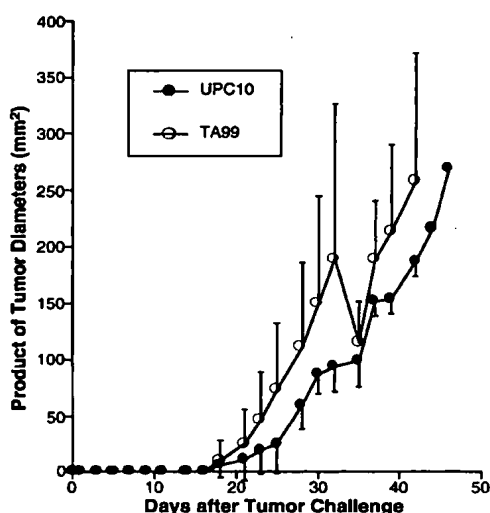


Fig. 3 TA99 treatment against B78gp75 melanoma. B78gp75 cells express intracellular gp75 but not cell surface gp75. B78gp75 cells (5×10^5) were injected s.c. into the flank of C57BL/6 mice. Mice were treated i.p. with control mouse IgG2a mAb UPC10 or mAb TA99 injected at a dose of 330 μ g (days 0, 2, 4, 7, and 9). This TA99 treatment inhibited the growth of B16F10 and JB/RH melanomas that express cell surface gp75 (12). Tumor growth was measured in millimeters using calipers. The longest surface length (a) and its perpendicular width (b) were measured, and tumor size was reported as $a \times b$. Tumors were checked at least three times/week and allowed to grow to 400 mm². Bars, SD of tumor size with 5–7 mice/group.

immunoglobulin conjugated to human type O RBCs were added to the wells. The plates were incubated for 1 h at room temperature. After blotting, the plates were washed six times with PBS, and rosetting was read under the light microscope.

ADCC Assay. Target cells were radiolabeled with 200 μ Ci (1 Ci = 37 GBq) of ⁵¹Cr for 1 h and then plated with the effector cells (50 μ l/well) in 96-well flat-bottom microplates (Falcon). The naive spleen cells, which were cultured with 500 units/ml of recombinant human IL-2 for 5 days, were used as effector cells. Purified antibodies (50 μ l/well) were added to each well. Plates were incubated at 37°C for 6 h. The supernatants were removed, and radioactivity was measured with a gamma counter.

Percent cytotoxicity

$$= \frac{(\text{sample release} - \text{spontaneous release})}{(\text{maximum release} - \text{spontaneous release})} \times 100$$

ELISA Assay for IFN- γ . NK cells were isolated from splenocytes with biotinylated anti-mouse NK1.1 mAb (PharMingen) and Dynabeads M-280 streptavidin (Dynal, Oslo, Norway) and cultured with 2000 units/ml of recombinant human IL-2 and 50 μ M 2-mercaptoethanol for 7 days. Fresh B16F10 cells (4×10^4 cells/well; 1 ml/well) were seeded as target cells in 24-well plates (Costar Corp., Cambridge, MA). Splenocytes or isolated NK cells (4×10^4 cells/well; 0.5 ml/well) were added as effector cells. Purified antibodies (50 μ g/ml; 0.5 ml/well) were added in each well. Supernatants were taken at 4, 6,

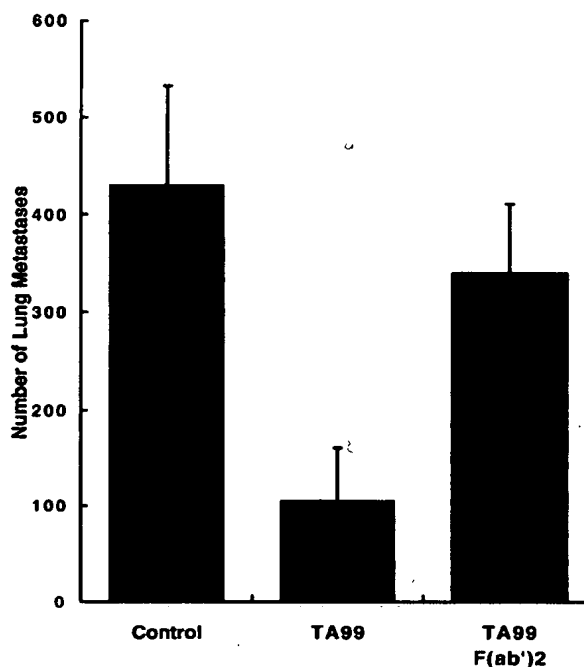


Fig. 4 Protective immunity with mAb TA99 and TA99 F(ab')₂ against B16F10 melanoma. The protective effect of TA99 F(ab')₂ on B16 mouse melanoma was analyzed. Groups included untreated controls (5 mice), mice injected with 0.15 mg of purified TA99 i.p. three times/week for 2 weeks except for day 0 (10 mice), and 10 mice injected with 0.09 mg of TA99 F(ab')₂ in the same manner. TA99 F(ab')₂ (0.09 mg) is the molar equivalent to 0.15 mg of whole IgG mAb TA99. Mice were challenged i.v. with 1×10^5 B16F10 cells. Fourteen days after tumor injection, lung tumor nodules were counted with the aid of a dissecting microscope.

14, 24, 46, 73, and 132 h and assayed for IFN- γ by means of a sandwich ELISA (PharMingen).

RESULTS AND DISCUSSION

The Melanosomal Membrane Protein gp75 is Expressed on the Cell Surface. The gp75 glycoprotein is a type I membrane molecule that is synthesized in the endoplasmic reticulum, transported through the Golgi complex, and sorted to the endosomal compartment and to melanosomes (15, 16). The gp75 glycoprotein contains an intracellular retention signal that sorts it to the endosomal compartment (16), leading to stable intracellular retention. An unexpected finding has been that mAb to gp75 can localize to melanoma tumors in xenografts and induce tumor rejection in syngeneic hosts, despite the intracellular location of gp75 (11, 12). To assess whether gp75 also reaches the plasma membrane, live unfixed B16F10 melanoma cells were analyzed for expression of gp75. Cell surface expression of gp75 was detected by MHA assays using mAb TA99 (Fig. 1). Plasma membrane expression was confirmed by flow cytometry (Fig. 2A). Similar cell surface expression was shown for the gp75⁺ murine melanoma JB/RH and the gp75⁺ human melanomas SK-MEL-19 and SK-MEL-23 (data not shown).

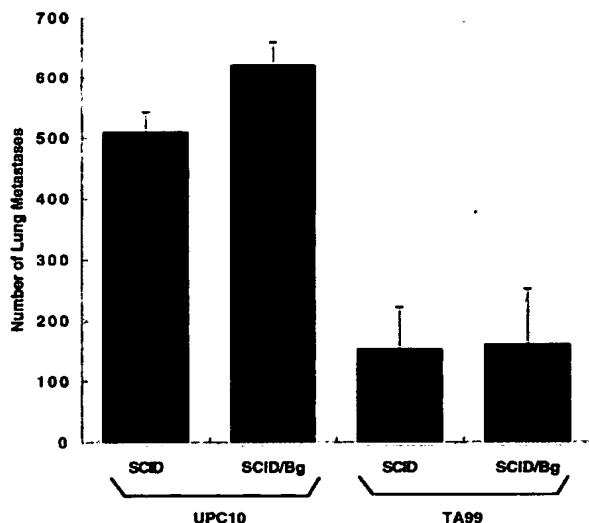


Fig. 5 Tumor rejection in mice deficient in T cells and NK cell activity. *scid/scid* (SCID) or *scid/scid;bg/bg* (SCID/Bg) CB-17 mice were challenged by injection through the tail vein with 1×10^5 B16F10 melanoma cells. Mice (5 mice/group) were treated i.p. with 300 µg of isotope-matched control mAb UPC10 or mAb TA99 three times/week for 2 weeks, starting on the day of tumor challenge. Lung tumor nodules were counted on day 14 after the tumor challenge. Bars, SD.

showing that cell surface expression is present on other pigmented mouse and human melanomas. Thus, despite the presence of an intracellular retention signal within the gp75 protein, a proportion of gp75 reaches the cell surface.

B16F10 melanoma cells freshly explanted from lung metastases expressed cell surface gp75 at a higher level than cultured B16F10 cells (Fig. 2B). When B16F10 melanoma cells explanted from lung metastases were carried in continuous tissue culture (>1 month), gp75 expression decreased, although cell surface expression was still present (Fig. 2A). These results showed that gp75 cell surface expression could be increased on B16F10 cells *in vivo* and suggested that expression of gp75 can be up-regulated by host factors.

Up-regulation of gp75 by IFN- γ . To investigate whether immune factors produced by host mononuclear cells can induce gp75, supernatants from splenocytes stimulated with conA were incubated with B16F10 melanoma cells. Addition of supernatants from 1 and 10% conA-induced syngeneic splenocytes increased the expression of gp75 measured by flow cytometry (Fig. 2C). One component in these supernatants that might be implicated in the induction of gp75 is IFN- γ . IFN- γ was present in these conA supernatants at a concentration of 800 units/ml, as measured by an ELISA assay, and therefore, was present at a final concentration of 8 units/ml in 1% conA medium. Purified recombinant mouse IFN- γ augmented the expression of gp75 at both 10 and 100 units/ml (Fig. 2D). This shows that a host factor, *i.e.*, IFN- γ , can induce increased expression of gp75 *in vitro*, implicating IFN- γ in the up-regulation of gp75 *in vivo*. This up-regulation of gp75 is remarkable because we have previously shown that a large number of other

melanocyte and melanoma antigens are unaffected by IFN- γ (17).

It is unclear why a melanosomal protein would be induced by an inflammatory cytokine. The gp75 protein plays a role in melanin synthesis, determining the type of pigment synthesized. The gp75 glycoprotein has 5,6-dihydroxyindole-2-carboxylic acid oxidase activity, which catalyzes an intermediate step in the melanin synthesis pathway (18, 19). The gp75 antigen is encoded by the *brown* locus and determines coat color in mice (*e.g.*, black, brown, and other colors). One possibility is that the proteins involved in melanin synthesis are coordinately up-regulated during inflammation. The production of epidermal pigmentation is a phenomenon that is commonly observed with cutaneous inflammatory conditions.

Passive Immunity to gp75 and its Relationship to Surface Expression of gp75. We have previously shown that treatment with mouse antibody TA99 in C57BL/6 mice bearing B16F10 and JB/RH melanomas leads to tumor rejection (12). As noted above, both B16F10 and JB/RH melanomas express cell surface gp75. B78H.1 melanoma is a gp75-negative variant of B16 melanoma that was selected for its ability to be stably transfected (20). The syngeneic gp75 cDNA expressed in the plasmid pcEXV-3 was transfected into B78H.1, and stable clones were selected that expressed gp75. A clone with relatively high expression of cellular gp75 was selected for further experiments (clone B78gp75). There was no detectable cell surface expression of gp75 in B78gp75 transfectants by the sensitive MHA assay even after induction with 100 units/ml IFN- γ , although abundant intracellular gp75 was demonstrated in vesicles inside B78gp75 cells and confirmed by immunoprecipitation with mAb TA99 (data not shown). It was estimated that B78gp75 expressed 62% of the total cellular gp75 level of B16F10 melanoma by ELISA binding to fixed permeabilized cells and by immunoprecipitation and approximately the same level of total cellular gp75 as JB/RH melanoma (data not shown). The lack of cell surface expression of gp75 by B78gp75 cells may reflect certain defects in sorting type I membrane glycoproteins to the cell surface because these cells are markedly deficient in expression of other surface glycoproteins including class I and II MHC molecules.⁴ Although treatment with TA99 antibody induced rejection of B16F10 and JB/RH (12), both of which express cell surface gp75, there was no effect on the growth of the B16 variant melanoma B78gp75 (Fig. 3).

These results show a relationship between expression of cell surface gp75 and tumor rejection, suggesting that surface expression is a requirement for tumor rejection. Results with the pair of melanomas derived from the B16 line (B16F10 with surface gp75 expression and B78gp75 without surface expression) support this model. Rejection of melanoma did not simply correspond to the total cellular level of gp75 because JB/RH melanoma was rejected by mAb TA99 treatment (12), but B78gp75 melanoma growth was not affected, although both tumors expressed approximately the same levels of gp75.

⁴ A. N. Houghton, unpublished observations.

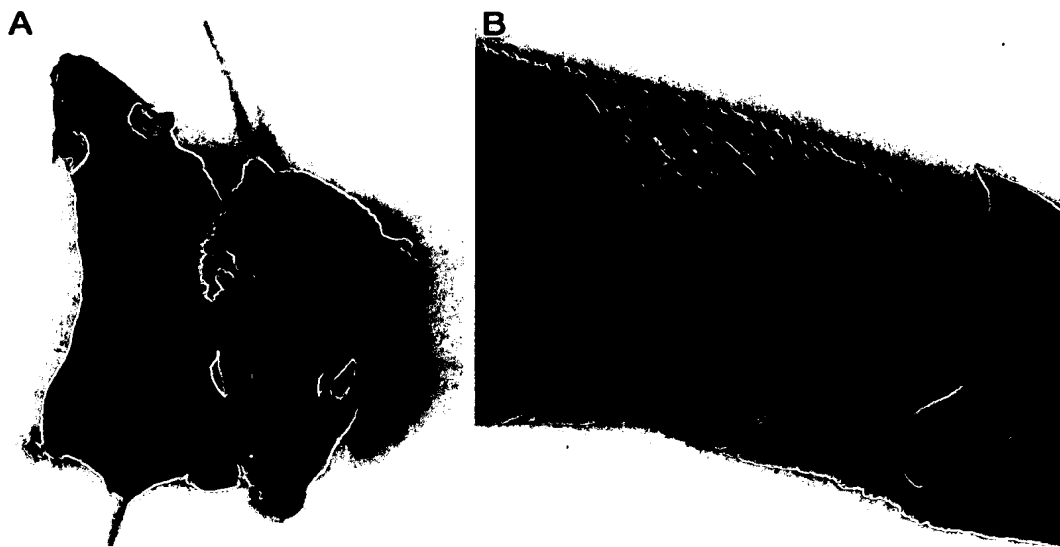


Fig. 6 Depigmentation of mice treated with mAb TA99. C57BL/6 mice were treated i.p. with 0.5 mg of mAb TA99 or control mouse IgG2a mAb UPC10 three times/week over 2 months. Continuous treatment with mAb TA99 induced patchy depigmentation in 4 of 4 mice, although the coat was not shaved or depilated. No depigmentation was observed in 6 of 6 untreated littermates. *A*, treated mouse (*right*) and untreated littermate (*left*). *B*, close-up of the coat of a treated mouse

Characterization of Antitumor Effects in Mice Treated with mAb TA99. In our previous studies, tumor rejection of B16 melanoma cells after treatment with mAb against gp75 was shown to require host NK1.1⁺ (12). The involvement of NK1.1⁺ cells suggests that NK cells are involved in tumor rejection mediated by mAb TA99. One possibility is that Fc receptors on NK cells are involved in ADCC mediated by TA99. We showed that the Fc region of TA99 is probably required for tumor rejection by comparing treatment with F(ab')₂ fragments of TA99 with whole IgG2a TA99 (Fig. 4). There were no detectable antitumor effects of F(ab')₂ fragments. A limitation of this experiment is that the biodistribution and pharmacokinetics of the TA99 fragment are likely different than those of whole IgG. However, even one-tenth of the dose of TA99 used in these experiments gives >70% reduction in melanoma, suggesting that a lower bioavailability of F(ab')₂ fragments of TA99 is not necessarily limiting.

In *in vitro* ADCC assays, no specific lysis (*i.e.*, specific lysis <5%) of B16F10 melanoma cells could be detected in ADCC assays using mouse splenocytes as effector cells (data not shown). No killing was detected with TA99, whether effector cells were fresh splenocytes, IL-2-activated splenocytes (lymphokine-activated killer cells), or adherent IL-2-activated splenocytes, nor whether B16F10 target cells were cultured or explanted from *in vivo* tumors (data not shown). Likewise, no release of IFN- γ was detected in supernatants when mouse splenocytes + mAb TA99 were incubated with B16F10 target cells (data not shown). Thus, despite the accessibility of cell surface gp75 to mAb TA99 and the potential involvement of NK cells in tumor rejection, there was no detectable ADCC or NK

IFN- γ release induced by mAb TA99 bound to target melanoma cells.

These results suggest that a noncytolytic mechanism involving NK1.1⁺ cells could mediate rejection induced by TA99. To further explore this possibility, we examined the antitumor effects of TA99 in *scid* and *scid* + *bg/bg* mice. The *beige* mutation causes intracellular vesicle dysfunction and lysosomal malformation, leading to a loss of NK cell activity (along with marked changes in neutrophil function, coagulation profiles, and other changes). TA99 decreased lung metastases by >70% in both *scid/scid* and *scid/scid;bg/bg* mice compared to isotype-matched antibody control treatment (Fig. 5). This experiment further supported a paradigm in which noncytolytic mechanisms of NK1.1⁺ cells were involved in melanoma rejection mediated by TA99.

At this point, we are unsure how NK1.1⁺ cells are involved in melanoma rejection mediated by mAb TA99. One possibility is that TA99 binding to gp75 antigen on melanoma cells and to Fc receptors on NK cells leads to NK activation but not to direct tumor lysis (ADCC). Cytokine release by activated NK cells could elicit other effector cells, *e.g.*, macrophages, to kill the tumor. We have not yet found evidence for this scenario because no IFN- γ release was detected when mAb TA99 was incubated with melanoma cells and host mononuclear cells. Another possibility is that traditional NK cells are not involved, but rather another NK1.1⁺ cell population, *e.g.*, NK1.1⁺ T cells (21).

Depigmentation in Mice Treated with mAb TA99. We have previously shown that depigmentation occurs after injection of mAb TA99 administered over 2 weeks, but loss of pigmentation in hairs was only observed in regenerating hairs

within depilated sites. When serum antibody levels against gp75 were maintained over a much longer period (2 months), patchy hair depigmentation appeared in nondepilated areas on four of four mice (Fig. 6). No other changes have been observed in these mice after 6 months of follow-up, including no changes in weight, behavior, or coat texture. These results show that hairs can be affected by TA99 treatment in areas that are not depilated if circulating levels of antibodies to gp75 are maintained over a long time. Presumably, hairs that go through a growth cycle naturally, as opposed to growth induced by depilation, can be depigmented by mAb TA99. It is interesting to note that depigmentation occurred in patches, and the pattern of depigmentation was distinct in each mouse. We have not examined melanocytes for surface expression of gp75, but these results suggest that there can be surface expression, at least in some circumstances (for instance, activated proliferating melanocytes). This provides a model for autoimmune vitiligo and further supports a relationship between immune recognition of self and tumor rejection. However, substantially less mAb TA99 was required for rejection of transplantable melanoma tumors than for depigmentation, suggesting that hair follicles remain a privileged immunological site relative to tumors.

ACKNOWLEDGMENTS

We thank Dr. S. Vijayasaradhi and Shakuntala Tiwari for useful discussions and assistance with these studies.

REFERENCES

- Houghton, A. N. Cancer antigens: immune recognition of self and altered self. *J. Exp. Med.*, **180**: 1-4, 1994.
- Houghton, A. N., Eisinger, M., Albino, A. P., Cairncross, J. G., and Old, L. J. Surface antigens of melanocytes and melanomas. *J. Exp. Med.*, **156**: 1755-1766, 1982.
- Livingston, P. O., Wong, G. Y. C., Adluri, S., Tao, Y., Pdavan, M., Parente, R., Hanlon, C., Calves, M. J., Helling, F., Ritter, G., Oettgen, H. F., and Old, L. J. Improved survival in stage III melanoma patients with GM2 antibodies: a randomized trial of adjuvant vaccination with GM2 ganglioside. *J. Clin. Oncol.*, **12**: 1036-1044, 1994.
- Vijayasaradhi, S., Bouchard, B., and Houghton, A. N. The melanoma antigen gp75 is the human homologue of the mouse *b* (*brown*) locus gene product. *J. Exp. Med.*, **171**: 1375-1380, 1990.
- Birchard, V., Pel, A. V., Wölfel, T., Wölfel, C., Plaen, E. D., Lethé, B., Coulie, P. G., and Boon, T. The tyrosinase gene codes for an antigen recognized by autologous cytolytic T lymphocytes on HLA-A2 melanomas. *J. Exp. Med.*, **178**: 489-495, 1993.
- Wang, R.-F., Robbins, P. F., Kawakami, Y., Kang, X.-Q., and Rosenberg, S. A. Identification of a gene encoding a melanoma tumor antigen recognized by HLA-A31-restricted tumor-infiltrating lymphocytes. *J. Exp. Med.*, **181**: 799-804, 1995.
- Gaugler, B., Eynde, B. V. d., Bruggen, P. v. d., Romero, P., Gaforio, J. J., Plaen, E. D., Lethé, B., Brasseur, F., and Boon, T. Human gene MAGE-3 codes for an antigen recognized on a melanoma by autologous cytolytic T lymphocytes. *J. Exp. Med.*, **179**: 921-930, 1994.
- Bakker, A. B. H., Schreurs, M. W. J., Boer, A. J. d., Kawakami, Y., Rosenberg, S. A., Adema, G. J., and Figdor, C. G. Melanocyte lineage-specific antigen gp100 is recognized by melanoma-derived tumor-infiltrating lymphocytes. *J. Exp. Med.*, **179**: 1005-1009, 1994.
- Kawakami, Y., Eliyahu, S., Delgado, C. H., Robbins, P. F., Rivoltini, L., Topalian, S. L., Miki, T., and Rosenberg, S. A. Cloning of the gene coding for a shared human melanoma antigen recognized by autologous T cells infiltrating into tumor. *Proc. Natl. Acad. Sci. USA*, **91**: 3515-3519, 1994.
- Song, Y.-H., Connor, E., Li, Y., Zorovich, B., Balducci, P., and Maclaren, N. The role of tyrosinase in autoimmune vitiligo. *Lancet*, **344**: 1049-1052, 1994.
- Welt, S., Mattes, M. J., Grando, R., Thomson, T. M., Leonard, R. W., Zanzonico, P. B., Bigler, R. E., Yeh, S., Oettgen, H. F., and Old, L. J. Monoclonal antibody to an intracellular antigen images human melanoma transplants in *nu/nu* mice. *Proc. Natl. Acad. Sci. USA*, **84**: 4200-4204, 1987.
- Hara, I., Takechi, Y., and Houghton, A. N. Implicating a role for immune recognition of self in tumor rejection: passive immunization against the *brown* locus protein. *J. Exp. Med.*, **182**: 1609-1614, 1995.
- Miller, J., and Germain, R. N. Efficient cell surface expression of class II MHC molecules in the absence of associated invariant chain. *J. Exp. Med.*, **164**: 1478-1489, 1986.
- Carey, T. E., Takahashi, T., Resnick, L. A., Oettgen, H. F., and Old, L. J. Cell surface antigens of human malignant melanoma: mixed hemadsorption assays for humoral immunity to cultured autologous melanoma cells. *Proc. Natl. Acad. Sci. USA*, **73**: 3278-3282, 1976.
- Vijayasaradhi, S., Doskoch, P. M., and Houghton, A. N. Biosynthesis and intracellular movement of the melanosomal membrane glycoprotein gp75, the human *b* (*brown*) locus product. *Exp. Cell Res.*, **196**: 233-240, 1991.
- Vijayasaradhi, S., Xu, Y., Bouchard, B., and Houghton, A. N. Intracellular sorting and targeting of melanosomal membrane protein: identification of signals for sorting of the human *brown* locus protein, gp75. *J. Cell Biol.*, **130**: 807-820, 1995.
- Houghton, A. N., Thomson, T. M., Gross, D., Oettgen, H. F., and Old, L. J. Surface antigens of melanoma and melanocytes. Specificity of induction of Ia antigens by human γ -interferon. *J. Exp. Med.*, **160**: 255-269, 1984.
- Jiménez-Cervantes, C., Solano, F., Kobayashi, T., Urabe, K., Hearing, V. J., Lozano, J. A., and García-Borrón, J. C. A new enzymatic function in the melanogenic pathway. *J. Biol. Chem.*, **269**: 17993-18001, 1994.
- Kobayashi, T., Urabe, K., Winder, A., Jiménez-Cervantes, C., Imokawa, G., Brewington, T., Solano, F., García-Borrón, J. C., and Hearing, V. J. Tyrosinase-related protein 1 (TRP1) functions as a DHICA oxidase in melanin biosynthesis. *EMBO J.*, **13**: 5818-5825, 1994.
- Lyoyd, H., Graf, J., Kaplan, P., and Silagi, S. Efficient DNA-mediated transfer of selectable genes and unselected sequences into differentiated and undifferentiated mouse melanoma clones. *Somatic Cell Mol. Genet.*, **10**: 139-151, 1984.
- Bendelac, A. Mouse NK1.1⁺ T cells. *Curr. Opin. Immunol.*, **7**: 367-374, 1995.

Fc receptors are required in passive and active immunity to melanoma

RAPHAEL CLYNES*†, YOSHIZUMI TAKECHI‡, YOICHI MOROI‡, ALAN HOUGHTON‡, AND JEFFREY V. RAVETCH*

*Laboratory of Molecular Genetics and Immunology, The Rockefeller University, 1230 York Avenue, and †Immunology Program and Department of Medicine, Memorial Sloan-Kettering Cancer Center, 1275 York Avenue, New York, NY 10021

Edited by Henry Metzger, National Institutes of Health, Chevy Chase, MD, and approved December 9, 1997 (received for review October 9, 1997)

ABSTRACT Effective tumor immunity requires recognition of tumor cells coupled with the activation of host effector responses. Fc receptor (FcR) $\gamma^{-/-}$ mice, which lack the activating Fc γ R types I and III, did not demonstrate protective tumor immunity in models of passive and active immunization against a relevant tumor differentiation antigen, the brown locus protein gp75. In wild-type mice, passive immunization with mAb against gp75 or active immunization against gp75 prevented the development of lung metastases. This protective response was completely abolished in Fc γ R-deficient mice. Immune responses were intact in $\gamma^{-/-}$ mice because IgG titers against gp75 develop normally in $\gamma^{-/-}$ mice immunized with gp75. However, uncoupling of the Fc γ R effector pathway from antibody recognition of tumor antigens resulted in a loss of protection against tumor challenge. These data demonstrate an unexpected and critical role for FcRs in mediating tumor cytotoxicity *in vivo* and suggest that enhancement of Fc γ R-mediated antibody-dependent cellular cytotoxicity by inflammatory cells is a key step in the development of effective tumor immunotherapeutics.

Effective immunity against cancer requires the specific recognition and elimination of malignant cells expressing targeted antigens. Antigens recognized on neoplastic cells include viral proteins, products of altered or mutated genes, developmentally reactivated silent gene products, and differentiation antigens expressed by tumor cells and their normal cell counterparts (1, 2). Much of the current effort of vaccine strategies is aimed at eliciting cytolytic T cell responses in which antigen recognition and cytotoxicity are functions shared by a single cell. In antibody-mediated cytotoxicity, however, antigen recognition and cytotoxicity mechanisms are functional properties of distinct cell types.

Therapeutic approaches to generate antigen-specific immune responses against tumors have included both passive immunization with mAbs and active immunization using antigens or genes expressing antigens. Passive immunity with antibodies could mediate its cytotoxic effects through complement activation or Fc receptor (FcR) engagement, and immunization with tumor antigens could elicit both cytolytic T cell responses and antibodies capable of triggering effector mechanisms. To clarify the roles of these various pathways in tumor immunity, we have examined the contributions of FcRs to the protective immune response induced against a tumor differentiation antigen by both passive and active immunization in a mouse model of tumor metastases.

Three classes of murine FcRs for IgG1, IgG2a, and IgG2b have been characterized—the high-affinity receptor Fc γ RI and the two low affinity receptors Fc γ RII and Fc γ RIII (3). Fc γ RI and III are heterooligomeric receptors, requiring co-

expression of the common γ chain for their assembly and signaling functions. Cross-linking these receptors results in cell activation. Fc γ RII, in contrast, is a single chain inhibitory receptor, aborting activation through ITAM (immune receptor tyrosine-based activation motif) containing receptors. In addition, a distinct Fc receptor for IgG3 has been described (4, 5). Mice containing genetic disruptions of the γ chain do not express either Fc γ RI or III and exhibit functionally impaired antibody-mediated responses, including loss of natural killer (NK) cell-mediated antibody-dependent cellular cytotoxicity (ADCC), macrophage phagocytosis, and mast cell degranulation in response to FcR cross-linking (6). Furthermore, γ chain deficiency ameliorates the pathogenesis of cytotoxic antibody in models of autoimmune hemolytic anemia and thrombocytopenia (7, 8) and the inflammatory cascade initiated by immune complexes in the Arthus reaction (7, 9) and autoimmune glomerulonephritis (10, 11). These studies have indicated that FcRs have a dominant role in mediating the effector responses to antibodies *in vivo*. This study was designed to address the role of FcR-mediated effector responses in tumor immunity.

The induction of immune responses to melanoma has been associated with improved clinical outcomes in melanoma patients (12). Immunotherapeutic approaches to this disease have been actively pursued. A number of differentiation antigens have been shown to be recognized by the immune system of patients with melanoma. The melanosome, a cellular organelle found in melanoma cells and normal melanocytes, expresses several glycoproteins that are potential targets for immunity (1). In particular, the product of the brown locus (protein gp75) is expressed both intracellularly and on the cell membrane by normal melanocytes and melanoma and is recognized by T cells and autoantibodies in melanoma patients (13, 14). In a model of passive immunization against gp75 using B16F10 melanoma lung metastases, the mAb TA99 against gp75 is highly effective in preventing and eradicating early-established metastases (15). In a model of active immunization against gp75, mice immunized with recombinant mouse gp75 expressed in insect cells develop a high-titer anti-gp75 antibody response and are likewise protected in the B16F10 lung metastases model (16). In the current study, we examine the mechanism of protection in these models and conclude that the FcR-mediated effector pathway is critical in both actively and passively immunized mice for tumor rejection.

METHODS

Mice and Tumors. γ chain-deficient mice were successively backcrossed to C57BL/6 mice (The Jackson Laboratories) for 12 generations. Six- to 8-week-old female γ chain-deficient congenic mice or wild-type (wt) C57BL/6 (The Jackson Lab-

The publication costs of this article were defrayed in part by page charge payment. This article must therefore be hereby marked "advertisement" in accordance with 18 U.S.C. §1734 solely to indicate this fact.

© 1998 by The National Academy of Sciences 0027-8424/98/95652-5\$2.00/0
PNAS is available online at <http://www.pnas.org>.

This paper was submitted directly (Track II) to the *Proceedings* office. Abbreviations: FcR, Fc receptor; NK, natural killer; ADCC, antibody-dependent cellular cytotoxicity; TNP, trinitrophenyl; wt, wild type. †To whom reprint requests should be addressed. e-mail: clynest@rockefeller.edu.

oratory) were used for all experiments. The B16F10 mouse melanoma cell line of C57BL/6 origin kindly provided by Isaiah Fidler (M.D. Anderson Cancer Center, Houston, TX) and were maintained in Eagle's MEM containing 1% nonessential amino acids, penicillin (100 $\mu\text{g}/\text{ml}$), streptomycin (100 $\mu\text{g}/\text{ml}$), and 2 mM glutamine and supplemented with 5% heat-inactivated fetal bovine serum (Sigma). B16F10 melanoma cells were detached with 0.02 mM EDTA in PBS and were washed twice with PBS. Mice were injected i.v. through the tail vein with 1×10^5 B16F10 melanoma cells in 0.2 ml of sterile PBS. Mice were sacrificed 14–17 days later and lung surface metastases were counted as black nodules under a dissecting microscope.

TA99 Passive Protection Model. Mice were injected intravenously with 10^5 B16 melanoma cells on day 0 and with 200 μg of purified TA99 or control mouse IgG2a mAb UPC10 (Sigma) on days 0, 2, 4, 7, 9, and 11. TA99 (IgG2a) mAb antibodies were purified from ascites fluid by protein A chromatography (Pharmacia LKB).

Sf9-gp75 Active Protection Model. A recombinant baculovirus expression vector containing the full-length murine gp75 cDNA has been described (16). Cell suspensions of Sf9 cells (Invitrogen) infected with wt or recombinant murine gp75 baculovirus were harvested by scraping and lysates prepared by three successive freeze-thaw cycles. Initial intraperitoneal immunizations were in complete Freund's adjuvant and the subsequent three intraperitoneal immunizations at 2-week intervals were in incomplete Freund's adjuvant (Sigma). Four weeks after the last immunization serum was obtained to check antibody responses and the mice were injected intravenously through the tail vein with 10^5 B16 melanoma cells.

Immunoprecipitation. Precleared serum obtained from immunized mice were mixed with [^{35}S]methionine-labeled B16F10 lysates ($3\text{--}10 \times 10^6$ cpm of trichloroacetic acid-insoluble precipitate) and pelleted with protein A-Sepharose. Disrupted complexes were subjected to denaturing PAGE and autoradiography. Purified anti-gp75 mAb TA99 was used as a positive control.

Macrophage-Mediated ADCC. Peritoneal macrophages were obtained from mice immunized with live attenuated bacillus Calmette-Guérin (Organon Teknika-Cappel) subcutaneously in complete Freund's adjuvant followed by i.p. administration 6 weeks later. Approximately 10^7 macrophages were obtained per animal 7 days after i.p. inoculation. Macrophages were cultured at an effector/target ratio of 10:1 (10^5 effector to 10^4 target cells per well) in 96-well plates. Target cells were chromium-51-labeled HSB-2 lymphoma cells derivitized with 2,4,6-trinitrophenyl (TNP) and opsonized with subagglutinating quantities of anti-TNP hybridoma supernatants. TNP-specific hybridomas included TIB191 (IgG1) obtained from the American Type Culture Collection and U7.12 (IgG2a) and U12.5 (IgG2b) both obtained from Jay Unkeless (Mt. Sinai Medical Center, New York, NY). ADCC reactions were for 6 h and specific activities were obtained as [(cpm from cultures with antibody) – (cpm from cultures with medium)] / (total cpm). Samples were assayed in triplicate with results expressed as the mean \pm SEM.

RESULTS

FcR Is Required for Passive Protection of Melanoma Metastases by mAb TA99. To determine the *in vivo* consequences of the loss of Fc γ R in tumor immunity, $\gamma^{-/-}$ C57BL/6 congenic mice were developed by 12 successive backcrosses to the FcR $\gamma^{-/-}$ mixed background (129/B1.6). To show that the genetic background of the congenic line was phenotypically similar to C57BL/6 mice, C57BL/6 $\gamma^{+/-}$ heterozygous mice were compared with wt C57BL/6 mice for baseline susceptibility to lung metastases in the B16F10 melanoma model. The number of lung metastases in congenic $\gamma^{+/-}$ mice were found to be similar to wt C57BL/6 mice (195 ± 15 vs. 187 ± 20 nodules). In addition, both strains were similarly protected from lung metastases by passive immunization with mAb TA99 against gp75 (85% vs. 78% reduction). Deletion of Fc γ R1 and -III by disruption of the common γ chain, however, results in loss of the protective effect of TA99, as shown in Fig. 1,

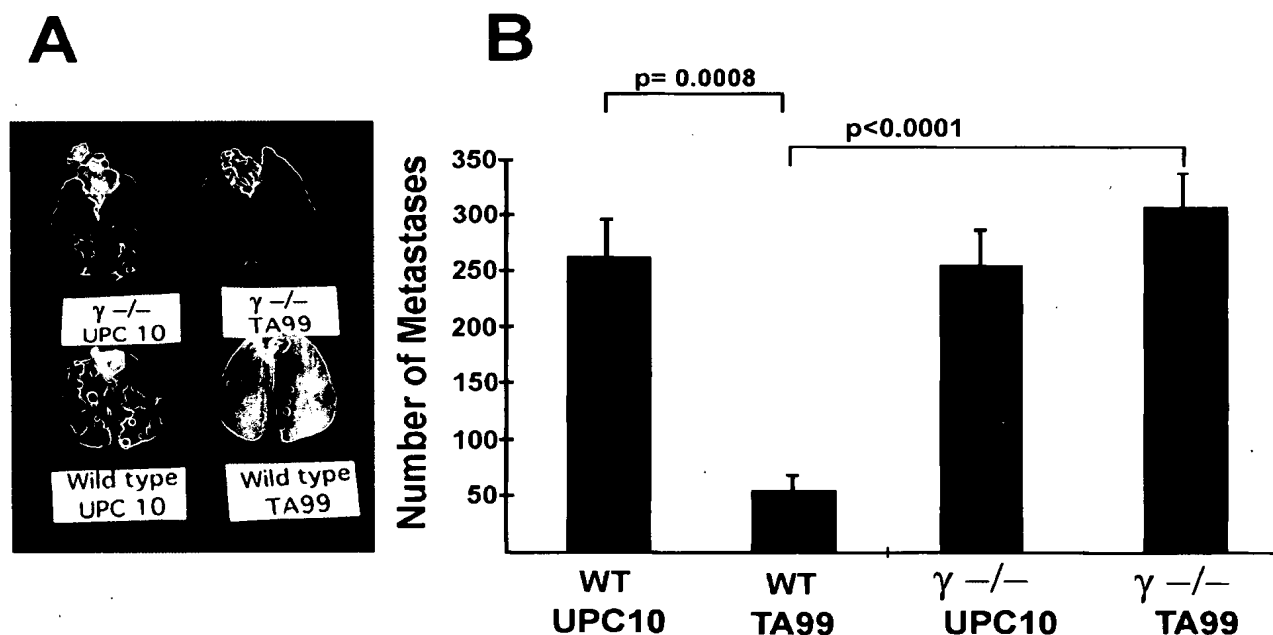


FIG. 1. Passive protection from melanoma metastases requires FcRs. (A) Representative lungs from wt and $\gamma^{-/-}$ mice injected i.v. with 10^5 B16 melanoma cells. Mice were injected with either anti-gp75 (TA99) or control isotype antibody (UPC10). Six mice were present in each group. (B) Data are the mean \pm SEM. *P* values of significant differences (Fisher exact test) are noted.

indicating that Fc γ R effector pathways are necessary for tumor rejection in mice passively immunized with mAb TA99.

FcR Is Required for Protection of Melanoma Metastases by Active Vaccination. In comparison with passive immunization, the situation in actively immunized mice is far more complex and is expected to include the polyclonal induction of both anti-gp75 T cells and antibodies, thus providing the host a number of possible cytotoxic effector systems including both cytotoxic T lymphocyte-mediated and antibody-mediated pathways. To determine the importance of the antibody-mediated Fc γ R effector pathway in actively immunized mice, $\gamma^{-/-}$ and wild-type (wt) mice were immunized with syngeneic gp75 expressed in cellular extracts of insect cells infected with mouse gp75 baculovirus constructs or with wt Sf9 cellular extracts. One consequence of Sf9-gp75 immunization is the induction of autoimmune depigmentation. This coat-color change recapitulates a possible clinical association of prolonged survival and vitiligo in melanoma patients (17–21). The typical appearance of depigmentation occurred in both wt and $\gamma^{-/-}$ Sf9-gp75-immunized mice, indicating that the effector arm of the anti-melanocyte immune response, probably T cell-mediated (15), does not require an intact Fc γ R γ chain (Fig. 2). Distinct from this autoimmune phenomenon, the anti-tumor effects of Sf9-gp75 immunization were strikingly different in the two strains of mice. Consistent with prior studies, Sf9-gp75-immunized wt mice had a significant reduction in lung metastases, with 83% fewer nodules (Fig. 3). In contrast Sf9-gp75-immunized $\gamma^{-/-}$ mice were afforded no protection against melanoma metastases. $\gamma^{-/-}$ mice have been shown to have normal immune responses to a variety of antigenic challenges (6, 22). This same situation is seen in the $\gamma^{-/-}$ congenic mice used in these studies because easily detectable anti-gp75 IgG were found in Sf9-gp75-immunized

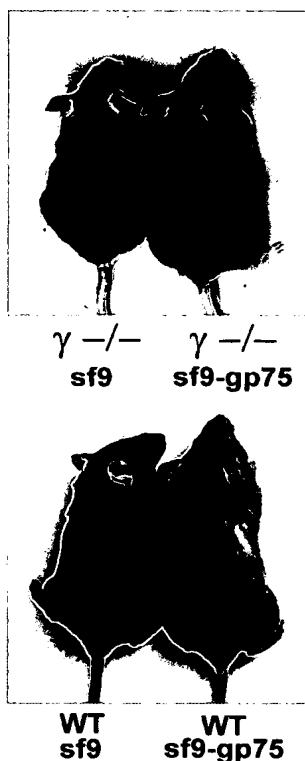


FIG. 2. Anti-gp75-induced depigmentation occurs normally in Fc γ R-deficient mice. $\gamma^{-/-}$ and wt mice were immunized with Sf9-gp75 (gray mice) or with control Sf9 extract (black mice).

wt and $\gamma^{-/-}$ mice (Fig. 4). Immunized $\gamma^{-/-}$ congenic mice exhibited normal CD4 and CD8 T cell responses when immunized with PCC (pigeon cytochrome c) peptide and OVA (ovalbumin) peptide, respectively. Class II-restricted T cell proliferative responses of CD4 + LN cells from wt and $\gamma^{-/-}$ -immunized mice were comparable when cocultured with PCC peptide (data not shown). Both wt and γ -deficient splenocytes were capable of T cell-mediated OVA-specific killing of OVA-pulsed EL-4 target cells at comparable effector/target ratios, thereby demonstrating that the cytolytic CD8⁺ T cell response is unaltered in γ -deficient mice (data not shown). Thus, these experiments demonstrate that both T cell immune recognition (anti-PCC response) and effector responses (anti-OVA-pulsed EL-4 cytotoxicity) are intact in $\gamma^{-/-}$ mice. Despite the fact that these mice are capable of developing normal B and T cell immune responses, the genetic disruption of the γ -mediated effector pathway is sufficient to abrogate the efficacy of a tumor vaccine. In the absence of Fc γ R, a requisite receptor for antibody-mediated tumor cytotoxicity, anti-melanoma responses are rendered incapable of tumor protection.

Macrophage-Mediated ADCC Is Abolished in $\gamma^{-/-}$ Mice. To determine the mechanism by which FcR-deficient mice are unable to mediate an ADCC response, FcR-expressing effector cells were studied *in vitro*. Both NK cells and myeloid cells express FcRs and are capable of antibody-mediated tumor cytotoxicity. *In vitro* data has indicated that ADCC mediated by NK cells, which express only the type III Fc γ R, is abolished in γ -chain deficient mice (6). It is unlikely that only NK cells are involved in ADCC in the B16 murine melanoma model, because studies have shown (23) that SCID/Beige mice, which lack NK cytolytic capacity, are capable of sustaining a TA99-mediated protective response. To ascertain whether macrophages, which express all three Fc γ Rs, also require the γ chain for anti-tumor ADCC, bacillus Calmette-Guérin-activated peritoneal macrophages were cocultured with TNP-derivitized HSB-2 tumor target cells in the presence of anti-TNP antibodies. Unlike the situation with TA99 and B16F10 tumor target cells (16, 23), this system efficiently produces ADCC reactions. Whereas wt macrophages killed 27% of IgG2a-opsonized HSB-2 tumor cells, there was no enhancement of $\gamma^{-/-}$ macrophage-mediated cytotoxicity with IgG1, IgG2a, or IgG2b opsonization (Fig. 5). Therefore, both NK and monocyte lineage effectors require the γ chain for affective ADCC of tumor target cells *in vitro*, suggesting that both cellular populations may be significant in tumor immunity and thus compromised in $\gamma^{-/-}$ mice.

DISCUSSION

The challenge of cancer immunotherapy is the induction of anti-tumor immune responses specific for self or altered-self tumor antigens. The resultant immune responses are, therefore, capable of triggering both clinical tumor responses and autoimmune phenomena. In this study the effector mechanisms responsible for these outcomes are explored in a melanoma model in which immunization can induce both anti-tumor responses and autoimmune vitiligo. The cytotoxic response mediated by antibodies is just one possible effector mechanism contributing to the efficacy of anti-tumor mAbs or tumor vaccines. Indeed, much of the current effort in tumor immunology is directed at the generation of effective cytolytic T cell responses. In the protection model described herein, however, the critical requirement for Fc γ R suggests that the development of cytotoxic IgG is the dominant anti-melanoma mechanism. Although it remains to be demonstrated that this is the case with other tumor vaccines, the results of this study presented herein imply that the Fc γ R-deficient mouse is a novel assay system that evaluates the role of cytotoxic IgG in immunotherapeutics.

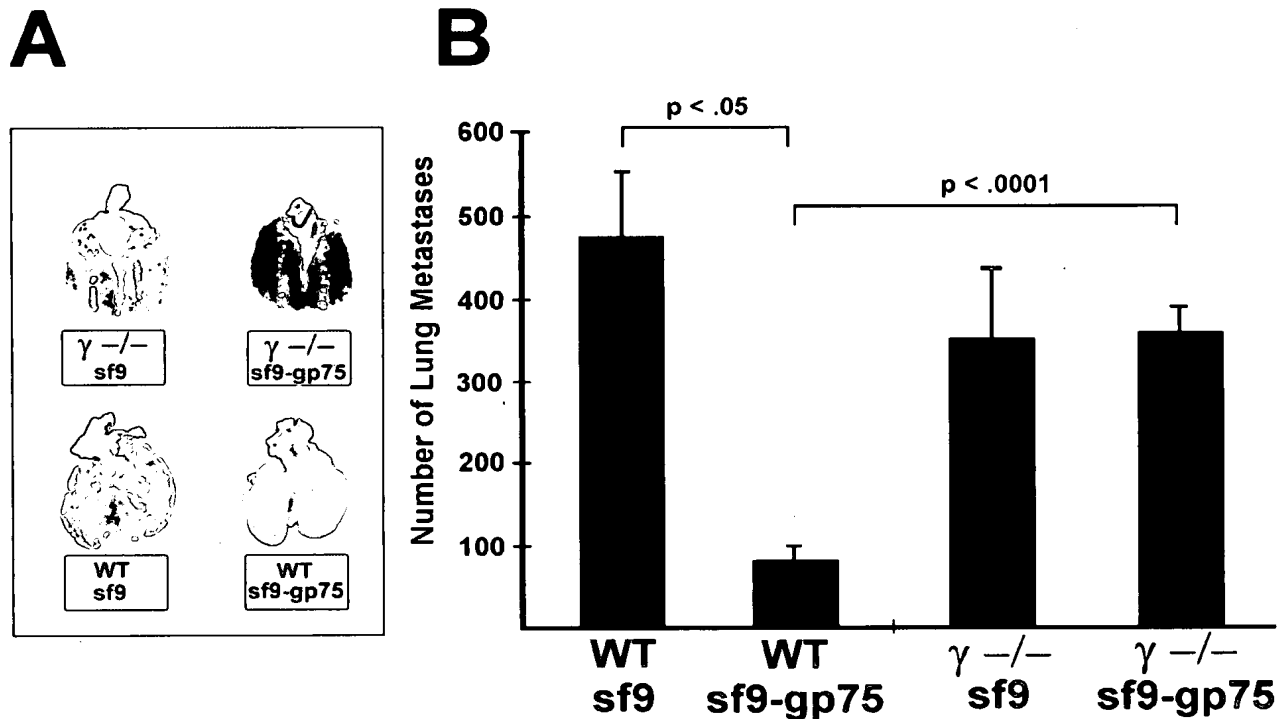


FIG. 3. Active protection from melanoma metastases requires FcRs. (A) Representative lungs from wt and $\gamma^{-/-}$ mice injected i.v. with 10^5 B16 melanoma cells. Mice were immunized with either anti-gp75 (Sf9-gp75) or control extract (Sf9). Six mice were present in each group. (B) Data are the mean \pm SEM. *P* values of significant differences (Fisher exact test) are noted.

The persistence of depigmentation induction in $\gamma^{-/-}$ mice reveals a distinction between the anti-tumor and anti-melanocyte effector pathways. Although antibody-mediated responses have been implicated in the pathogenesis of vitiligo (19, 20, 24–28), the data presented herein are more consistent with prior Thy1.2 depletion studies (15) in which depigmentation was abrogated in gp75-immunized mice and suggest instead a role for T cell responses rather than cytotoxic IgG in the anti-melanocyte autoimmune response. The dissociation of depigmentation from tumor immunity in $\gamma^{-/-}$ mice argues that the anti-melanocyte response is not sufficient to convey tumor immunity and suggests that the clinical correlation of vitiligo with tumor responses is not necessarily the result of a shared immunological response.

The identity of the FcR-bearing effector cell that mediates the anti-gp75 cytotoxicity in tumor protection is currently unknown. Prior cell depletion experiments showed that both

NK1.1-bearing cells and to a much lesser extent, $CD4^+$ cells were required for TA99 protection (15). On the other hand in the SCID/Beige mouse, which lacks mature T and B cells, as well as NK cells with cytolytic capacity, tumor protection by mAb TA99 is intact (23), suggesting instead that cytotoxic T lymphocyte- and NK-mediated cytotoxicity are not required. These findings can be reconciled with the hypotheses that macrophage-mediated ADCC is critical to anti-tumor efficacy and that $CD4^+$ and $NK1.1^+$ cells are required as immunoregulatory cells for stimulation of macrophage activity. The lack of ADCC by $\gamma^{-/-}$ macrophages is consistent with this hypothesis.

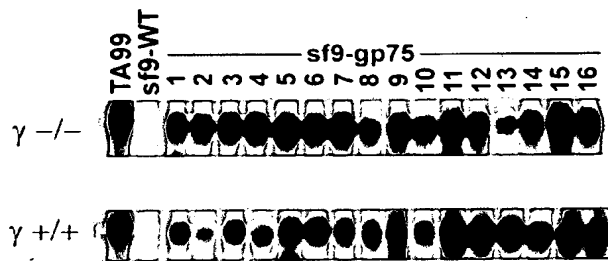


FIG. 4. Anti-gp75 titers in Sf9-gp75-immunized $\gamma^{+/+}$ and $\gamma^{-/-}$ mice are indistinguishable. Immunoprecipitations of diluted serum samples from Sf9-immunized (negative control) and Sf9-gp75-immunized mice. Diluted TA99 anti-gp75 mAb is used as a positive control.

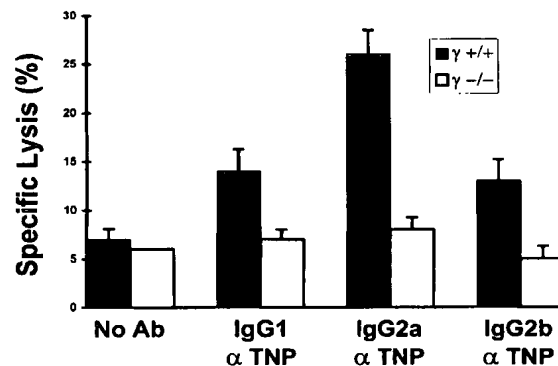


FIG. 5. Macrophage ADCC of tumor target cells requires Fc γ R γ chain. Bacillus Calmette–Guérin-elicited peritoneal $\gamma^{+/+}$ and $\gamma^{-/-}$ macrophages were cultured with chromium-labeled TNP-opsonized HSB-2 target cells at an effector/target ratio of 10:1. Data are expressed as the mean \pm SEM of triplicate samples assayed in the presence or absence of subagglutinating quantities of IgG1, IgG2a, or IgG2b anti-dinitrophenyl antibody.

Regardless of the lineage of the effector cell(s) involved, these studies substantiate a critical role *in vivo* for Fc γ R-mediated ADCC in tumor immunity. Although anti-gp75-mediated ADCC has not been demonstrated *in vitro*, data have shown that transfer of serum from Sf9-gp75-immunized mice can protect naïve mice from melanoma metastases, suggesting that serum anti-gp75 IgG is sufficient to provide protection (16, 23). The evidence presented herein indicates that the Fc γ R effector pathway is the dominant mechanism of protection of this humoral response and is necessary for the efficacy of a tumor vaccine. Uncoupling of the Fc γ R pathway from antibody recognition of tumor antigens resulted in a loss of protection against tumor challenge. These observations suggest that enhancement of the functional activity of anti-tumor antibody-Fc γ R interactions would improve the efficacy of immunotherapeutic agents.

We thank the members of the Ravetch and Houghton labs for helpful discussions, and Fred Vital and Cynthia Ritter for technical and administrative assistance. This work was supported by Swim Across America (A.H.), Louis and Anne Abrons (A.H.), and National Institutes of Health Grants K08DK02468 (R.C.), R01CA56821 (A.H.), and R01A135875 (J.V.R.).

- Houghton, A. N. (1994) *J. Exp. Med.* **180**, 1–4.
- Jaffee, E. M. & Perdoll, D. M. (1996) *Curr. Opin. Immunol.* **8**(5), 622–627.
- Ravetch, J. V. (1997) *Curr. Opin. Immunol.* **9**, 121–125.
- Diamond, B. & Yelton, D. E. (1981) *J. Exp. Med.* **153**, 514–519.
- Yuan, R., Clynes, R., Oh, J., Ravetch, J. V. & Scharff, M. D. (1998) *J. Exp. Med.*, in press.
- Takai, T., Li, M., Sylvestre, D., Clynes, R. & Ravetch, J. V. (1994) *Cell* **76**, 519–529.
- Clynes, R., Sylvestre, D., Ma, M., Warren, H., Carroll, M. C. & Ravetch, J. V. (1996) *J. Exp. Med.* **184**, 2385–2392.
- Clynes, R. & Ravetch, J. V. (1995) *Immunity* **3**, 21–26.
- Sylvestre, D. L. & Ravetch, J. V. (1994) *Science* **265**, 1095–1098.
- Clynes, R., Dumitru, C. & Ravetch, J. V. (1998) *Science*, in press.
- Suzuki, Y., Shirato, I., Tomin, Y., Okomura, K., Ravetch, J. V., Takai, T. & Ra, C. (1998) *J. Clin. Invest.*, in press.
- Livingston, P. O., Wong, G. Y., Adluri, S., Tao, Y., Padavan, M., Parente, R., Hanlon, C., Calves, M. J., Helling, F., Ritter, G., Oettgen, H. F. & Old, L. J. (1994) *J. Clin. Oncol.* **12**, 1036–1044.
- Wang, R. F., Robbins, P. F., Kawakami, Y., Kang, X. Q. & Rosenberg, S. A. (1995) *J. Exp. Med.* **181**, 799–804.
- Vijayasarithi, S., Bouchard, B. & Houghton, A. N. (1990) *J. Exp. Med.* **171**, 1375–1380.
- Hara, I., Takechi, Y. & Houghton, A. N. (1995) *J. Exp. Med.* **182**, 1609–1614.
- Naftzger, C., Takechi, Y., Kohda, H., Hara, I., Vijayasarithi, S. & Houghton, A. N. (1996) *Proc. Natl. Acad. Sci. USA* **93**, 14809–14814.
- Nordlund, J. J., Kirkwood, J. M., Forget, B. M., Milton, G., Albert, D. M. & Lerner, A. B. (1983) *J. Am. Acad. Dermatol.* **9**, 689–696.
- Duhra, P. & Ilchyshyn, A. (1991) *Clin. Exp. Dermatol.* **16**, 303–305.
- Cui, J. & Bystry, J. C. (1995) *Arch. Dermatol.* **131**, 314–318.
- Merimsky, O., Shoenfeld, Y., Baharav, E., Altomonte, M., Chaitchik, S., Maio, M., Ferrone, S. & Fishman, P. (1996) *Am. J. Clin. Oncol.* **19**, 613–618.
- Rosenberg, S. A. & White, D. E. (1996) *J. Immunother. Emphasis Tumor Immunol.* **19**, 81–84.
- Vora, K. A., Ravetch, J. V. & Manser, T. (1997) *J. Immunol.* **159**, 2116–2124.
- Takechi, Y., Hara, I., Naftzger, C., Xu, Y. Q. & Houghton, A. N. (1996) *Clin. Cancer Res.* **2**, 1837–1842.
- Fishman, P., Merimsky, O., Baharav, E. & Shoenfeld, Y. (1997) *Cancer* **79**, 1461–1464.
- Hann, S. K., Koo, S. W., Kim, J. B. & Park, Y. K. (1996) *J. Dermatol.* **23**, 100–103.
- Merimsky, O., Baharav, E., Shoenfeld, Y., Chaitchik, S., Tsigelman, R., Cohen-Aloro, D. & Fishman, P. (1996) *Cancer Immunol. Immunother.* **42**, 297–302.
- Hann, S. K. & Kim, J. B. (1995) *Yonsei Med. J.* **36**, 457–461.
- Merimsky, O., Shoenfeld, Y., Yecheskel, G., Chaitchik, S., Azizi, E. & Fishman, P. (1994) *Cancer Immunol. Immunother.* **38**, 411–416.

Inhibitory Fc receptors modulate *in vivo* cytotoxicity against tumor targets

RAPHAEL A. CLYNES¹, TERRI L. TOWERS¹, LEONARD G. PRESTA² & JEFFREY V. RAVETCH¹

¹Laboratory of Molecular Genetics and Immunology, The Rockefeller University, 1230 York Ave, New York, New York 10021, USA

²Dept. of Immunology, Genentech, 1 DNA Way, South San Francisco, California 94080, USA

Correspondence should be addressed to J.V.R.; email: ravetch@rockefeller

Inhibitory receptors have been proposed to modulate the *in vivo* cytotoxic response against tumor targets for both spontaneous and antibody-dependent pathways¹. Using a variety of syngenic and xenograft models, we demonstrate here that the inhibitory FcγRIIB molecule is a potent regulator of antibody-dependent cell-mediated cytotoxicity *in vivo*, modulating the activity of FcγRIII on effector cells. Although many mechanisms have been proposed to account for the anti-tumor activities of therapeutic antibodies, including extended half-life, blockade of signaling pathways, activation of apoptosis and effector-cell-mediated cytotoxicity, we show here that engagement of Fcγ receptors on effector cells is a dominant component of the *in vivo* activity of antibodies against tumors. Mouse monoclonal antibodies, as well as the humanized, clinically effective therapeutic agents trastuzumab (Herceptin®) and rituximab (Rituxan®), engaged both activation (FcγRIII) and inhibitory (FcγRIIB) antibody receptors on myeloid cells, thus modulating their cytotoxic potential. Mice deficient in FcγRIIB showed much more antibody-dependent cell-mediated cytotoxicity; in contrast, mice deficient in activating Fc receptors as well as antibodies engineered to disrupt Fc binding to those receptors were unable to arrest tumor growth *in vivo*. These results demonstrate that Fc-receptor-dependent mechanisms contribute substantially to the action of cytotoxic antibodies against tumors and indicate that an optimal antibody against tumors would bind preferentially to activation Fc receptors and minimally to the inhibitory partner FcγRIIB.

Passive and active protection against pulmonary metastasis in the syngenic B16 melanoma model has been demonstrated to require the presence of activation Fc receptors² on effector cells, such as natural killer (NK) cells. To determine whether the inhibitory molecule FcγRIIB (Genome DataBase designation, Fcgr2b) is a factor in determining the *in vivo* anti-tumor activity of monoclonal antibody TA99 (ref. 2), a protective immunoglobulin (Ig)G2a antibody specific for the melanoma differentiation antigen gp75, we crossed C57Bl/6 mice to an FcγRIIB-deficient strain and then back-crossed to establish a syngenic strain. Metastases of B16 melanoma cells in the FcγRIIB-deficient background were identical to those in wild-type mice (Fig. 1), demonstrating that the inhibitory receptor was not involved in tumor growth or spread. In contrast, when FcγRIIB-deficient mice received the protective IgG2a antibody, there was much more activity of this antibody than in mice wild-type for FcγRIIB (Fig. 1). Quantification of the tumor nodules in excised lungs showed that wild-type, treated mice reduced tumor load by three-fold (300 ± 30 compared with 100 ± 10) whereas antibody treatment of FcγRIIB^{-/-} mice resulted in a 100-fold reduction (300 compared

to 3). As shown before², deletion of the activation γ subunit eliminated the *in vivo* protective effect of this antibody (Fig. 1). NK cells, a principal cell type involved in antibody-dependent cell-mediated cytotoxicity (ADCC), express the activation Fcγ receptor, FcγRIII (Genome DataBase designation, Fcgr3), but do not express the inhibitory counterpart, FcγRIIB. Thus, the increase seen in FcγRIIB-deficient mice cannot be attributed to NK cell hyper-responsiveness. Instead, monocytes and macrophages, which express both FcγRIII and FcγRIIB, may therefore function as the dominant effector cell in this antibody-dependent protection *in vivo*. Thus the activity attributed to the protective IgG2a antibody in a wild-type animal represents the sum of the opposing activation and inhibitory pathways contributed by NK cells, monocytes and macrophages.

To determine the generality of this pathway of antibody-mediated cytotoxicity mediated by FcγRIIB, we investigated other well-defined tumor models for which therapeutic antibodies against tumors have been developed. Antibodies against the HER2/neu growth factor receptor prevent the growth of breast carcinoma cells *in vitro* and *in vivo*³. Similarly, antibodies against the CD20 antigen on B cells arrest the growth of non-Hodgkin's lymphoma⁴. These antibodies were developed based on their ability to interfere with tumor cell growth *in vitro* and are representative of a class that includes those with specificities for the epidermal growth factor receptor⁵, interleukin-2 receptor⁶ and others⁷. Trastuzumab (Herceptin®), a humanized IgG1 antibody specific for the cellular proto-oncogene p185HER-2/neu (refs. 8,9), and rituximab (Rituxan®), the chimeric monoclonal IgG1 antibody specific for the B-cell marker CD20 (ref. 10), were recently approved for the treatment of HER-2 positive breast cancer and B-cell lymphoma, respectively. Some *in vitro* studies have indicated that the essential mechanisms responsible for the anti-tumor activities of trastuzumab and its mouse 'parent' IgG1 antibody against HER2, 4D5, are due to receptor-ligand blockade^{11,12}; others have indicated that factors such as ADCC may be important^{9,12}. *In vitro* studies with rituximab and its mouse 'parent' antibody 2B8 have indicated a direct pro-apoptotic activity may be associated with this antibody¹³.

To determine the contribution of interactions between the Fc domain and effector cell FcγRs to the *in vivo* activities of trastuzumab and rituximab, we modified the orthotopic athymic nude mouse tumor model to generate a suitable model to address the role of FcγRIIB and FcγRIII in the anti-tumor response. Mice deficient in the common γ chain (FcRγ^{-/-}) (14), lacking the activation Fcγ receptors FcγRI and FcγRIII, and mice deficient in FcγRIIB (ref. 15) were each mated with athymic nude mice (nu/nu) to generate FcRγ^{-/-}/nu/nu and FcγRIIB^{-/-}/nu/nu mice for

ARTICLES

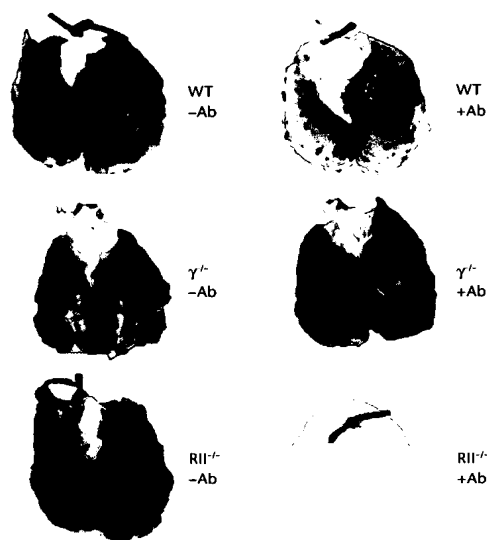


Fig. 1 Passive protection from pulmonary metastasis is increased considerably in FcRIIB-deficient mice. Mice were injected intravenously with B16 melanoma cells on day 0 and with antibody TA99 on days 0, 2, 4, 7, 9 and 11. Lungs were collected on day 14 WT, wild-type; -Ab, without antibody; +Ab, with antibody; $\gamma^{-/-}$, FcR $\gamma^{-/-}$; RII $^{-/-}$, FcRIIB $^{-/-}$.

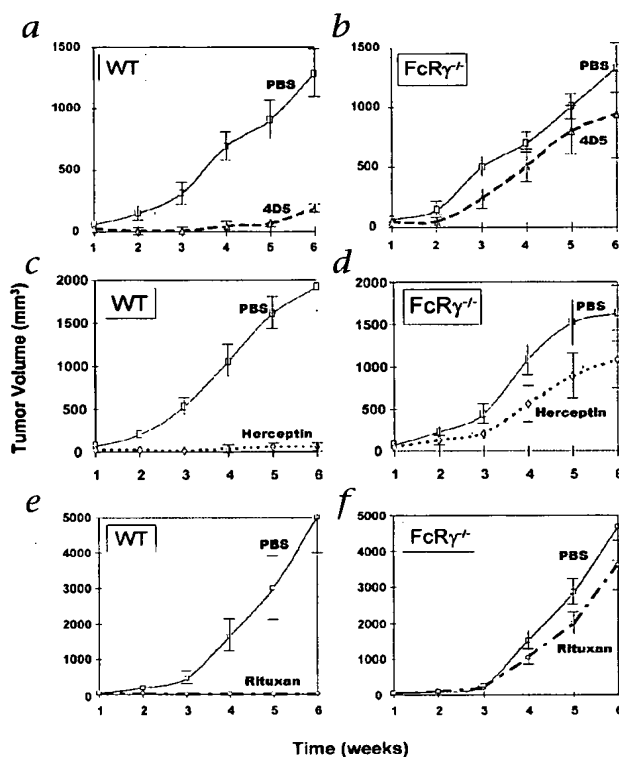
use in xenograft human tumor models. We then studied the anti-tumor activity of trastuzumab and 4D5 in preventing the growth of the human breast carcinoma BT474M1, which over-expresses p185/HER-2/neu, in FcR $\gamma^{-/-}$ and FcR $\gamma^{+/+}$ athymic nude mice (Fig. 2a–d). Tumor growth, measured as volume, was identical in homozygous FcR $\gamma^{-/-}$ /nu/nu and FcR $\gamma^{+/+}$ /nu/nu mice injected subcutaneously with 5×10^6 BT474M1 cells. In FcR $\gamma^{+/+}$ mice, a single intravenous dose of 4 μ g/g antibody, followed by weekly intravenous injections of 2 μ g/g antibody, resulted in near-complete inhibition of tumor growth (tumor mass reductions of 90 and 96% in mice treated with 4D5 and trastuzumab, respectively) with only 4 of 17 mice developing palpable tumors. However, this protective effect of trastuzumab and 4D5 was reduced in FcR $\gamma^{-/-}$ mice. Tumor mass in antibody-treated FcR $\gamma^{-/-}$ mice was reduced by 29 and 44%, respectively, by trastuzumab and 4D5, and 14 of 15 mice developed palpable tumors. We obtained similar results with the FcR $\gamma^{-/-}$ /nu/nu xenograft model for the mechanism by which rituximab inhibits B-cell lymphoma growth *in vivo*. Tumor growth of the human B-cell lymphoma cell line Raji was indistinguishable in FcR $\gamma^{-/-}$ /nu/nu and FcR $\gamma^{+/+}$ /nu/nu mice (Fig. 2e and f). However, the protective effect of weekly, intravenous, 10- μ g/g doses of rituximab seen in FcR $\gamma^{+/+}$ /nu/nu mice was reduced in FcR $\gamma^{-/-}$ /nu/nu mice. Treatment of wild-type athymic mice with rituximab resulted in reductions of tumor mass of more than 99%, and no wild-type mice devel-

Fig. 2 Anti-tumor activities of 4D5, trastuzumab and rituximab require activation Fc γ receptors. Nude mice ($n = 6$ –10 per group) were injected with BT474M1 cells (a–d) or Raji B cells (e and f), followed by weekly injections of 4D5 (a and b), trastuzumab (c and d) or rituximab (e and f). PBS, phosphate buffered saline (control). The antibody-dependent tumor protection seen in BALB/c nude mice (WT; a, c and e) is absent in FcR $\gamma^{-/-}$ nude mice (b, d and f). All experiments were repeated three times with similar results.

oped palpable tumors. In contrast, in FcR $\gamma^{-/-}$ mice, little protection was afforded by rituximab; six of seven mice developed palpable tumors, and tumor mass reductions averaged just 23%.

In contrast, FcRIIB $^{-/-}$ mice were more effective at arresting BT474 growth in this nude mouse model (Fig. 3). At a sub-therapeutic dose of antibody (a 0.4- μ g/g loading dose and 0.2 μ g/g given weekly), tumor growth in FcRIIB-deficient mice was arrested, demonstrating the involvement of the inhibitory FcRIIB pathway in this model as well. Nude mice have increased numbers of NK cells, leading to the presumption that antibody protection in those mice are not representative of the protection seen in syngenic systems, as in human disease. The observation that deletion of FcRIIB increases protection in nude mice indicates the involvement of effector cells other than NK cells, such as monocytes and macrophages, in the protective response and further indicates that the Fc-receptor-dependent pathways are not restricted to a system biased to NK cells, but, as in the syngenic melanoma system, is likely to be relevant in other syngenic systems as well.

To further demonstrate the involvement of interactions between Fc and Fc γ receptors in the protective response, we engineered a modification of 4D5 to disrupt the ability of the antibody to engage cellular Fc γ receptors while retaining its affinity for its cognate antigen p185 HER-2/neu. We systematically mutated the CH2 and CH3 domains of mouse IgG1 Fc sequence, replacing each amino acid, in turn, with alanine (alanine scanning). We then expressed each mutant antibody thus generated and determined its binding to mouse Fc receptors. Based on this alanine-scanning mutagenesis mapping, a single amino-acid replacement at residue 265 in the C μ 2 domain of the mouse IgG1 heavy chain reduced binding of IgG1-containing immune com-



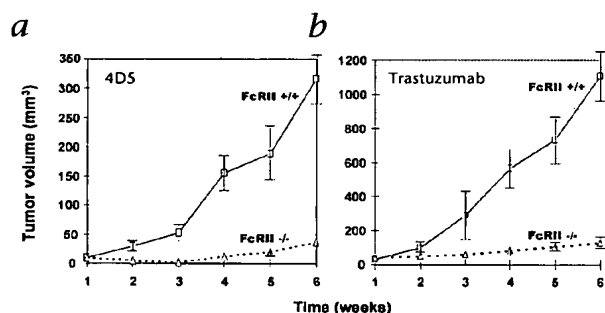


Fig. 3 Anti-breast tumor activity of 4D5 and trastuzumab is enhanced FcRIII-deficient mice. Nude mice ($n = 8$ per group) were injected with BT474M1 cells and treated with a 0.4- μ g loading dose and 0.2 μ g/g weekly (a sub-therapeutic dose for wild-type mice) of 4D5 (**a**) or trastuzumab (**b**). There is complete inhibition of tumors in FcRIII-deficient mice (dotted lines) at sub-therapeutic antibody doses.

plexes to both Fc γ RIIB and Fc γ RIII in a receptor-coated plate assay (Fig. 4a). This residue was located at a site within the Fc portion of the IgG molecule thought to interact directly with surfaces of Fc receptors. We put the mutation of Asp to Ala at residue 265 into the 4D5 IgG1 heavy chain gene and expressed this in parallel with the wild-type 4D5 IgG1 heavy chain in A293 cells along with the 4D5 kappa chain to produce 4D5 and mutant (D265A) antibodies. As the mutation would not be expected to disrupt antibody-antigen interactions, as predicted, both 4D5 and D265A antibodies purified from transfected-cell supernatants bound cellular p185HER-2/neu with equivalent avidity and had similar *in vitro* growth inhibitory activity when added to BT474M1-expressing breast carcinoma cells in tissue culture (Fig. 4b). However, although D265A retained the wild-type characteristics of *in vivo* half-life (data not shown), antigenic targeting and functional p185HER-2/neu receptor blockade, the *in vitro* ADCC capacity of the mutant was lost as a consequence of its reduced affinity for Fc γ RIII on effector cells (Fig. 4c). *In vivo*, D265A, when tested in the breast carcinoma BT474M1 xenograft model, had less anti-tumor activity than 4D5 (Fig. 4d). Palpable tumors developed in all wild-type athymic mice treated with D265A but developed in only two of five mice treated with 4D5. D265A treatment reduced tumor volumes by 30%, compared with a reduction of 85% with 4D5. The attenuated anti-tumor responses of D265A correlate with its impaired ability to activate Fc-receptor-bearing effector cells despite its ability to inhibit tumor

growth *in vitro*, supporting the conclusion that Fc receptor engagement is a substantial contributing component of anti-tumor activity *in vivo*.

Many mechanisms have been proposed for the ability of antibodies against tumors to mediate their effects *in vivo*. The data presented here indicate that Fc γ receptor binding contributes substantially to *in vivo* activity. This Fc γ -receptor dependence seems to apply to more than a single antibody, as it has been seen in both syngenic and xenograft models for the three unrelated tumors and target antigens presented here. Fc γ receptor engagement involves both activation and inhibitory receptors and thus indicates involvement of monocytes and macrophages in the effector cell component of the protective response. Supportive evidence for this interpretation is found in the ability of trastuzumab to mediate ADCC *in vitro* and the ability of antibodies against Fc receptor to inhibit some of the *in vivo* activity of antibodies against CD20 (ref. 16). Although the studies presented here demonstrate the importance of interactions between Fc and Fc γ receptors, triggering the growth and apoptotic regulatory pathways by antibody engagement of p185HER2/neu and CD20 may still contribute to the total *in vivo* efficacy of antibodies against tumors. Support for this interpretation can be seen in the partial protection in Fc γ R^{-/-} mice treated with antibodies against HER2/neu (Fig. 2), in which the anti-tumor activity of these antibodies against the BT474M1 breast carcinoma cells was reduced but not ablated. Similarly, previous studies showed that the 225 antibody against epidermal growth factor receptor was able to reduce the epithelial tumor cell A431 growth *in vivo* as an F(ab')₂, although with only 50% of the activity shown by the intact antibody¹⁷. Blocking the signaling on tumor cells by antibodies may also act synergistically with immune effector responses by rendering the tumor cells more susceptible to immune effector cell triggered apoptotic or lytic cell death¹⁸. Our results thus indicate the importance of selection and engineering of therapeutic antibodies against tumor to maximize their interactions with Fc γ RIII and minimize their interaction with Fc γ RIIB, which along with the appropriate antigenic target will potentiate their therapeutic capacity. In addition, these studies emphasize the fundamental

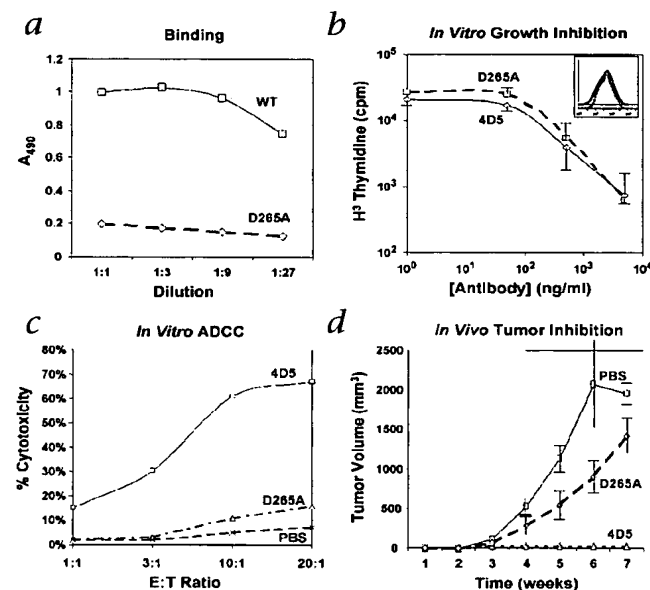


Fig. 4 *In vitro* and *in vivo* properties of the D265A mutant antibody. **a**, Fc γ RIII binding. Both wild-type and mutant Fc fragments were grafted onto an anti-human IgE Fab fragment. Solid-phase binding assays used hexameric complexes of human IgE and anti-human IgE and plates coated with recombinant Fc γ RIII. A₄₉₀, absorbance at 490 nm. **b**, Growth inhibition of BT474M1 cells. Inset, Fluorescence-activated cell sorting analysis of BT474M1 cells demonstrates equivalent avidities of 4D5 (solid line) and D265A (dotted line) for cell surface p185 HER2/neu. Main graph, ³H-thymidine incorporation of BT474M1 cells, measured in the presence of either 4D5 or D265A. **c**, NK-cell ADCC of chromium-labeled tumor targets. Chromium-labeled SKBR-3 cells were incubated with NK effector cells (effector:target (E:T) ratios, horizontal axis), and release of label was quantified. **d**, *In vivo* growth of breast carcinoma cells. Athymic BALB/c nu/nu mice were implanted with BT474M1 xenografts and their growth in response to treatment with 4D5, D265A or PBS was measured.

ARTICLES

importance of the inhibitory pathways *in vivo* and indicate that individual responses to antibodies against tumors may depend on the expression of these inhibitory pathways.

Methods

Melanoma metastasis model. Mice were injected intravenously with 1×10^6 B16 melanoma cell on day 0 and with either phosphate-buffered saline (PBS) or 20 μ g purified TA99 intraperitoneally on days 0, 2, 4, 7, 9 and 11. In previous experiments², a dose of 200 μ g of monoclonal antibody TA99 induced a reduction of more than 90% in tumor metastasis in wild-type but not *FcR γ ^{-/-}* mice. However, at this lower dose of TA99 (20 μ g), only limited protection was provided against tumor metastasis in wild-type mice. Mice were killed on day 14 and surface lung metastasis were counted under a dissecting microscope.

Tumor xenograft models. For breast carcinoma xenograft experiments, 5×10^6 BT474M cells (BT474 subclone derived at Genentech, South San Francisco, California) were injected subcutaneously on day 1 in 0.1 ml PBS mixed with 0.1 ml Matrigel (Collaborative Research, Bedford, Massachusetts). BALB/c nude mice, *FcR γ ^{-/-}* BALB/c nude mice or *Fc γ RII^{-/-}* BALB/c nude mice 2–4 months old were injected subcutaneously with 17 β -estradiol 60-day release pellets (0.75 mg/pellet; Innovative Research of America, Sarasota, Florida) 24 h before tumor cell injection. Therapeutic antibodies (obtained from clinical material, in vials; Genentech, South San Francisco, California) were injected intravenously beginning on day 1 at a loading dose of 4 μ g/mg, with weekly injections of 2 μ g/mg for BALB/c nude and *FcR γ ^{-/-}* BALB/c nude. A dose 10% of this (0.4 μ g/mg, loading; 0.2 μ g/mg, weekly) was used for the experiments in Fig. 3. For B-cell lymphoma xenograft experiments, BALB/c nude mice or *FcR γ ^{-/-}* BALB/c nude mice 2–4 months old were irradiated with 3.0 cGy before subcutaneous injection of 5×10^6 Raji B-lymphoma cells. Rituximab (Rituxan[®]; IDEC Pharmaceuticals, San Diego, California) was given at a dose of 10 μ g/kg weekly. Tumor measurements were obtained weekly.

Engineering of D254A mutant antibody and binding assays. Site-directed mutagenesis was accomplished using the QuikChange Mutagenesis Kit (Stratagene, La Jolla, California). Mutant antibody was transiently expressed in A293 cells in the pRK expression vector, and conditioned supernatants were collected and purified by protein G affinity column chromatography. The ability of various mutants to bind recombinant Fc γ Rs was measured using an *in vitro* binding assay¹⁹. Microtiter plates were coated with 100 ng/well of a fusion protein of recombinant Fc γ RIII and glutathione S-transferase in PBS. Plates were washed with PBS supplemented with 0.05% Tween-20 (wash buffer) then blocked for 1 h at room temperature with 0.5% BSA, 50 mM Tris-buffered saline, 0.05% Tween 20, 2mM EDTA, pH 8.0 (ELISA buffer). The IgG1 Fc fragment of murine 4D5 as well as D265A was grafted onto the Fab of anti-human IgE (monoclonal antibody E27) and recombinant antibody was produced as described above. The addition of human IgE to E27 with wild-type or mutant Fc domains in a molar ratio of 1:1 in ELISA buffer led to the formation of homogeneous hexameric complexes. Complexes were added to the plates, washed five times in wash buffer, and were detected by the addition of goat F(ab')₂ antibody against mouse IgG, with subsequent colorimetric development.

Growth inhibition assays. BT474M cells were plated at a density of 1×10^4 cells per well and allowed to adhere for 24 h. Antibody was added for 48 h, followed by a 14-hour pulse with ³H-thymidine. Cells were collected onto filter mats and incorporated radioactivity was counted in a Wallac Microbeta scintillation counter. BT474M cells were incubated with 4D5 or D265A, and stained with FITC-conjugated goat antibody against mouse IgG. Fluorescence intensity was measured on a FACScan flow cytometer (Becton-Dickinson, San Jose, California).

In vitro ADCC assay. Adherent NK effector cells were obtained from interleukin-2-stimulated (250 U/ml; Sigma), 14-day cultures of splenocytes non-adherent to nylon-wool. Four-hour ADCC reactions used as target cells 5×10^4 chromium-labeled, HER2-overexpressing, SK-BR3 breast carcinoma cells (American Type Culture Collection, Rockville, Maryland) in 96-well plates in the presence or absence of 10 μ g/ml antibody. Percent cytotoxicity is expressed as [counts in supernatant-spontaneous release (without effectors)]/[total counts incorporated-spontaneous release]. Data are expressed as the mean of three replicate wells.

Acknowledgments

We thank D. White for his technical expertise, C. Ritter for her administrative assistance and R. Steinman and M. Nussenzweig for their comments on the manuscript. These studies were supported by grants from the National Institutes of Health, Cancer Research Institute and Genentech.

RECEIVED 9 NOVEMBER 1999; ACCEPTED 2 FEBRUARY 2000

- Bolland, S. & Ravetch, J.V. Inhibitory pathways triggered by ITIM-containing receptors. *Adv. Immunol.* **72**, 149–177 (1999).
- Clynes, R.A., Tekechi, Y., Moroi, Y., Houghton, A. & Ravetch, J.V. Fc receptors are required in passive and active immunity to melanoma. *Proc. Natl. Acad. Sci. USA* **95**, 652 (1998).
- Hudziak, R. *et al.* p185HER2 monoclonal antibody has antiproliferative effects *in vitro* and sensitizes human breast tumor cells to tumor necrosis factor. *Mol. Cell Biol.* **9**, 1165 (1989).
- Taji, H. *et al.* Growth inhibition of CD20 positive B lymphoma cell lines by IDEC-C288 anti-CD20 monoclonal antibody. *Jpn. J. Cancer Res.* **89**, 748 (1998).
- Masui, H., Moroyama, T. & Mendelsohn, J. Mechanism of antitumor activity in mice for anti-epidermal growth factor receptor monoclonal antibodies with different isotypes. *Cancer Res.* **46**, 5592 (1986).
- Waldmann, T.A. Lymphokine receptors: a target for immunotherapy of lymphomas. *Ann. Oncol. Suppl.* **13**, S, 1–45 (1994).
- Tutt, A.L. *et al.* Monoclonal antibody therapy of a B cell lymphoma: signaling activity on tumor cells appears more important than recruitment of effectors. *J. Immunol.* **161**, 3176 (1998).
- Pegram, M.D. *et al.* Phase II study of receptor enhanced chemosensitivity using recombinant humanized anti-p185HER2/neu monoclonal antibody plus cisplatin in patients with HER2/neu overexpressing metastatic breast cancer refractory to chemotherapy treatment. *J. Clin. Oncol.* **16**, 2659 (1998).
- Carter, P.L. *et al.* Humanization of an anti-p185HER2 antibody for human cancer treatment. *Proc. Natl. Acad. Sci. USA* **89**, 4285 (1992).
- Leget, G.A. & Czuczman, M.S. Use of Rituximab, the new FDA-approved antibody. *Curr. Opin. Oncol.* **10**, 548–551 (1998).
- Kopreski, M., Lipton, A., Harvey, H.A. & Kumar, R. Growth inhibition of breast cancer cell lines by combinations of anti-p185 monoclonal antibody and cytokines. *Anticancer Res.* **16**, 433–436 (1996).
- Lewis, G.D. *et al.* Differential responses of human tumor cell lines to anti-p185HER2 monoclonal antibodies. *Cancer Immunol. Immunother.* **37**, 255–263 (1993).
- Shan, D., Ledbetter, J.A. & Press, O.W. Apoptosis of malignant human B cells by ligation of CD20 with monoclonal antibodies. *Blood* **91**, 1644–1652 (1998).
- Takai, T., Li, M., Sylvestre, D., Clynes, R. & Ravetch, J.V. Fc γ chain deletion results in pleiotropic effector cell defects. *Cell* **76**, 519–529 (1994).
- Takai, T., Ono, M., Hikida, M., Ohmori, H. & Ravetch, J.V. Augmented humoral and anaphylactic responses in Fc γ RIII deficient mice. *Nature* **379**, 346–349 (1996).
- Funakoshi, S., Longo, D.L. & Murphy, W.J. Differential *in vitro* and *in vivo* antitumor effects mediated by anti-CD40 and anti-CD20 monoclonal antibodies against human B-cell lymphomas. *J. Immunother.* **19**, 93–101 (1996).
- Fan, Z., Masui, H., Altas, I. & Mendelsohn, J. Blockade of epidermal growth factor receptor function by bivalent and monovalent fragments of 225 anti-epidermal growth factor receptor monoclonal antibodies. *Cancer Res.* **53**, 4322–4328 (1993).
- Baselga, J., Norton, L., Albanell, J., Kim, Y.M. & Mendelsohn, J. Recombinant humanized anti-HER2 antibody (Herceptin) enhances the anti-tumor activity of paclitaxel and doxorubicin against HER2/neu overexpressing human breast cancer xenografts. *Cancer Res.* **58**, 2825–2831 (1998).
- Liu, J., Lester, P., Builder, S. & Shine, J. Characterization of complex formation by humanized anti-IgE monoclonal antibody and monoclonal human IgE. *Biochemistry* **34**, 10474–10482 (1995).

REPORTS

38. X. He, M. Semenov, K. Tamai, X. Zeng, *Development* 131, 1663 (2004).
39. G. Liu, A. Bafico, V. K. Harris, S. A. Aaronson, *Mol. Cell. Biol.* 23, 5825 (2003).
40. T. Liu et al., *Science* 292, 1718 (2001).
41. Y. Xing, W. K. Clements, D. Kimelman, W. Xu, *Genes Dev.* 17, 2753 (2003).
42. This research was partially supported by the Intra-

mural Research Program of NIH, National Institute of Dental and Craniofacial Research.

Supporting Online Material

www.sciencemag.org/cgi/content/full/310/5753/1504/DC1
Materials and Methods
SOM Text

Figs. S1 to S5
References

16 June 2005; accepted 2 November 2005
Published online 17 November 2005
10.1126/science.1116221

Include this information when citing this paper.

Divergent Immunoglobulin G Subclass Activity Through Selective Fc Receptor Binding

Falk Nimmerjahn and Jeffrey V. Ravetch*

Subclasses of immunoglobulin G (IgG) display substantial differences in their ability to mediate effector responses, contributing to variable activity of antibodies against microbes and tumors. We demonstrate that the mechanism underlying this long-standing observation of subclass dominance in function is provided by the differential affinities of IgG subclasses for specific activating IgG Fc receptors compared with their affinities for the inhibitory IgG Fc receptor. The significant differences in the ratios of activating-to-inhibitory receptor binding predicted the *in vivo* activity. We suggest that these highly predictable functions assigned by Fc binding will be an important consideration in the design of therapeutic antibodies and vaccines.

Antibodies have evolved into classes with specific assigned functions. Within these classes, further subclassification extends immunoglobulin diversity, most strikingly in the four subclasses of IgG of mammals (1). In rodents and primates, these subclasses have evolved specialized effector responses, such as cytotoxicity, phagocytosis, and release of inflammatory mediators (2, 3). IgG subclass expression is influenced by multiple factors, including the prevailing cytokine environment. For example, the T helper cell T_H2 cytokine interleukin 4 (IL-4) preferentially induces switching to IgG1 and IgE, whereas transforming growth factor- β (TGF- β) induces switching to IgG2b and IgA (4–6). Alternatively, T_H1 cytokines such as interferon- γ (IFN- γ) result in IgG2a, 2b, and 3 switching (7). Switching is also strongly influenced by the nature of the stimulating antigen. For example, protein antigens elicit a thymus-dependent response generally dominated by IgG1, 2a, and 2b, whereas carbohydrate antigens can induce so-called thymus-independent responses that result in IgG3 antibody expression (8). Among IgG subclasses, IgG2a and 2b are generally considered to be the most potent for activating effector responses and dominate antiviral immunity and autoimmune diseases (9–11). Such functional dis-

tinctions among these IgG subclasses have been attributed to differences in their capacity to fix complement (12, 13). However, studies in complement-deficient mice have challenged this assumption and have focused attention on the cellular receptors for IgG, the Fc γ Rs, as the primary mediators of IgG effector responses (14, 15). We hypothesized that unified mechanisms accounting for the different potencies of IgG subclasses might be based on the differential binding to the known FcRs.

Activation Fc γ Rs are expressed on all myeloid cells, and their cross-linking results in sustained cellular responses (3). Balancing these activation receptors is the inhibitory Fc receptor, Fc γ RIIB, which, when coligated to activation receptors, dampens the cellular response (3, 16). The coexpression of activation and inhibitory receptors establishes a threshold for cellular triggering by IgG antibodies. Although all Fc γ Rs can bind IgG immune complexes, we have observed that individual Fc receptors display significantly different affinities for IgG subclasses (17). We described this differential affinity for functionally distinct FcRs by specific IgG subclasses as a ratio, referred to as the activating-to-inhibitory (or A/I) ratio (17). These A/I ratios were found to differ by several orders of magnitude between IgG subclasses and thus raised the possibility that the variation in *in vivo* IgG subclass activity could be directly linked to the specific A/I ratio. To address this hypothesis, we established an *in vivo* system for testing antibodies that differed in their

A/I ratios. The variable portions of the immunoglobulin heavy chain (V_H regions) of the cloned hybridomas that recognize either the melanosome gp75 antigen (TA99) or a platelet integrin antigen (6A6) were grafted onto IgG1, 2a, 2b, or 3 Fc regions and coexpressed with the appropriate light chains (17, 18). These recombinant antibodies were purified, and subsequent testing revealed that switching the constant regions of IgG did not affect antigen binding affinity (18) (table S1). As expected, however, specific differences in binding affinity of each subclass to specific Fc γ Rs were observed, resulting in different A/I ratios for each subclass (17) (fig. S1, table S2).

To determine whether the differences in A/I ratios for individual subclasses correlate to *in vivo* biological activity, we investigated the ability of these class-switched antibodies to mediate their specific biological functions: tumor clearance and platelet depletion (14, 19). Both TA99 (Fig. 1, A and B) and 6A6 (Fig. 1C) carrying IgG2a constant regions (A/I = 70) displayed enhanced activity compared with these antibodies bearing IgG1 constant regions (A/I = 0.1). IgG2a and 2b were equivalent in their ability to mediate platelet clearance, whereas IgG2a resulted in enhanced antibody-dependent cellular cytotoxicity (ADCC) in the metastatic melanoma model compared with IgG2b (A/I = 7) (Fig. 1, A and B). The hierarchy of activity for the IgG subclasses in these immune functions was thus IgG2a \geq IgG2b > IgG1 \gg IgG3, mirroring the hierarchy based on the A/I ratios (Fig. 1D).

We next tested the mechanism of this observed differential activity by repeating the experiments using strains of mice carrying specific deficiencies in, or blocked activation of, different activating Fc γ Rs or complement components (Fig. 2; fig. S2). No differences in *in vivo* activity were observed in complement-deficient (C4, C3, or CR1/2) strains (fig. S2). In contrast, IgG1, 2a, and 2b all depended on expression of activating Fc γ R, because activity was abrogated in the common γ chain-deficient background (Fig. 2, A, B, and E). Because IgG2a has been shown to bind to all of the γ chain-containing activating Fc γ Rs *in vitro* [with high affinity (10^8 to 10^9 M $^{-1}$) to Fc γ RI, intermediate affinity (10^7 M $^{-1}$) to Fc γ RIV, and low affinity (10^6 M $^{-1}$) to Fc γ RIII], its *in vivo* capacity to deplete platelets or to mediate ADCC could, in principle, result from engagement of one or more of these Fc γ Rs. We tested the contributions of each of these

Laboratory of Molecular Genetics and Immunology, The Rockefeller University, 1230 York Avenue, New York, NY 10021, USA.

*To whom correspondence should be addressed.
E-mail: ravetch@rockefeller.edu

Fig. 1. Hierarchy of antibody isotype-mediated effector functions in vivo. (A and B) B16-F10 lung metastasis in mice treated with TA99 switch variants (mean \pm SEM). Mice were injected as described (18); the number of surface lung metastasis was evaluated on day 15. * $P < 0.0001$; ** $P < 0.01$. (C) Platelet depletion with 6A6 switch variants (mean \pm SEM). Mice were injected as described (18); platelet counts were determined at the indicated time points. (D). A/I ratio for the indicated switch variants.

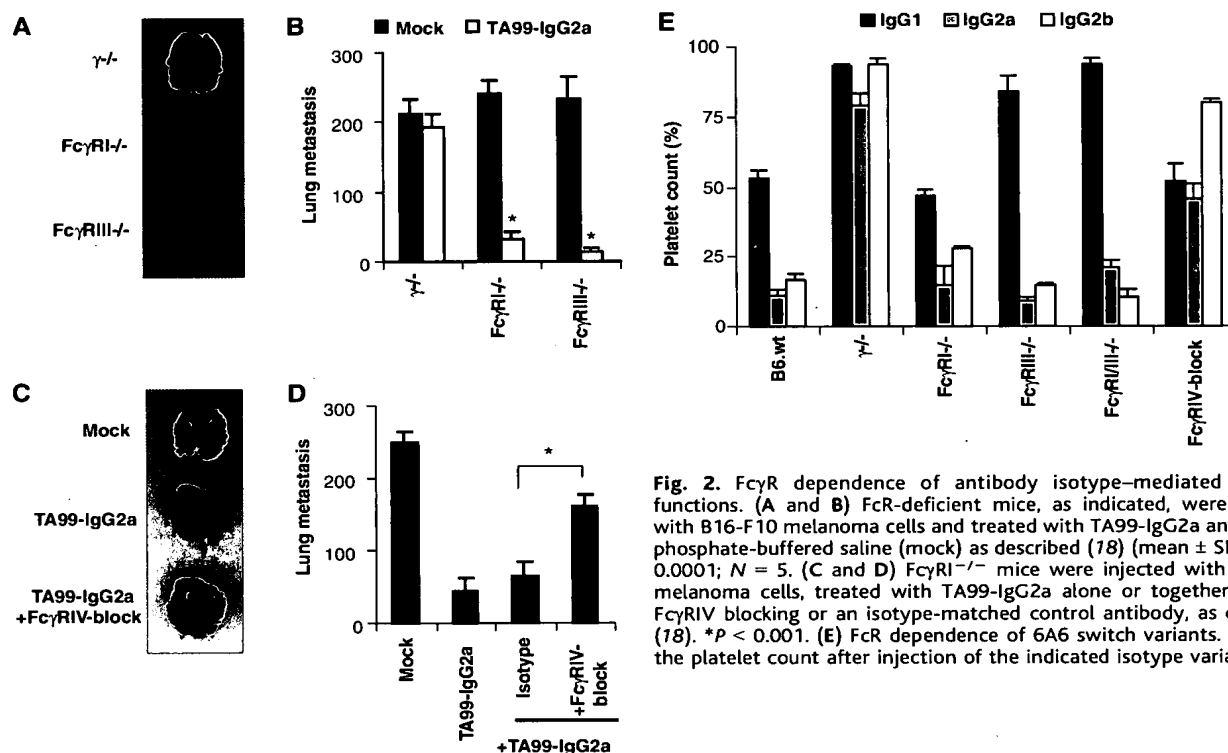
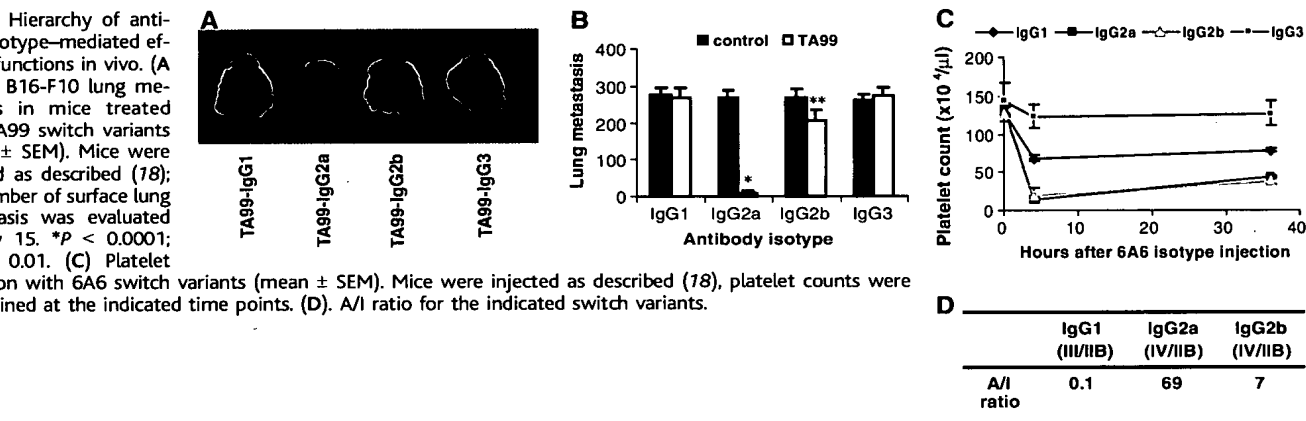


Fig. 2. Fc γ R dependence of antibody isotype-mediated effector functions. (A and B) Fc γ R-deficient mice, as indicated, were injected with B16-F10 melanoma cells and treated with TA99-IgG2a antibody or phosphate-buffered saline (mock) as described (18) (mean \pm SEM). * $P < 0.0001$; $N = 5$. (C and D) Fc γ RI $^{-/-}$ mice were injected with B16-F10 melanoma cells, treated with TA99-IgG2a alone or together with an Fc γ RIV blocking or an isotype-matched control antibody, as described (18). * $P < 0.001$. (E) Fc γ R dependence of 6A6 switch variants. Shown is the platelet count after injection of the indicated isotype variants (18):

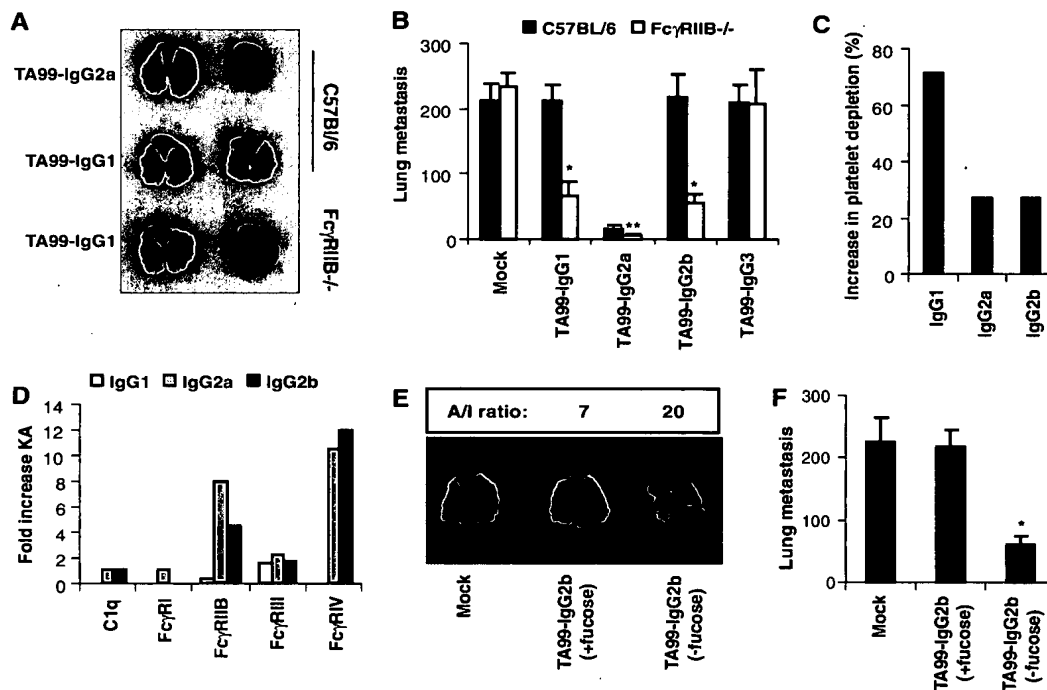
receptors to the in vivo activity of this subclass using mice deficient in or blocked for each receptor. TA99-IgG2a-mediated tumor clearance and 6A6-IgG2a-mediated platelet depletion were undiminished in mice deficient in either Fc γ RI or III (Fig. 2, C to E); in contrast, blocking Fc γ RIV binding with a specific monoclonal antibody significantly reduced these IgG2a-mediated activities (Fig. 2, C to E). Similarly, 6A6-IgG2b activity was only dependent on Fc γ RIV engagement, despite its in vitro binding to both Fc γ RIII and IV (17) (Fig. 2E). In contrast, the 6A6-IgG1 switch variant was only dependent on Fc γ RIII engagement (17) (Fig. 2E).

The A/I ratio of 0.1 for IgG1 suggested that IgG1 might exhibit a greater dependence in its in vivo activity on Fc γ RIIB expression. Consistent with this prediction, we observed that IgG1 displayed the most significant enhancement in activity in mice lacking the inhibitory receptor, both in tumor clearance (Fig. 3, A and B) and platelet depletion (Fig. 3C) relative to IgG2a or 2b switch variants (Fig. 3, A to C). In contrast, IgG2a (A/I = 70) showed the least enhancement in biological activity in Fc γ RIIB-deficient mice (Fig. 3, B and C). By comparison, IgG2b (A/I = 7) differed in the magnitude of enhancement displayed in the Fc γ RIIB-deficient

strains between each of the two models, with a significant increase in tumor clearance (Fig. 3B), but only minimal enhancement in platelet depletion (Fig. 3C). The intermediate A/I ratio of this subclass may render it more sensitive to the absolute level of inhibitory receptor surface expression and the specific effector cell engaged. This makes the dependence of IgG2b on Fc γ RIIB consistent with the observation that expression of this Fc γ R is minimal on splenic macrophages (15, 20), the cell type responsible for platelet clearance, but higher on alveolar macrophages, which are involved in the metastatic melanoma model (21).

REPORTS

Fig. 3. A/I ratio determines in vivo efficacy of native and modified antibodies. (A to C) Differential effects of inhibitory receptor expression on IgG subclass activity. (A and B) C57BL/6 wild-type or FcγRIIB^{-/-} mice were injected with B16-F10 melanoma cells and treated with TA99 switch variants, as described (18). **P* < 0.0001; ****P* < 0.05; *N* = 5. (C) C57BL/6 or FcγRIIB^{-/-} mice were injected with 6A6 antibody switch variants, as described (18). (D to F) Modified antibodies with increased A/I ratio display enhanced cytotoxic activity. (D) Fold increase in association constants (*K_A*) for C1q and FcγRs I-IV in binding to fucosylated or non-fucosylated TA99 switch variants. (E and F) Clearance of B16 melanoma lung metastasis with TA99-IgG2b with or without fucose (18). **P* < 0.0001.



To further explore the relation between the A/I ratio of IgG subclasses and their activity, modified IgG constant regions were generated. FcR binding to IgG depends on the presence of N-linked glycosylation at position 297, and deglycosylation abrogates all FcR binding (22). However, selective removal of specific carbohydrates, such as fucose, has been suggested to enhance human IgG1 binding to human FcγRIII and, thus, to enhance NK cell-mediated ADCC in vitro (23, 24). We therefore prepared fucose-sufficient and fucose-deficient TA99-IgG1, 2a, and 2b subclasses and compared their binding to antigen, complement, and FcγRI, II, III, and IV (18). Fucose-deficient antibodies ranged in their binding affinities to their respective FcγRs, but not for antigen or C1q, the first component of complement (23) (table S1, S2; Fig. 3D). TA99-IgG1, with or without fucose, displayed minimal differences in binding to FcγRIIB and III, whereas fucose-deficient IgG2a and 2b antibodies bound with higher affinity (by an order of magnitude) to FcγRIIB and IV compared with fucose-sufficient versions. These differences in binding affinities resulted in alterations to the respective A/I ratios that were most pronounced for IgG2b, with defucosylation increasing its A/I ratio from 7 to 20 (Fig. 3E; table S2). Furthermore, this translated into significantly enhanced in vivo activity for fucose-deficient TA99-IgG2b (Fig. 3, E and F). This selective effect of IgG defucosylation on FcR binding further illustrates the specificity of IgG subclassing in their inter-

actions with individual FcRs and the contribution of these affinities for IgG to in vivo activity.

The studies described here provide a mechanistic basis for the observed variation in IgG subclass activity in both active and passive vaccination and in the variable pathogenicity of the IgG subclasses in autoimmune conditions. The selective FcR binding affinities for the IgG subclasses and fucose-deficient antibodies appeared to be predictive of the in vivo activity for cytotoxic antibodies in models of tumor clearance and platelet depletion. Although significant differences between the mouse and human IgG subclasses and the FcγRs have been described (25), the principles that have emerged from these mouse studies are likely to apply to human antibodies as well as their respective FcRs. Such considerations may prove important in the design of antibody-based therapeutics and active vaccination protocols.

References and Notes

- G. W. Litman, M. K. Anderson, J. P. Rast, *Annu. Rev. Immunol.* 17, 109 (1999).
- D. R. Burton, J. M. Woof, *Adv. Immunol.* 51, 1 (1992).
- J. V. Ravetch, S. Bolland, *Annu. Rev. Immunol.* 19, 275 (2001).
- F. D. Finkelman et al., *Annu. Rev. Immunol.* 8, 303 (1990).
- J. Stavnezer, *J. Immunol.* 155, 1647 (1995).
- C. M. Snapper, J. J. Mond, *Immunol. Today* 14, 15 (1993).
- T. R. Mosmann, R. L. Coffman, *Annu. Rev. Immunol.* 7, 145 (1989).
- J. J. Mond, Q. Vos, A. Lees, C. M. Snapper, *Curr. Opin. Immunol.* 7, 349 (1995).

- J. P. Coutelier, J. T. van der Logt, F. W. Heessen, G. Warnier, J. Van Snick, *J. Exp. Med.* 165, 64 (1987).
- D. Markine-Goriaynoff, J. P. Coutelier, *J. Virol.* 76, 432 (2002).
- L. Fossati-Jimack et al., *J. Exp. Med.* 191, 1293 (2000).
- A. R. Duncan, G. Winter, *Nature* 332, 738 (1998).
- C. A. Janeway, P. Travers, M. Walport, M. Shlomchik, *Immunobiology 5: The Immune System in Health and Disease* (Garland Press, New York, 2001).
- D. Sylvestre et al., *J. Exp. Med.* 184, 2385 (1996).
- R. Clynes, J. V. Ravetch, *Immunology* 3, 21 (1995).
- J. V. Ravetch, L. L. Lanier, *Science* 290, 84 (2000).
- F. Nimmerjahn, P. Bruhns, K. Horiuchi, J. V. Ravetch, *Immunology* 23, 41 (2005).
- Materials and methods are available as supporting material on Science Online.
- S. Vijayasaradhi, B. Bouchard, A. N. Houghton, *J. Exp. Med.* 171, 1375 (1990).
- A. Samuelsson, T. L. Towers, J. V. Ravetch, *Science* 291, 484 (2001).
- N. Shushakova et al., *J. Clin. Invest.* 110, 1823 (2002).
- R. Jefferis, J. Lund, *Immunol. Lett.* 82, 57 (2002).
- R. L. Shields et al., *J. Biol. Chem.* 277, 26733 (2002).
- T. Shinkawa et al., *J. Biol. Chem.* 278, 3466 (2003).
- M. D. Hulett, P. M. Hogarth, *Adv. Immunol.* 57, 1 (1994).
- We are grateful to M. Carroll (Harvard University) for providing CR2^{-/-}, C3^{-/-}, and C4^{-/-} mice, B. Collier (Rockefeller University) for access to the Advia hematology system, and A. Savage for expert technical assistance. This work was supported by grants from the NIH to J.V.R. and from the Deutsche Forschungsgemeinschaft (NI711/2-1) and Cancer Research Institute to F.N.

Supporting Online Material

www.sciencemag.org/cgi/content/full/310/5753/1510/DC1

Materials and Methods
Figs. S1 and S2
Tables S1 and S2
References and Notes

16 August 2005; accepted 27 October 2005
10.1126/science.1118948

Mac-1 (CD11b/CD18) is crucial for effective Fc receptor-mediated immunity to melanoma

Annemiek B. van Spriel, Heidi H. van Ojik, Annie Bakker, Marco J. H. Jansen, and Jan G. J. van de Winkel

Antibody-reliant destruction of tumor cells by immune effector cells is mediated by antibody-dependent cellular cytotoxicity, in which Fc receptor (FcR) engagement is crucial. This study documents an important role for the β_2 integrin Mac-1 (CD11b/CD18) in FcR-mediated protection against melanoma. CD11b-deficient mice, those that lack Mac-1, were less

protected by melanoma-specific monoclonal antibody TA99 than wild-type (WT) mice. Significantly more lung metastases and higher tumor loads were observed in Mac-1^{-/-} mice. Histologic analyses revealed no differences in neutrophil infiltration of lung tumors between Mac-1^{-/-} and WT mice. Importantly, Mac-1^{-/-} phagocytes retained the capacity to bind tumor

cells, implying that Mac-1 is essential during actual FcR-mediated cytotoxicity. In summary, this study documents Mac-1 to be required for FcR-mediated antimelanoma immunity in vivo and, furthermore, supports a role for neutrophils in melanoma rejection. (Blood. 2003;101:253-258)

© 2003 by The American Society of Hematology

Introduction

Antibody (Ab)-dependent cellular cytotoxicity (ADCC) is considered crucial for Ab-mediated tumor cell degradation. Specific Ab-Fc receptor (FcR) interactions establish close contacts between tumor targets and immune effector cells, which triggers cytotoxicity and cytokine release. Neutrophils, monocytes, macrophages, and natural killer (NK) cells can mediate ADCC via activating FcRs, which include Fc γ R1a (CD64), Fc γ R1b (CD32), Fc γ R1c (CD16), and Fc γ R2 (CD89) in man, and Fc γ R1 and Fc γ R2 in mice.¹⁻⁴ Although Abs may affect tumor growth via FcR-unrelated mechanisms (such as complement-dependent lysis, blockade of growth factor receptors, or via induction of apoptosis),⁵ in vivo antitumor effects of Abs have been documented to depend on immune activation through FcRs.⁶⁻⁸

Numerous studies in cancer immunology focused on melanoma and melanoma-specific differentiation antigens that induce immune responses.⁹ If tolerance is broken, melanosomal proteins can be recognized by T cells, which may provide B-cell help and participate in Ab production. Actual tumor rejection seems dependent on phagocytes, which may be activated by CD4⁺ or NK cells.¹⁰⁻¹² Improved clinical outcome has, furthermore, been correlated with the presence of melanoma-specific Abs in patients.¹³ Ab-mediated protection in the murine B16F10 melanoma model is well established. Monoclonal antibody (mAb) TA99, specific for melanoma differentiation antigen gp75 (*brown* locus protein, or TRP-1), is effective in preventing and eradicating early established metastases.¹¹ Studies with mice deficient in the FcR γ chain, lacking expression of Fc γ R1 and Fc γ R2, revealed activating FcR to be critical in TA99-mediated tumor rejection.⁶ Further evidence supporting FcR dependence in Ab-mediated melanoma rejection was established by (1) the documented inability of F(ab')₂ fragments to mediate protection,¹² (2) lack of Ab effects on tumor cells

in the absence of effector cells,¹² and (3) enhancement of antitumor immunity in Fc γ R2 (inhibitory murine FcR) knock-out mice.⁷

Mac-1 (CD11b/CD18) represents the leukocyte $\alpha_m\beta_2$ integrin, which is expressed on neutrophils, monocytes, macrophages, and NK cells. Mac-1 binds multiple ligands and is important in leukocyte adhesion, chemotaxis, migration, phagocytosis, and cytotoxicity.¹⁴ CD18 linkage to the actin cytoskeleton and associated proteins enables Mac-1 signaling.^{15,16} Furthermore, Mac-1 has been proposed to act as a signaling partner for other leukocyte receptors, including lipopolysaccharide (LPS)/LPS binding protein (LBP) receptors (CD14), formyl-methionyl-leucyl-phenylalanine (FMLP) receptors, urokinase plasminogen activator receptors (CD87), and FcRs.¹⁷

Involvement of Mac-1 in phagocyte FcR-mediated phagocytosis and respiratory burst activity has been documented.¹⁸⁻²⁰ Phagocytes from leukocyte adhesion deficiency patients lack β_2 integrins, and are defective in phagocytosis and ADCC.^{14,21} An important role has been shown for Mac-1 in FcR-mediated cytotoxicity toward tumor cells, parasites, virus-infected cells, and erythrocytes.²²⁻²⁶ Recently, Mac-1 was shown to be crucial for neutrophil spreading on Ab-coated tumor cells and formation of immunologic synapses. This was postulated to underlie the mechanism of Mac-1 requirement for Ab-mediated tumor cytotoxicity.²⁷ Although all these studies point to an essential role for Mac-1 in ADCC, Mac-1 involvement in Ab-mediated tumor rejection has not been documented in vivo. Therefore, we established the syngeneic B16F10 melanoma model in Mac-1-deficient mice and studied Ab-mediated protection. This study documents Mac-1 to be required for FcR-mediated immunity to melanoma and, furthermore, supports an active role for neutrophils in antimelanoma responses.

From the Immunotherapy Laboratory, Department of Immunology, Department of Internal Medicine and Oncology, Medarex Europe, and Genmab, University Medical Center Utrecht, The Netherlands.

Submitted May 4, 2001; accepted August 29, 2002.

A.B. van S. and H.H. van O. contributed equally to this study.

Reprints: Jan G. J. van de Winkel, Immunotherapy Laboratory, Department of

Immunology, University Medical Center Utrecht, Room KC02.085.2, Lundlaan 6, 3584 EA, Utrecht, The Netherlands; e-mail: janvandewinkel@aol.com.

The publication costs of this article were defrayed in part by page charge payment. Therefore, and solely to indicate this fact, this article is hereby marked "advertisement" in accordance with 18 U.S.C. section 1734.

© 2003 by The American Society of Hematology

Materials and methods

Antibodies and peg-G-CSF

mAb TA99 (mouse IgG2a), which is directed against the gp75 antigen, was purified from hybridoma HB-8704 (American Type Culture Collection, Manassas, VA) by protein A Sepharose chromatography (Amersham, Uppsala, Sweden). mAb 17-1A (mIgG2a), used as an isotype control, was kindly provided by Dr T. Valcrius (Erlangen, Germany). mAb 520C9 (mIgG1, directed against the proto-oncogene product HER-2/neu) was obtained from Medarex (Annandale, NJ). mAb GR-1 (PharMingen, San Diego, CA) and F4/80 (Serotec, Oxford, United Kingdom) were used in immunohistochemistry to examine neutrophil and monocyte/macrophage infiltration, respectively. Human recombinant polyethylene-glycol granulocyte colony-stimulating factor (peg-G-CSF) was kindly provided by Dr J. Andresen (Amgen, Thousand Oaks, CA). Covalent attachment of polyethylene-glycol (peg) to G-CSF extends its half-life.²⁸ Previous work indicated peg-G-CSF to exhibit similar *in vivo* biologic effects as uncoupled G-CSF.²⁹

Tumor cell lines and gp75 expression

The B16F10 mouse melanoma cell line of C57BL/6 origin was from NCI (Frederick, MD). Cells were grown in RPMI 1640 medium (Gibco BRL, Grand Island, NY) supplemented with 10% heat-inactivated fetal calf serum (FCS), penicillin (50 IU/mL), and streptomycin (50 µg/mL). B16F10 cells were detached with 0.02 mM EDTA (ethylenediaminetetraacetic acid) in phosphate-buffered saline (PBS), and washed twice with PBS. Gp75 expression was determined by incubating B16F10 cells with mAb TA99 (25 µg/mL) at 4°C for 30 minutes, followed by staining with fluorescein isothiocyanate (FITC)-labeled F(ab')₂ fragments of goat anti-mouse immunoglobulin G (IgG) (Protos, San Francisco, CA). Total gp75 expression in B16F10 cells was assayed upon permeabilization with methanol/acetone (1:1) at 4°C for 15 minutes. In addition, B16F10 cells were incubated with control mIgG2a (17-1A) and FITC-labeled goat anti-mouse IgG. FITC-fluorescence intensities were analyzed on a FACScan flow cytometer (Becton Dickinson, San Jose, CA). SK-BR-3 (human breast carcinoma) cells (ATCC, HTB-30) were used as controls in ADCC experiments.

ADCC assay

To increase circulating effector cells, mice were injected subcutaneously with 15 µg peg-G-CSF, and blood was collected from the retro-orbital plexus 3 days later. Erythrocytes were removed by hypotonic lysis, followed by washing remaining leukocytes 3 times with RPMI 1640 medium with 10% FCS. Cell viability determined by trypan blue exclusion was always more than 95%. Fluorescence activated cell sorting (FACS) analyses revealed leukocytes to consist of, approximately, 55% neutrophils, 40% lymphocytes, 3% monocytes, and 1% eosinophils. The capacity of leukocytes to lyse tumor cells was evaluated in ⁵¹Chromium (⁵¹Cr) release assays.³⁰ Briefly, ⁵¹Cr-labeled B16F10 or SK-BR-3 cells were plated in round-bottom 96-well plates (5 × 10³ cells/well) in RPMI 1640 medium with 10% FCS. Isolated mouse leukocytes were added in the absence or presence of mAb TA99 (concentrations ranging from 1 µg/mL-100 µg/mL) or 2 µg/mL mAb 520C9, giving different effector-to-target ratios, and incubated for 4 hours at 37°C, after which ⁵¹Cr release was measured in supernatants.

Mice

C57BL/6 wild-type (WT) mice were purchased from Harlan (Horst, The Netherlands). CD11b-deficient mice (Mac-1^{-/-}), in the C57BL/6 background, were kindly provided by Dr T. N. Mayadas (Harvard Medical School, Boston, MA).^{25,27,31} Experiments were performed with 8- to 12-week-old female and male mice. Mice were maintained at the Central Laboratory Animal Institute (Utrecht University) and experiments were approved by the Utrecht University animal ethics committee.

Melanoma model

C57BL/6 WT and Mac-1^{-/-} mice were injected intravenously with 1 × 10⁵ B16F10 tumor cells (in 100 µL saline) on day 0. Mice were treated intraperitoneally with 200 µL saline (control), or with 200 µg mAb TA99 (in 200 µL saline) on days 0, 2, 4, 7, 9, and 11. In other experiments, mice were treated with peg-G-CSF or with mAb TA99 and peg-G-CSF. Peg-G-CSF was administered as a subcutaneous injection of 20 µg (in 150 µL saline) on days -3 and -4. Mice were observed daily and killed when they became seriously ill (inactive/blurred fur) or paralyzed. Surviving mice were killed at day 21. Since metastases of B16F10 melanoma are readily visually detected, they were scored at the macroscopical level by 2 independent investigators, who were blinded for the treatment. Lungs from all mice were excised and scored for (1) the number of surface metastases and (2) tumor load. Tumor load was defined by the sum of the following scores: metastases less than 1 mm were scored as 1; metastases of 1 mm to 2 mm scored as 3; and metastases more than 2 mm scored as 10. Tumor load correlated closely with the number of metastases (Figure 2). Secondary target organs, including thoracic and abdominal lymph nodes, liver, kidneys, spleen, and the central nervous system (CNS) were also examined for the presence of melanoma metastases, and the mean number of metastases per target organ was calculated (n ≥ 6 per group). In additional experiments, mice were killed and lungs were excised at day 7, 11, or 15 after tumor inoculation and frozen in liquid nitrogen for immunohistochemical analyses. Mean numbers of GR-1-positive cells in lungs with detectable metastases were quantified by 2 independent investigators using light microscopy.

Immunohistochemistry

Frozen sections of lungs (6 µm thick) were placed on superfrost slides (Menzel, Braunschweig, Germany), air-dried overnight, and fixed in acetone for 10 minutes at 20°C. Slides were incubated with 0.3% H₂O₂ to quench endogenous peroxidase activity. After fixation, slides were blocked with 10% normal mouse serum, and incubated with mAb GR-1 (1:250) or mAb F4/80 (1:2) for 1 hour. After repeated washing with PBS 0.05% Tween, sections were incubated with peroxidase-labeled rabbit anti-rat IgG (DAKO, Glostrup, Denmark) (1:1200) for 30 minutes at 20°C. Primary antibodies were diluted in 2% normal mouse serum, and a secondary Ab was diluted in 1% normal mouse and 2% normal rabbit serum. Upon washing with PBS 0.05% Tween and with sodium acetate buffer (0.1 M, pH 5.0), peroxidase activity was detected by incubating slides with 0.4 mg/mL 3-amino-9-ethylcarbazole (Sigma) for 15 minutes. Subsequently, slides were rinsed in distilled water, counterstained with Mayer hematoxylin (Merck, Darmstadt, Germany), and mounted in aquamount (BHD, Poole, England).

Statistical analysis

Unpaired Student *t* tests and Welch tests were used to determine statistical differences. Significance was accepted at the *P* < .05 level.

Results

mAb TA99 recognizes gp75 antigen on B16F10 melanoma cells

We first examined the binding of mAb TA99 to B16F10 melanoma cells. Low gp75 expression (mean fluorescence intensity [MFI] of 9.94, vs MFI of 3.55 in the control) was found on B16F10 cell membranes, whereas high levels were detectable in permeabilized cells (MFI of 551.3) (Figure 1). Control mIgG2a and FITC-labeled anti-mouse IgG did not bind B16F10 cells. Next, we assessed whether isolated murine leukocytes mediated ADCC of melanoma cells. Leukocytes of WT mice did not mediate Ab-dependent cytotoxicity of B16F10 cells at a range of effector-to-target ratios (data not shown). This was in contrast to breast carcinoma cells

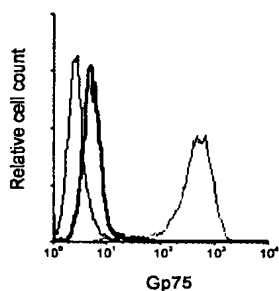


Figure 1. Gp75 expression on B16F10 melanoma cells. The interaction of mAb TA99, which binds the gp75 melanocyte differentiation antigen, with in vitro-grown B16F10 cells was analyzed by flow cytometry. B16F10 cells were incubated with control mlgG2a (thin solid line) or TA99 (thick solid line), and FITC-conjugated anti-mouse IgG, to assess gp75 membrane expression. Total gp75 expression was assayed by TA99 staining on permeabilized B16F10 cells (dashed line).

(SK-BR-3), which were effectively lysed ($56.3\% \pm 2.5\%$ cytotoxicity, $n = 4$) by WT leukocytes in the presence of mAb 520C9. mAb 520C9 recognizes the antigen HER-2/neu on SK-BR-3 cell membranes (MFI of 90.86 vs MFI of 2.9 in the control).

Ab-mediated protection against melanoma is enhanced by G-CSF

Previous work indicating that T and NK cells do not play a direct role in Ab-mediated rejection of B16F10 melanoma¹⁰⁻¹² prompted us to study the effect of peg-G-CSF on Ab-induced antitumor responses. Peg-G-CSF mediates *in vivo* activity similar to G-CSF, but has a prolonged half-life.^{28,29} WT mice were inoculated with 1×10^5 B16F10 cells, treated with either saline, mAb TA99, peg-G-CSF, or both TA99 and peg-G-CSF, and the number of lung metastases (Figure 2A) and tumor load (Figure 2B) were determined after 21 days. TA99 treatment led to protection against melanoma (61% reduction in number of lung metastases and 78% reduced tumor load, compared with controls). Peg-G-CSF, however, enhanced TA99-mediated antitumor activity significantly (95% reduction in number of metastases and 99% reduced tumor load). Upon combination treatment with TA99 and peg-G-CSF, 64% of mice were tumor-free at day 21. In additional experiments, mice were followed up after TA99/peg-G-CSF combination treatment, and were found to be alive without symptoms at the last observation at day 70. Peg-G-CSF treatment, by itself, did not lead to decreased tumor growth ($12.9 \pm 1.1\%$ metastases and $61 \pm 6.6\%$ tumor load; $n = 14$).

Excitingly, the combination treatment was also protective when started 7 days after tumor cell injection (75% reduction in number

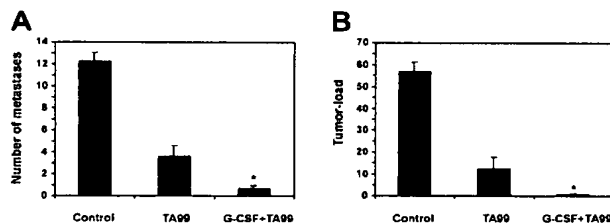


Figure 2. Peg-G-CSF augments Ab-induced protection against melanoma. WT mice were challenged intravenously with 1×10^5 B16F10 melanoma cells and treated with saline (control), mAb TA99, or TA99 and peg-G-CSF. Number of lung metastases (A) and pulmonary tumor load (B) were determined on day 21. Data are expressed as means \pm SEMs from at least 14 mice per group of 2 individual experiments. *Significant difference compared with TA99 treatment ($P < .05$, determined with unpaired Student *t* tests).

of lung metastases and 72% reduced tumor load, compared with controls; $n = 6$). Moreover, 33% of the treated mice were tumor-free after 21 days in this therapy model.

Mac-1 is required for Ab-induced antimelanoma activity

To assess the relevance of Mac-1 in FcR-mediated tumor cytotoxicity *in vivo*, we established the syngeneic B16F10 melanoma model in CD11b-deficient mice, which were of the same background as WT mice (C57Bl/6). B16F10 cells grew well in Mac-1^{-/-} mice, leading to advanced lung metastases after 3 weeks, similar to WT mice (Figure 3). A striking difference in melanoma growth was observed, however, between Mac-1^{-/-} and WT mice upon treatment. MAb TA99 combined with peg-G-CSF treatment resulted in almost complete tumor remission in lungs of WT mice, whereas Mac-1^{-/-} mice still contained clear melanoma infiltration despite treatment (Figure 3A). Quantification of pulmonary metastases revealed WT mice to be significantly better protected than Mac-1^{-/-} mice by mAb TA99 therapy (Figure 3Bi), as well as TA99 combined with peg-G-CSF (Figure 3Bii). Combination treatment reduced the number of metastases in WT mice by 95%, and in Mac-1^{-/-} mice by only 44%, compared with saline controls. Similarly, pulmonary tumor load was significantly higher in treated Mac-1^{-/-} mice than in WT mice. Treatment with TA99 combined with peg-G-CSF resulted in mean tumor loads of $0.79 (\pm 0.25, n = 14)$ in WT mice and $21.3 (\pm 7.5, n = 12)$ in Mac-1^{-/-} mice (data not shown). In addition, control experiments revealed peg-G-CSF to increase circulating neutrophil numbers in WT and Mac-1^{-/-} mice with similar kinetics (data not shown).

To study whether Ab-mediated protection was also diminished in secondary melanoma target organs of Mac-1^{-/-} mice, we evaluated melanoma infiltration into lymph nodes, liver, kidneys, and CNS (Table 1). Similar to the situation in lungs, Ab treatment (with or without peg-G-CSF) was more effective in WT than in Mac-1^{-/-} mice in protecting secondary target organs from melanoma infiltration. Taken together, these results reveal an important role for Mac-1 in Ab-induced antimelanoma immunity *in vivo*.

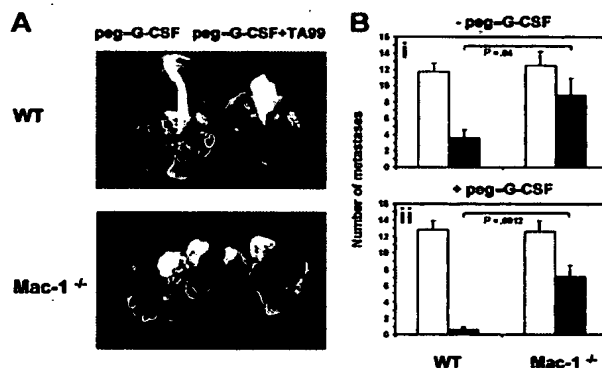


Figure 3. Mac-1 requirement in Ab-mediated antimelanoma immunity. The effect of mAb TA99 and peg-G-CSF on melanoma growth was studied in WT and Mac-1^{-/-} mice. Upon tumor inoculation, mice were treated with saline or TA99 combined with or without peg-G-CSF. (A) Lungs were excised at day 21 to analyze surface metastases. (B) Numbers of metastases in saline-treated (□) or TA99-treated mice (■) combined without (i) or with (ii) peg-G-CSF were quantified. Results represent means \pm SEMs from 2 individual experiments (WT: $n = 14$; Mac-1^{-/-}: $n = 12$). *P* values of significant differences were determined using unpaired Welch *t* tests.

Table 1. TA99-mediated protection from melanoma metastases in secondary target organs is dependent on Mac-1

	Lymph nodes		Liver/spleen	Kidney	CNS
	Thoracic	Abdominal			
WT saline	1.43 ± 0.46	1.57 ± 0.32	0.71 ± 0.31	0.86 ± 0.15	1.86 ± 0.15
WT TA99	0	0.43 ± 0.32	0	0	0.43 ± 0.32
Mac-1 ^{-/-} saline	1.33 ± 0.37	1.33 ± 0.37	0.67 ± 0.37	0.50 ± 0.24	0.33 ± 0.23
Mac-1 ^{-/-} TA99	0.67 ± 0.37	1.33 ± 0.46	0.17 ± 0.18	0	0.50 ± 0.37

WT and Mac-1^{-/-} mice were challenged with 1×10^5 B16F10 melanoma cells and treated with saline or TA99 combined with peg-G-CSF. Secondary target organs (thoracic and abdominal lymph nodes, liver, spleen, kidney, and CNS) were analyzed for presence of metastases on day 21. Results represent mean numbers (\pm SEMs) of metastases per target organ (WT: n = 7; Mac-1^{-/-}: n = 6).

Phagocytic cell migration into melanoma

Because our data pointed to a role for phagocytes in immunity to B16F10 melanoma, we examined the capacity of WT and Mac-1^{-/-} neutrophils and monocytes/macrophages to infiltrate tumor sites. Lungs of WT and Mac-1^{-/-} mice, treated with TA99 and peg-G-CSF, were analyzed 7, 11, and 15 days after tumor challenge. B16F10 cells were distributed as clustered neoplastic cells on days 11 and 15. Histology of lungs of treated WT mice revealed close-to-normal alveolar morphology with sporadic malignant cells and few neutrophils present (Figure 4, lower left). Lungs of WT mice not receiving TA99 and lungs of Mac-1^{-/-} mice (treated with saline or TA99), on the other hand, contained large metastatic lesions with occasional neutrophil infiltrates (Figure 4, arrows). We quantified the number of GR-1-positive cells in lung metastases of WT and Mac-1^{-/-} mice not receiving TA99 11 and 15 days after tumor inoculation. Comparable neutrophil infiltration (mean number of cells \pm SEM, n = 3) was observed in established tumors of WT and Mac-1^{-/-} mice (26 ± 4.9 vs 40.7 ± 18.7 at day 11, and 118 ± 41.2 vs 115 ± 35.9 at day 15, respectively). Analyzing effector-target cell interactions in more detail revealed both WT and Mac-1^{-/-} neutrophils to be situated in close contact with melanoma cells (Figure 4, inserts). On the contrary, macrophages and monocytes (visualized by F4/80 staining) hardly infiltrated into metastases of WT or Mac-1^{-/-} mice (data not shown). These data show Mac-1 not to be essential for phagocytic cell recruitment into metastatic sites and, furthermore, reveal Mac-1^{-/-} neutrophils capable of binding tumor cells.

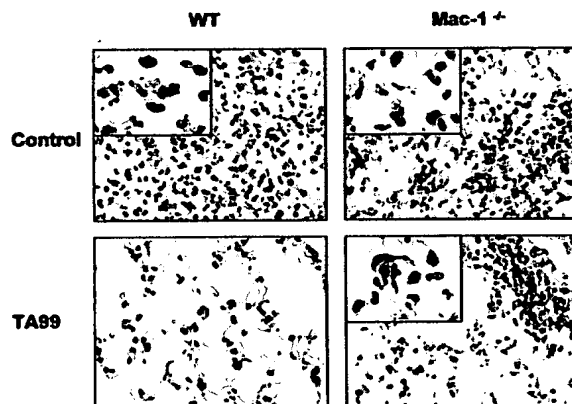


Figure 4. Phagocyte infiltration into pulmonary metastases of WT and Mac-1^{-/-} mice. WT and Mac-1^{-/-} mice were challenged intravenously with 1×10^5 B16F10 cells, and treated with peg-G-CSF and saline (control), or TA99 and peg-G-CSF as detailed in "Materials and methods." Lungs were removed 15 days after tumor inoculation for immunohistochemistry. GR-1 staining (mouse neutrophil marker, shown in brown) of pulmonary tissue of WT (left panels) and Mac-1^{-/-} (right panels) mice treated with (bottom panels) or without (top panels) TA99. Red arrows point at GR-1-positive cells. Original magnifications: $\times 400$ (main panels) and $\times 1000$ (insets).

Discussion

Melanoma differentiation antigens serve as a hallmark of tumor targets for immune cells. Antibodies directed against the gp75 antigen mediate effective protection in murine melanoma models. The mechanisms by which antibodies initiate antitumor activity remain incompletely understood. In the present study we document a requirement for Mac-1, an important β_2 integrin, in FcR-mediated cytotoxicity toward melanoma.

Our data and the data of others^{6,12} show that the gp75 glycoprotein is predominantly expressed intracellularly in cultured B16F10 melanoma cells, making them resistant to ADCC. However, gp75 membrane expression increases upon *in vivo* growth, and gp75-specific antibodies induce FcR-dependent melanoma rejection.^{6,7} In the present study, Mac-1-deficient mice proved significantly less protected against B16F10 melanoma infiltration than WT mice by an antibody targeting gp75, evidenced by higher tumor loads in lungs and secondary target organs. Since Mac-1 also serves as an adhesion molecule, we hypothesized that effector cell infiltration of tumor sites possibly depends on Mac-1. However, our data showed that WT and Mac-1^{-/-} neutrophils exhibit a comparable capability to enter metastases, which was determined by quantifying GR-1-expressing cells. This corresponds with the unaffected capacity of Mac-1^{-/-} neutrophils to migrate *in vivo*.³¹ Importantly, Mac-1^{-/-} phagocytes were found to bind well to tumor cells (Figure 4). This is consistent with our earlier data, which showed that the abrogated ADCC capacity of Mac-1^{-/-} neutrophils was not attributable to a defect at the level of FcR-antibody binding. Moreover, Mac-1^{-/-} neutrophils were fully capable of degranulation and oxygen radical production. However, Mac-1 was found to be crucial in neutrophil spreading on tumor cells and the formation of immunologic synapses *in vitro*.²⁷ Open intercellular clefts between effector cells and tumor cells can result in the leakage of toxic metabolites, and may represent the mechanism by which tumoricidal activity of Mac-1^{-/-} neutrophils is abrogated. We postulate Mac-1 to act as a costimulatory molecule for FcR-mediated cytotoxicity toward malignancies. Although we cannot conclude from the present data whether the Mac-1 requirement is general or restricted to FcR-mediated cytotoxicity of melanoma, a universal role for Mac-1 may be expected given that Mac-1 is crucial in ADCC toward various targets, including a number of tumor cell lines and parasites.^{23,26,27} The molecular basis of Mac-1/FcR cooperation has not been clarified, albeit that physical interactions between both molecules have been detected.^{17,32,33} Mac-1 may transmit signals elicited by Fc and other leukocyte receptors via its linkage to the actin cytoskeleton and associated signal transduction proteins.³⁴ The interaction of the cytoplasmic tail of the Mac-1 β -chain with talin and alpha-actinin has a dynamic nature and is dependent on the

activation status of neutrophils.^{15,35} Signaling pathways linking β_2 integrins to the various neutrophil functions are incompletely understood, but key roles for Syk-2, FAK, and Src-family kinases (Fgr/Hck) and their downstream substrates (Cbl, vav, PLC γ) have been reported.^{36,37}

Mac-1-mediated tumor cytotoxicity was recently shown in therapy models with β -glucan, which was dependent on C3bi deposition on tumor cells.³⁸ However, complement components are unlikely to be involved in our model, because neutrophil ADCC toward tumor targets has been shown independent of active complement.²⁷ Moreover, complement depletion with cobra venom factor does not reduce antibody-induced protection in the B16F10 melanoma model.¹¹ Melanoma cells are known to express intracellular adhesion molecule 1 (ICAM-1),³⁹ enabling direct Mac-1 interactions; in addition, Mac-1 is capable of clustering in the absence of ligand.⁴⁰ In any case, Ab-mediated melanoma rejection is crucially dependent on FcR and requires Mac-1 for efficient cytotoxicity.

A number of earlier studies focused on identification of the effector cells responsible for Ab-mediated melanoma eradication. An important role for phagocytes seems plausible on the following grounds: (1) enhanced Ab-induced melanoma rejection by macrophage colony-stimulating factor,^{10,41} (2) intact Ab-mediated protection upon T-cell depletion,^{10,11} and (3) Ab-mediated immunity in both *SCID* (lacking lymphocytes) and *beige* (lacking NK cells) mice.¹² Establishing a requirement for Mac-1 in Ab immunity to melanoma is in line with this earlier work and may allude to neutrophil involvement. To further support this, peg-G-CSF was found to augment antimelanoma Ab responses *in vivo*. Peg-G-CSF proved not tumoricidal by itself, underlining FcR-antibody interactions as a prerequisite. Since peg-G-CSF has a documented capacity to increase circulating neutrophil numbers and to enhance their tissue recruitment,²⁹ the present findings support the involvement of neutrophils in Ab-mediated protection against melanoma. Consistent with our data, G-CSF transduction of adenocarcinoma

results in antitumor activity mediated by neutrophils.^{42,43} Furthermore, phagocytes have been shown to infiltrate tumor sites including melanoma,⁴⁴⁻⁴⁷ and neutrophils have earlier been found important for tumor cell elimination *in vivo*.^{8,43,48-50}

Ab-mediated protection against melanoma was reduced by approximately 50% in Mac-1^{-/-} mice, pointing to a Mac-1-independent pathway in FcR-mediated tumor cytotoxicity. Since Mac-1 deficiency abrogates neutrophil ADCC capacity,²⁵ we hypothesize that Ab-reliant melanoma destruction results from cross-talk between neutrophils and other cytotoxic effectors.^{47,51} Although we did not observe apparent macrophage infiltration into tumor sites, Mac-1-deficient macrophages are capable of killing tumor cells, in contrast to neutrophils. This likely reflects differences in cytolytic effector mechanisms between these types of phagocytic cells.²⁷

In summary, the data presented here provide evidence for an important role of Mac-1 in Ab-mediated immunity to melanoma. Furthermore, this study implicates neutrophils to be important for Ab-reliant tumor cytotoxicity. Antibody treatment of human tumors has been studied extensively, with a number of clinical successes reported.^{5,7,52} FcRs play an important role in direct Ab-mediated tumor cytotoxicity and are, furthermore, important in the induction of vaccine responses.^{8,53,54} Better insight into the mechanisms of FcR-mediated tumor cytotoxicity may well facilitate the design of more effective therapeutic concepts.

Acknowledgments

We thank Tanya Mayadas for kindly providing the CD11b-deficient mice, Cora Damen for technical assistance, Theo Thepen and Gerard Groenewegen for critically reading the manuscript, and Toon Hesp, Herma Boere, Anja van der Sar, and Ingrid van den Brink for excellent animal care.

References

- Takai T, Li M, Sylvestre D, Clynes R, Ravetch JV. FcR gamma chain deletion results in pleiotropic effector cell defects. *Cell*. 1994;76:519-529.
- Heijnen IAFM, Rijks LJ, Schiel A, et al. Generation of HER-2/neu-specific cytotoxic neutrophils *in vivo*: efficient arming of neutrophils by combined administration of granulocyte colony-stimulating factor and Fc gamma receptor I bispecific antibodies. *J Immunol*. 1997;159:5629-5639.
- Gavin AL, Barnes N, Dijkstra-Hoem HM, Hogarth PM. Identification of the mouse IgG3 receptor: implications for antibody effector function at the interface between innate and adaptive immunity. *J Immunol*. 1998;160:20-23.
- Van de Winkel JGJ, Hogarth PM. The Immunoglobulin Receptors and Their Physiological and Pathological Roles in Immunity. Dordrecht, The Netherlands: Kluwer Academic Publishers; 1998.
- Houghton AN, Scheinberg DA. Monoclonal antibody therapies—a 'constant' threat to cancer. *Nat Med*. 2000;6:373-374.
- Clynes R, Takechi Y, Moroi Y, Houghton A, Ravetch JV. Fc receptors are required in passive and active immunity to melanoma. *Proc Natl Acad Sci U S A*. 1998;95:652-656.
- Clynes RA, Towers TL, Presta LG, Ravetch JV. Inhibitory Fc receptors modulate *in vivo* cytotoxicity against tumor targets. *Nat Med*. 2000;6:443-446.
- Honeychurch J, Tutt AL, Valerius T, Heijnen IAFM, Van de Winkel JGJ, Glennie MJ. Therapeutic efficacy of Fc gamma RI/CD64-directed bispecific antibodies in B-cell lymphoma. *Blood*. 2000;96:3544-3552.
- Houghton AN, Gold JS, Blachere NE. Immunity against cancer: lessons learned from melanoma. *Curr Opin Immunol*. 2001;13:134-140.
- Hara I, Nguyen H, Takechi Y, Gansbacher B, Chapman PB, Houghton AN. Rejection of mouse melanoma elicited by local secretion of interleukin-2: implicating macrophages without T cells or natural killer cells in tumor rejection. *Int J Cancer*. 1995;61:253-260.
- Hara I, Takechi Y, Houghton AN. Implicating a role for immune recognition of self in tumor rejection: passive immunization against the brown locus protein. *J Exp Med*. 1995;182:1609-1640.
- Takechi Y, Hara I, Naftzger C, Xu Y, Houghton AN. A melanosomal membrane protein is a cell surface target for melanoma therapy. *Clin Cancer Res*. 1996;2:1837-1842.
- Livingston PO, Wong GY, Adluri S, et al. Improved survival in stage III melanoma patients with GM2 antibodies: a randomized trial of adjuvant vaccination with GM2 ganglioside. *J Clin Oncol*. 1994;12:1036-1044.
- Amaout MA. Structure and function of the leukocyte adhesion molecules CD11/CD18. *Blood*. 1990;75:1037-1050.
- Pavalko FM, LaRoche SM. Activation of human neutrophils induces an interaction between the integrin beta 2-subunit (CD18) and the actin binding protein alpha-actinin. *J Immunol*. 1993;151:3795-3807.
- Clark EA, Brugge JS. Integrins and signal transduction pathways: the road taken. *Science*. 1995;268:233-239.
- Petty HR, Todd III RF. Receptor-receptor interactions of complement receptor type 3 in neutrophil membranes. *J Leukoc Biol*. 1993;54:492-494.
- Krauss JC, Poo H, Xue W, Mayo-Bond L, Todd III RF, Petty HR. Reconstitution of antibody-dependent phagocytosis in fibroblasts expressing Fc gamma receptor IIIB and the complement receptor type 3. *J Immunol*. 1994;153:1769-1777.
- Worth RG, Mayo-Bond L, Van de Winkel JGJ, Todd III RF, Petty HR. CR3 (alphaM beta2; CD11b/CD18) restores IgG-dependent phagocytosis in transfectants expressing a phagocytosis-defective Fc gammaRIIA (CD32) tail-minus mutant. *J Immunol*. 1996;157:5660-5665.
- Zhou MJ, Brown EJ. CR3 (Mac-1, alpha M beta 2, CD11b/CD18) and Fc gamma RIII cooperate in generation of a neutrophil respiratory burst: requirement for Fc gamma RIII and tyrosine phosphorylation. *J Cell Biol*. 1994;125:1407-1416.
- Anderson DC, Schmalstieg FC, Finegold MJ, et al. The severe and moderate phenotypes of heritable Mac-1, LFA-1 deficiency: their quantitative definition and relation to leukocyte dysfunction and clinical features. *J Infect Dis*. 1985;152:668-689.
- Kohl S, Loo LS, Schmalstieg FS, Anderson DC. The genetic deficiency of leukocyte surface glycoprotein Mac-1, LFA-1, p150,95 in humans is associated with defective antibody-dependent

- cellular cytotoxicity in vitro and defective protection against herpes simplex virus infection in vivo. *J Immunol.* 1986;137:1688-1694.
23. Capron M, Kazatchkine MD, Fischer E, et al. Functional role of the alpha-chain of complement receptor type 3 in human eosinophil-dependent antibody-mediated cytotoxicity against schistosomes. *J Immunol.* 1987;139:2059-2065.
 24. Majima T, Ohashi Y, Nagatomi R, Iizuka A, Konno T. Defective mononuclear cell antibody-dependent cellular cytotoxicity (ADCC) in patients with leukocyte adhesion deficiency emphasizing on different CD11/CD18 requirement of Fc gamma RI versus Fc gamma RII in ADCC. *Cell Immunol.* 1993;148:385-396.
 25. Van Egmond M, Van Vuuren AJ, Morton HC, et al. Human immunoglobulin A receptor (Fc alphaRI, CD89) function in transgenic mice requires both FcR gamma chain and CR3 (CD11b/CD18). *Blood.* 1999;93:4387-4394.
 26. Ottonello L, Epstein AL, Dapino P, Barbera P, Morone P, Dallegri F. Monoclonal Lym-1 antibody-dependent cytotoxicity by neutrophils exposed to granulocyte-macrophage colony-stimulating factor: intervention of Fc gamma RII (CD32), CD11b-CD18 integrins, and CD66b glycoproteins. *Blood.* 1999;93:3505-3511.
 27. Van Spriel AB, Leusen JHW, Van Egmond M, et al. Mac-1 (CD11b/CD18) is essential for Fc receptor-mediated neutrophil cytotoxicity and immunologic synapse formation. *Blood.* 2001;97:2478-2486.
 28. Tanaka H, Satake-Ishikawa R, Ishikawa M, Matsuki S, Asano K. Pharmacokinetics of recombinant human granulocyte colony-stimulating factor conjugated to polyethylene glycol in rats. *Cancer Res.* 1991;51:3710-3714.
 29. Van Spriel AB, Van den Herik-Oudijk IE, Van de Winkel JGJ. A single injection of polyethylene-glycol granulocyte colony-stimulating factor strongly prolongs survival of mice with systemic candidiasis. *Cytokine.* 2000;12:666-670.
 30. Valerius T, Repp R, De Wit TP, et al. Involvement of the high-affinity receptor for IgG (Fc gamma RI; CD64) in enhanced tumor cell cytotoxicity of neutrophils during granulocyte colony-stimulating factor therapy. *Blood.* 1993;82:931-939.
 31. Coxon A, Rieu P, Barkalow FJ, et al. A novel role for the beta 2 integrin CD11b/CD18 in neutrophil apoptosis: a homeostatic mechanism in inflammation. *Immunity.* 1996;5:653-666.
 32. Zhou M, Todd III RF, Van de Winkel JGJ, Petty HR. Cocapping of the leuko adhesion molecules complement receptor type 3 and lymphocyte function-associated antigen-1 with Fc gamma receptor III on human neutrophils: possible role of lectin-like interactions. *J Immunol.* 1993;150:3030-3041.
 33. Petty HR, Worth RG, Todd III RF. Interactions of integrins with their partner proteins in leukocyte membranes. *Immunol Res.* 2002;25:75-95.
 34. Todd III RF, Petty HR. Beta 2 (CD11/CD18) integrins can serve as signaling partners for other leukocyte receptors. *J Lab Clin Med.* 1997;129:492-498.
 35. Sampath R, Gallagher PJ, Pavalko FM. Cytoskeletal interactions with the leukocyte integrin beta2 cytoplasmic tail. *J Biol Chem.* 1998;273:33588-33594.
 36. Berton G, Lowell CA. Integrin signaling in neutrophils and macrophages. *Cell Signal.* 1999;11:621-635.
 37. Mocsai A, Zhou M, Meng F, Tybulewicz VL, Lowell CA. Syk is required for integrin signaling in neutrophils. *Immunity.* 2002;16:547-558.
 38. Yan J, Velvicka V, Xia Y, et al. Beta-glucan, a "specific" biologic response modifier that uses antibodies to target tumors for cytotoxic recognition by leukocyte complement receptor type 3 (CD11b/CD18). *J Immunol.* 1999;163:3045-3052.
 39. Renard N, Lienard D, Lespagnard L, Eggemont A, Heimann R, Lejeune F. Early endothelium activation and polymorphonuclear cell invasion precede specific necrosis of human melanoma and sarcoma treated by intravascular high-dose tumour necrosis factor alpha (rTNF alpha). *Int J Cancer.* 1994;57:656-663.
 40. Detmers PA, Wright SD, Olsen E, Kimball B, Cohn ZA. Aggregation of complement receptors on human neutrophils in the absence of ligand. *J Cell Biol.* 1987;105:1137-1145.
 41. Bock SN, Cameron RB, Kragel P, Mule JJ, Rosenberg SA. Biological and antitumor effects of recombinant human macrophage colony-stimulating factor in mice. *Cancer Res.* 1991;51:2649-2654.
 42. Colombo MP, Ferrari G, Stoppacciaro A, et al. Granulocyte colony-stimulating factor gene transfer suppresses tumorigenicity of a murine adenocarcinoma in vivo. *J Exp Med.* 1991;173:889-897.
 43. Colombo MP, Lombardi L, Stoppacciaro A, et al. Granulocyte colony-stimulating factor (G-CSF) gene transduction in murine adenocarcinoma drives neutrophil-mediated tumor inhibition in vivo: neutrophils discriminate between G-CSF-producing and G-CSF-nonproducing tumor cells. *J Immunol.* 1992;149:113-119.
 44. Schmidt KG, Rasmussen JW, Wedebye IM, Frederiksen PB, Pedersen NT. Accumulation of indium-111-labeled granulocytes in malignant tumors. *J Nucl Med.* 1988;29:479-484.
 45. Colombo MP, Forni G. Cytokine gene transfer in tumor inhibition and tumor therapy: where are we now? *Immunol Today.* 1994;15:48-51.
 46. Zatloukal K, Schneeberger A, Berger M, et al. Elicitation of a systemic and protective anti-melanoma immune response by an IL-2-based vaccine: assessment of critical cellular and molecular parameters. *J Immunol.* 1995;154:3406-3419.
 47. Shinohara H, Yano S, Bucana CD, Fidler IJ. Induction of chemokine secretion and enhancement of contact-dependent macrophage cytotoxicity by engineered expression of granulocyte-macrophage colony-stimulating factor in human colon cancer cells. *J Immunol.* 2000;164:2728-2737.
 48. Cavallo F, Giovarelli M, Gulino A, et al. Role of neutrophils and CD4+ T lymphocytes in the primary and memory response to nonimmunogenic murine mammary adenocarcinoma made immunogenic by IL-2 gene. *J Immunol.* 1992;149:3627-3635.
 49. Noffz G, Qin Z, Kopf M, Blankenstein T. Neutrophils but not eosinophils are involved in growth suppression of IL-4-secreting tumors. *J Immunol.* 1998;160:345-350.
 50. Di Carlo E, Forni G, Lollini P, Colombo MP, Modesti A, Musiani P. The intriguing role of polymorphonuclear neutrophils in antitumor reactions. *Blood.* 2001;97:339-345.
 51. Musiani P, Modesti A, Giovarelli M, et al. Cytokines, tumour-cell death and immunogenicity: a question of choice. *Immunol Today.* 1997;18:32-36.
 52. Weiner LM. Monoclonal antibody therapy of cancer. *Semin Oncol.* 1999;26:43-51.
 53. Snider DP, Segal DM. Targeted antigen presentation using crosslinked antibody heteroaggregates. *J Immunol.* 1987;139:1609-1616.
 54. Gosselin EJ, Wardwell K, Gosselin DR, Alter N, Fisher JL, Guyre PM. Enhanced antigen presentation using human Fc gamma receptor (monocyte/macrophage)-specific immunogens. *J Immunol.* 1992;149:3477-3481.

The High-Affinity IgG Receptor, FcγRI, Plays a Central Role in Antibody Therapy of Experimental Melanoma

Lisette Bevaart,¹ Marco J.H. Jansen,¹ Martine J. van Vugt,² J. Sjef Verbeek,³ Jan G.J. van de Winkel,^{1,2} and Jeanette H.W. Leusen¹

¹Immunotherapy Laboratory, Department of Immunology, University Medical Center Utrecht; ²Genmab, Utrecht, the Netherlands; and

³Center for Human and Clinical Genetics, Leiden University Medical Center, Leiden, the Netherlands

Abstract

We examined the role of FcγR in antibody therapy of metastatic melanoma in wild-type and different FcγR knock-out mice. Treatment of B16F10-challenged wild-type mice with TA99 antibody specific for the gp75 tumor antigen resulted in a marked decrease in numbers of lung metastases. Treatment of individual FcγR knock-out mice revealed the high-affinity IgG receptor, FcγRI (CD64), to represent the central FcγR for TA99-induced antitumor effects. The potential of immune-modulating agents to further enhance the protective effect induced by monoclonal antibody (mAb) TA99 was examined in combination treatments consisting of mAb TA99 and a TLR-4 agonist, monophosphoryl lipid A (MPL). MPL did potently boost TA99 antibody-induced effects, and combination therapy was, again, found to be dependent on the presence of FcγRI. (Cancer Res 2006; 66(3): 1261-4)

Introduction

Antibodies represent promising therapeutic candidates due to their high specificity and low toxicity profiles. The exact variables and mechanisms contributing to the therapeutic potential of anticancer antibodies remain unclear. Antibodies can initiate various effects, including antibody-dependent cell-mediated cytotoxicity (ADCC), complement dependent cytotoxicity, and induction of apoptosis (1). A better understanding of the working mechanisms of therapeutic antibodies is essential to further enhance the efficacy of antibody therapy. In this study, we address the role of IgG receptors (FcγR) in antibody-induced antitumor activity. Four classes of murine leukocyte FcγR are currently distinguished [FcγRI (CD64), FcγRII (CD32), FcγRIII (CD16), and the recently described FcγRIV], which differ in cell distribution and function. FcγRI, FcγRIII, and FcγRIV are activatory receptors, whereas FcγRII can mediate inhibitory effects (2, 3). The B16F10 lung metastasis model represents a validated model to study antibody therapy using TA99, a mouse IgG2a antibody recognizing the gp75 tumor antigen (4). Treatment of wild-type mice with TA99 after tumor challenge has been shown to markedly reduce numbers of lung metastases (5). A role for FcγR in TA99 antibody-mediated effects has been documented with the use of FcR γ-chain knock-out mice, which lack all activatory leukocyte FcγR (6, 7). The relative contribution of individual FcγR classes, however, has not been previously assessed. Antibody therapy is often combined with other

treatment regimens, such as anti-angiogenic or cytostatic drugs, to further enhance therapeutic efficacy. Agonists of Toll-like receptors (TLR) can effectively boost antibody-induced effects (8). Monophosphoryl lipid A (MPL), a TLR-4 agonist, is a chemically modified lipopolysaccharide (LPS) derived from *Salmonella minnesota* (9). As adjuvant effects of MPL *in vivo* have been documented (10, 11), we tested the influence of MPL on the outcome of treatment when administered in combination with TA99 antibody. In this report, we observed FcγRI to be essential for TA99 antibody-induced antitumor effects in C57Bl/6 mice. MPL further enhanced TA99-mediated antitumor effects.

Materials and Methods

Mice. C57Bl/6 wild-type mice were obtained from Janvier (Le Genest Saint Isle, France). FcγRI (CD64) knock-out mice (12), FcγRIII (CD16) knock-out mice (13), and FcR γ-chain knock-out mice (7), all in the C57Bl/6 background, were bred and maintained in the Central Animal Laboratory, Utrecht University. Experiments were done with 7- to 12-week-old mice and were all approved by the Utrecht University animal ethics committee.

Cell lines and TA99 antibody. The B16F10 mouse melanoma cell line was obtained from the National Cancer Institute (Frederick, MD). Cells were cultured in RPMI 1640 (Life Technologies, Paisley, United Kingdom) supplemented with 10% fetal bovine serum (Integro, Dieren, the Netherlands), 50 units/mL penicillin (Life Technologies), and 50 μg/mL streptomycin (Life Technologies). Hybridoma HB-8704 (American Type Culture Collection, Manassas, VA), which produces TA99 antibody, was cultured under serum-free conditions with HyQ ADCF-monoclonal antibody (mAb) medium (Hyclone, Logan, UT). Monoclonal antibody TA99 (mouse IgG2a), directed against the gp75 antigen present on B16F10 melanoma cells, was purified from hybridoma supernatants by protein A-Sepharose chromatography.

MPL. MPL, a derivative of lipid A from *Salmonella minnesota*, was obtained from Corixa (Seattle, WA).

Melanoma model. Wild-type mice, FcR γ-chain knock-out, FcγRI knock-out, or FcγRIII knock-out mice, were injected i.v. with 1.5×10^5 B16F10 tumor cells (in 100 μL saline) on day 0. For treatments with an antibody dosage of 200 μg (6), mice were injected i.p. with TA99 antibody (or PBS as control) on days 0, 2, 4, 7, 9, and 11. For combination treatments with suboptimal antibody and MPL concentrations, mice were injected with MPL (0.5 μg in 100 μL PBS) or 100 μL PBS s.c. on days -1, 4, and 8. A suboptimal dose of TA99 antibody (10 μg in 100 μL PBS) or 100 μL PBS (as control) were injected i.p. at days 0, 2, 4, 7, 9, and 11. At day 21, mice were sacrificed, and lungs were scored for numbers of metastases and tumor load. Tumor load was defined as the sum of the following scores: metastases <1 mm were scored as 1; metastases between 1 and 2 mm were scored as 3; and metastases >2 mm were scored as 10, as detailed in ref. (14).

Statistical analyses. ANOVA analyses were done using SPSS software (Chicago, IL). All experiments were done a minimum of two times. *Ps* < 0.05 were considered significant.

Results and Discussion

To dissect the role of individual FcγR in antibody therapy of melanoma, we injected wild-type and FcγR knock-out mice i.v.

Note: J.G.J. van de Winkel and J.H.W. Leusen contributed equally to this work.

Requests for reprints: Jan G.J. van de Winkel, Immunotherapy Laboratory, Department of Immunology, University Medical Center Utrecht, Lundlaan 6, KC.02.085.2, 3584 EA Utrecht, the Netherlands. Phone: 31-30-212-3100; Fax: 31-30-212-111; E-mail: j.vandewinkel@azu.nl.

©2006 American Association for Cancer Research.
doi:10.1158/0008-5472.CAN-05-2856

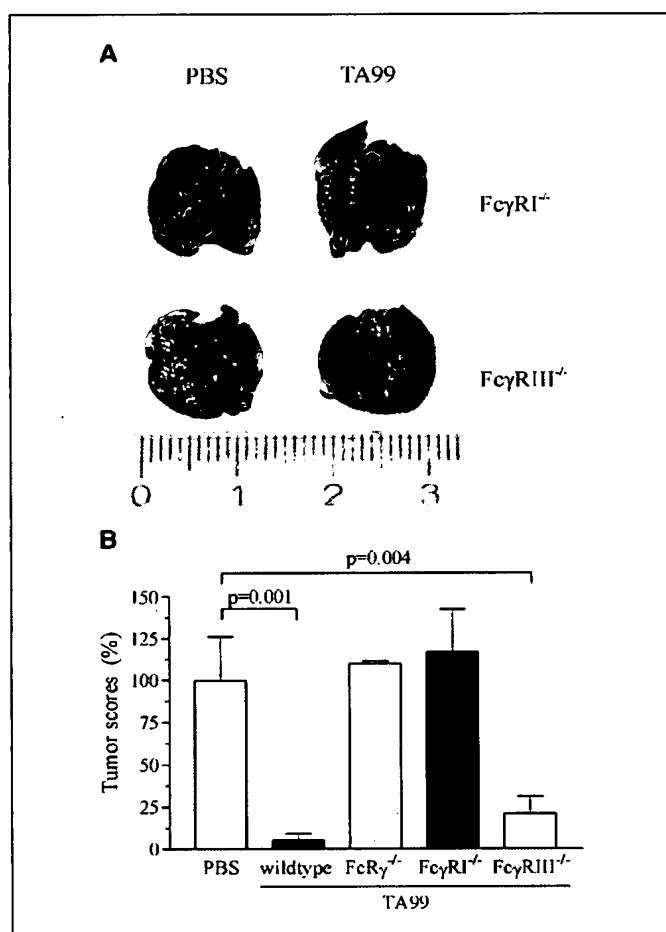


Figure 1. FcγRI is essential for antitumor effects induced by TA99 antibody. Wild-type, FcR γ-chain^{-/-}, FcγRI^{-/-}, or FcγRIII^{-/-} mice were challenged i.v. with 1.5×10^5 B16F10 tumor cells and injected i.p. with 200 μg mAb TA99 or PBS (control) on days 0, 2, 4, 7, 9, and 11. After 21 days, mice were sacrificed, lungs were excised, and tumor loads were scored as detailed in Materials and Methods. A, lungs of FcγRI^{-/-} and FcγRIII^{-/-} mice treated with PBS or mAb TA99; black nodules represent metastases. B, tumor load scores in wild-type, FcR γ-chain^{-/-}, FcγRI^{-/-}, and FcγRIII^{-/-} mice. Tumor loads in PBS-treated mice were set at 100%. Columns, average; bars, SE. Representative for two experiments, each with six mice per group.

with B16F10 tumor cells and studied the effect of antibody treatment. The TA99 antibody, specific for the gp75 tumor antigen, induced a profound protective effect in wild-type mice, which was abrogated in FcR γ-chain^{-/-} mice (Fig. 1). These results confirmed an earlier report, exemplifying the importance of activating FcγR in antibody-mediated antitumor effects (6). We then did experiments in FcγRI and FcγRIII knockout mice. FcγRI represents the sole FcγR class capable of binding monomeric IgG with high affinity (2) and can potentially initiate various immune cell functions, including antibody dependent cell-mediated cytotoxicity; antigen uptake; and induction of antigen presentation (12). FcγRI^{-/-} mice exhibit various defects, such as an impaired phagocytosis of IgG2a-immune complexes, impaired ADCC, and antigen presentation (12). FcγRIII plays a role in anaphylactic and inflammatory responses (13). Antibody TA99 induced a profound antitumor effect in FcγRIII knockout mice (Fig. 1). Expression of FcγRI proved essential for mAb

TA99-mediated effects, as antibody treatment in FcγRI^{-/-} mice induced no therapeutic effect (Fig. 1). These data indicated FcγRI to be instrumental for the TA99-induced effects.

Choice of antibody isotype can influence binding to Fcγ receptors. Mouse IgG2a antibodies can bind FcγRI and FcγRIII, albeit with far higher affinity to FcγRI (12). However, in the case of the absence of FcγRI, the TA99 antibody should still be able to bind to FcγRIII, thus not explaining the dramatic effect on antitumor response in FcγRI^{-/-} mice. If an antibody of another subclass would be employed (e.g., IgG1), different results might be expected, although this antibody would still be able to bind to FcγRI. Very recently, a new class of murine FcγR, FcγRIV, has been characterized as an IgG2a and IgG2b receptor (3). Because the effect of TA99 antibody was observed to be absent in FcγRI^{-/-} mice, FcγRIV may play only a minor role, if any, in TA99 antibody-induced effects.

We next evaluated the influence of MPL on TA99-induced antitumor effects. MPL is a TLR-4 agonist, which has similar adjuvant properties as LPS, without inducing toxicity (9). With suboptimal amounts of TA99 or MPL used as monotherapies, mice developed metastases (Fig. 2). Combination of TA99

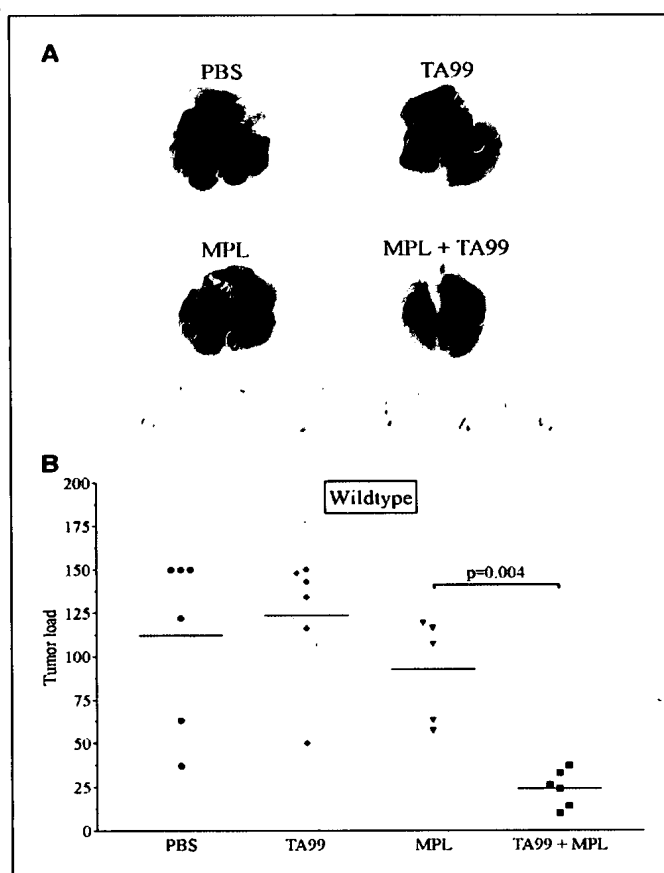


Figure 2. Effect of MPL on therapeutic efficacy of TA99 antibody. Wild-type mice were challenged i.v. with tumor cells and treated with PBS, a suboptimal dose of mAb TA99 (10 μg), a suboptimal dose of MPL (0.5 μg), or with TA99 plus MPL. After 21 days, mice were sacrificed, lungs were excised, and tumor loads scored as detailed in Materials and Methods. A, lungs of wild-type mice; black nodules represent metastases. B, tumor loads scored in wild-type mice. Representative for two experiments, each with six mice per group.

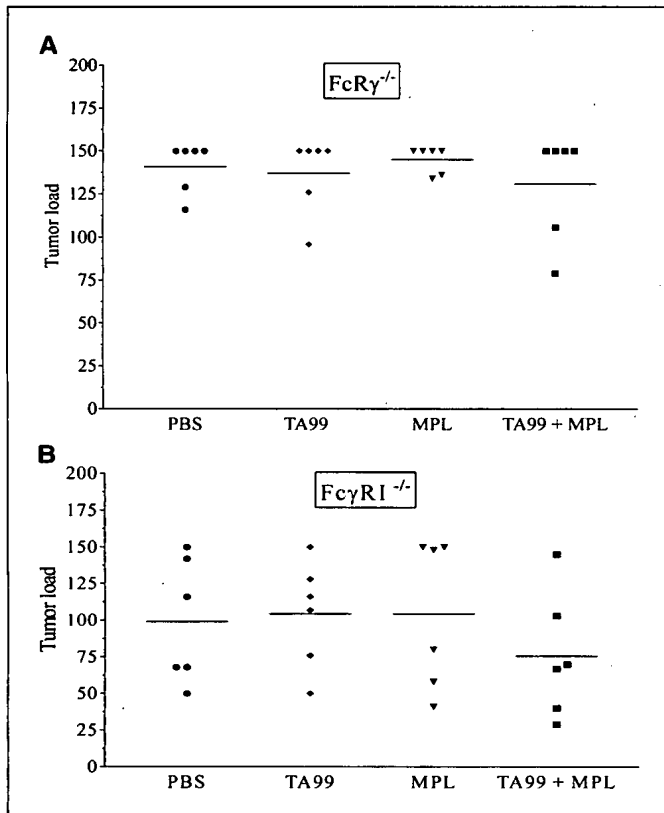


Figure 3. FcγRI is essential for combination therapy. FcγRI^{-/-} (A) or FcγRI^{-/-} mice (B) were challenged i.v. with tumor cells and treated with PBS, a suboptimal dose of mAb TA99 (10 μg), a suboptimal dose of MPL (0.5 μg), or with TA99 combined with MPL. After 21 days, mice were sacrificed, lungs were excised, and tumor loads scored. Representative for two experiments, each with six mice per group.

antibody and MPL, however, consistently led to lower numbers of metastases (Fig. 2). The FcγR dependency of TA99 effects in the presence of MPL was analyzed in FcγRI^{-/-} mice. These animals were challenged with tumor cells and injected with antibody or MPL alone or in combination. The protective effect of the combination was abrogated in FcγRI^{-/-} mice (Fig. 3A). We evaluated the contribution of FcγRI by challenging FcγRI^{-/-} mice with B16F10 tumor cells followed

by treatment with antibody, MPL, or antibody plus MPL. FcγRI was, again, found essential for induction of a therapeutic effect with the combination therapy (Fig. 3B).

MPL is known to activate macrophages and dendritic cells, and adjuvant studies *in vivo* documented MPL to induce antigen-specific CTL and to skew T-helper balance toward a Th1 phenotype (11, 15). MPL improve the capacity of B cells and macrophages to prime T and B cells and induce the maturation of splenic dendritic cells *in situ*. Furthermore, MPL triggers cytokine production, which can have an effect on the development of both humoral and cellular immune responses (16), indicating MPL to be a suitable candidate adjuvant for antibody therapy.

The effector cells, which can be involved in antibody-mediated antitumor effects, are natural killer (NK) cells, polymorphonuclear (PMN), monocytes, and macrophages. Earlier studies examining effector cells in the B16 model during antibody treatment excluded a role for NK cells, B and T cells (17). In these studies, microscopic analyses of lung tissues documented abundant infiltration of macrophages (5), supporting a role for macrophages during antibody therapy. Murine FcγRI is expressed on monocytes, macrophages, and dendritic cells but not on PMN (12). As we observed FcγRI to be central for antibody-mediated antitumor effects, we hypothesize FcγRI-expressing monocytes/macrophages to be of importance for the TA99-induced antitumor effects and not NK cells or PMN. We are currently performing studies (e.g., monocytes/macrophage depletion with use of clodronate liposomes) to further address the role of the effector cells involved in this model.

The importance of human Fcγ receptors for tumor therapy has been documented, where FcγR polymorphisms were shown to affect the outcome of antibody treatments in cancer patients (18–20). A better understanding of the role of individual FcγR in antibody therapies is important to further optimize antibody therapeutic approaches in man.

Acknowledgments

Received 8/11/2005; revised 10/18/2005; accepted 12/21/2005.

Grant support: Dutch Cancer Society "K.W.F." grant UU 2001-2496.

The costs of publication of this article were defrayed in part by the payment of page charges. This article must therefore be hereby marked *advertisement* in accordance with 18 U.S.C. Section 1734 solely to indicate this fact.

We thank Anja van der Sar, Toon Hesp, Wendy Kaspers, Sabine Versteeg, Agnes Goderie, and Gerard Geelen for excellent animal care; Esther Rudolph and Patrick Luijk for help with digital photography; and Soeniel Jhakrie, Edwin van Voskuilen, Marcel Brandhorst, and Judy Bos-de Ruijter for culturing and purification of TA99 antibody.

References

- Harris M. Monoclonal antibodies as therapeutic agents for cancer. *Lancet Oncol* 2004;5:292–302.
- Ravetch JV, Bolland S. IgG Fc receptors. *Annu Rev Immunol* 2001;19:275–90.
- Nimmerjahn F, Bruhns P, Horiuchi K, Ravetch JV. FcγRIIIb: a novel FcγR with distinct IgG subclass specificity. *Immunity* 2005;23:41–51.
- Thomson TM, Real FX, Murakami S, Cordon-Cardo C, Old LJ, Houghton AN. Differentiation antigens of melanocytes and melanoma: analysis of melanosome and cell surface markers of human pigmented cells with monoclonal antibodies. *J Invest Dermatol* 1988;90:459–66.
- Hara I, Takechi Y, Houghton AN. Implicating a role for immune recognition of self in tumor rejection: passive immunization against the brown locus protein. *J Exp Med* 1995;182:1609–14.
- Clynes R, Takechi Y, Moroi Y, Houghton A, Ravetch JV. Fc receptors are required in passive and active immunity to melanoma. *Proc Natl Acad Sci U S A* 1998;95:652–6.
- Takai T, Li M, Sylvestre D, Clynes R, Ravetch JV. FcγRIII chain deletion results in pleiotropic effector cell defects. *Cell* 1994;76:519–29.
- Ulevitch RJ. Therapeutics targeting the innate immune system. *Nat Rev Immunol* 2004;4:512–20.
- Ulrich JT, Myers KR. Monophosphoryl lipid A as an adjuvant. Past experiences and new directions. *Pharm Biotechnol* 1995;6:495–524.
- Drachenberg KJ, Wheeler AW, Stuebner P, Horak F. A well-tolerated grass pollen-specific allergy vaccine containing a novel adjuvant, monophosphoryl lipid A, reduces allergic symptoms after only four preseasonal injections. *Allergy* 2001;56:498–505.
- Wijburg OL, van den Dobbelsteen GP, Vadolos J, Sanders A, Strugnell RA, van Rooijen N. The role of macrophages in the induction and regulation of immunity elicited by exogenous antigens. *Eur J Immunol* 1998;28:479–87.
- Ioan-Facsinay A, de Kimpe SJ, Hellwig SM, et al. FcγRI (CD64) contributes substantially to severity of arthritis, hypersensitivity responses, and protection from bacterial infection. *Immunity* 2002;16:391–402.
- Hazenbos WL, Gessner JE, Hofhuis FM, et al. Impaired IgG-dependent anaphylaxis and Arthus

- p>reaction in FcγRIII (CD16) deficient mice.
- Immunity*
- 1996;5:181–8.
14. van Spriel AB, van Ojik HH, Bakker A, Jansen MJ, van de Winkel JG. Mac-1 (CD11b/CD18) is crucial for effective Fc receptor-mediated immunity to melanoma. *Blood* 2003;101:253–8.
 15. De Becker G, Moulin V, Pajak B, et al. The adjuvant monophosphoryl lipid A increases the function of antigen-presenting cells. *Int Immunol* 2000;12:807–15.
 16. Evans JT, Cluff CW, Johnson DA, Lacy MJ, Persing DH, Baldrige JR. Enhancement of antigen-specific immunity via the TLR4 ligands MPL adjuvant and Ribi.529. *Expert Rev Vaccines* 2003;2:219–29.
 17. Takechi Y, Hara I, Naftzger C, Xu Y, Houghton AN. A melanosomal membrane protein is a cell surface target for melanoma therapy. *Clin Cancer Res* 1996;2:1837–42.
 18. Cartron G, Dacheux L, Salles G, et al. Therapeutic activity of humanized anti-CD20 monoclonal antibody and polymorphism in IgG Fc receptor FcγRIIIa gene. *Blood* 2002;99:754–8.
 19. Weng WK, Levy R. Two immunoglobulin G fragment C receptor polymorphisms independently predict response to rituximab in patients with follicular lymphoma. *J Clin Oncol* 2003;21:3940–7.
 20. Weng WK, Czerwinski D, Timmerman J, Hsu FJ, Levy R. Clinical outcome of lymphoma patients after idiotype vaccination is correlated with humoral immune response and immunoglobulin G Fc receptor genotype. *J Clin Oncol* 2004;22:4665–72.

Exchanging human Fc γ 1 with murine Fc γ 2a highly potentiates anti-tumor activity of anti-EpCAM antibody adecatumumab in a syngeneic mouse lung metastasis model

Petra Lutterbuese · Klaus Brischwein · Robert Hofmeister · Sandrine Crommer · Grit Lorenczewski · Laetitia Petersen · Sandra Lippold · Antonio da Silva · Mathias Locher · Patrick A. Baeuerle · Bernd Schlereth

Received: 22 March 2006 / Accepted: 25 July 2006 / Published online: 26 August 2006
© Springer-Verlag 2006

Abstract An important mode of action shared by human IgG1 antibody therapies is antibody-dependent cellular cytotoxicity (ADCC). ADCC relies on the interaction of the antibody's Fc portion with Fc-gamma receptors (Fc γ R) on immune effector cells. The anti-tumor activity of human IgG1 antibodies is frequently assessed in mouse models. Binding of human IgG1 to murine Fc γ Rs is however of reduced affinity. We here show that ADCC of adecatumumab (MT201), a fully human IgG1 antibody specific for epithelial cell adhesion molecule (EpCAM/CD326), is drastically lower if human peripheral blood mononuclear cells are replaced by murine splenocytes as effector cells. When the variable domains of adecatumumab were genetically fused to a murine IgG2a backbone (yielding mu-adecatumumab), ADCC with murine effector cells was much improved, but at the same time significantly reduced with human effector cells. The serum half-lives of adecatumumab and mu-adecatumumab were determined in mice and dosing schedules established that gave similar serum trough levels during a 4-week antibody treatment. The anti-tumor activities of adecatumumab and mu-adecatumumab were then compared side-by-side in a lung metastasis mouse model established with a syngeneic B16 melanoma line expressing human EpCAM at physiologically relevant levels. Treatment of mice with mu-adecatumumab led to an almost complete prevention of lung metastases,

while the human version of the antibody was much less active. This shows that adecatumumab has high anti-tumor activity when tested in a form that is better compatible with the species' immune system. Moreover, our data suggest to routinely compare in mouse models human IgG1 and murine IgG2a versions of antibodies to properly assess the contribution of ADCC to overall anti-tumor activity.

Keywords Adecatumumab · Monoclonal antibody · Fc domain · EpCAM · ADCC · Syngeneic mouse model

Introduction

During the past decade, chimeric, humanized and human monoclonal antibodies of the IgG1 isotype have been successfully added to the arsenal of anti-cancer therapies. There are currently four registered IgG1 therapies that recognize surface targets on tumor cells and may share antibody-dependent cellular cytotoxicity (ADCC) as a common mode of action. These are anti-CD20 rituximab (Rituxan[®]/MabThera[®]) for treatment of non-Hodgkin lymphoma, anti-HER-2 trastuzumab (Herceptin[®]) for treatment of metastatic breast cancer, anti-EGFR cetuximab (Erbix[®]) for treatment of metastatic colorectal cancer, and anti-CD52 alemtuzumab (Campath[®]) for treatment of refractory chronic lymphatic leukemia. Other registered antibodies in cancer therapy work by different mechanisms, e.g., neutralization of pro-angiogenic VEGF (Avastin[®]), delivery of toxin (Mylotarg[®]) or of radioisotopes (Bexxar[®], Zevalin[®]). While ADCC was demonstrated for trastuzumab [16, 13], rituximab [9]

P. Lutterbuese · K. Brischwein · R. Hofmeister · S. Crommer · G. Lorenczewski · L. Petersen · S. Lippold · A. da Silva · M. Locher · P. A. Baeuerle (✉) · B. Schlereth
Micromet AG, Staffelseestr. 2, 81477 Munich, Germany
e-mail: Patrick.baeuerle@micromet.de

and alemtuzumab [6] and is there considered to be a prime mode of action [10], very little is known about ADCC by cetuximab. Several other IgG1 antibodies, which have been shown to predominantly work by ADCC, are in different stages of clinical development. Examples are the anti-CEA IgG1 labetuzumab [1], anti-carboanhydrase IX IgG1 Rencarex® [17] and anti-EpCAM IgG1 adecatumumab [11, 13].

Antibody-dependent cellular cytotoxicity is mediated by a bifunctional binding activity of IgG1. Via its Fc domain, the antibody transiently tethers Fc-gamma receptor (FcγR)-positive cytotoxic immune cells to antibody-decorated tumor cells. This leads to (i) formation of a cytolytic synapse between cells, (ii) a targeted delivery of cytotoxic proteins, such as perforin and granzymes, by the immune cell and (iii) ultimately induction of apoptosis in tumor cells. Important immune cells participating in ADCC are natural killer (NK) cells bearing the low-affinity Fcγ receptor FcγRIIa (CD16) in humans, and its corresponding receptor FcγRIII in the mouse. The affinities of these receptors are $< 1 \times 10^7/\text{M}$ for murine FcγRIII to mouse IgG2a and about $2 \times 10^7/\text{M}$ for human FcγRIIIA to human IgG1 [18]. The importance of NK cells for ADCC is genetically supported by a correlation of reduced efficacy of rituximab with a polymorphism in CD16 that reduces the receptor's affinity for antibody ligand [2, 4]. A similar correlation was identified for a polymorphism of CD32 [19], suggesting that CD32-positive immune cells also contribute to ADCC although NK cells are major contributors to ADCC when blood cell subpopulations are analyzed [14]. The observation that all IgG1 therapies require high serum trough levels for several months to achieve anti-tumor responses supports that a sustained activation of immune cells is required involving a low-affinity recognition element. In vivo, recruitment of CD16-positive cells by antibody-coated tumor cells is further impeded by high serum concentrations of other IgG1 antibodies that compete for binding [11, 14].

In non-clinical development, the efficacy of novel human IgG1 therapies is frequently assessed in xenotransplant models employing immunodeficient nude mice. Due to the absence of T cells in these mice, many human tumor cell lines are accepted and grow out into measurable tumors. Because nude mice still have NK cells, they are considered to also mediate ADCC by human antibodies. Immunocompetent mouse models employ syngeneic tumor cell lines transfected with the human target antigen. In these models, tumor cells are intravenously injected, get then trapped in lung capillaries and subsequently grow to macroscopically visible lung tumor colonies. A drawback of conventional

mouse models could be that the Fcγ1 domain of human IgG1 antibodies binds with much reduced affinity to mouse FcγRs than, for instance, its murine equivalent Fcγ2a. In this case, which requires further analysis, ADCC reactions of human antibodies with murine immune cells are expected to be suboptimal.

Adecatumumab is a fully human IgG1 antibody against EpCAM, which has been shown to act by ADCC and CDC [11]. If the efficacy of a human IgG1 antibody solely relies on ADCC, its anti-tumor activity would be underestimated in conventional mouse models. To test this hypothesis we generated a murine version of adecatumumab by grafting the variable heavy (vH) domain of adecatumumab on a mouse IgG2a domain and fusing the variable light (vL) domain with a mouse cκ region. Both antibodies were compared side-by-side with respect to ADCC using human and mouse effector cells. Further, we explored the anti-tumor activity of both antibodies in a lung metastasis model using immunocompetent C57BL/6 mice.

Materials and methods

Cell lines

Chinese hamster ovary (CHO) dhfr negative cells were obtained from the German Collection of Microorganisms and Cell Cultures (DSMZ, Braunschweig, Germany) and the KATO III human gastric carcinoma cell line from the European Collection of Cell Cultures (ECACC, Salisbury, UK). CHO dhfr negative cells were grown at 37°C in roller bottles with HyClone culture media (HyClone, Logan, UT, USA) for 7 days before harvest. KATO III cells were cultured in RPMI 1640 media (Invitrogen, Karlsruhe, Germany), supplemented with 10% fetal bovine serum (Invitrogen, Karlsruhe, Germany), at 37°C, in a 5% CO₂ incubator.

The cell line B16F10/EpCAM (clone 3E3), which is stably expressing human EpCAM, was generated at Micromet AG, Munich, Germany. In brief, the parental cell line B16F10 was transfected with the expression vector pEF-ADA-EpCAM and selected with increasing amounts of adenosine/alanosine/uridine and desoxicoformycin. A highly EpCAM-positive clone (3E3) was picked by limiting dilution analysis.

Construction of mu-adecatumumab

Generation and production of human adecatumumab has been described elsewhere [15]. For the generation of the murine version of adecatumumab, the constant regions were cloned by reverse transcription-PCR

from RNA isolated from OKT3 hybridoma cells expressing a mouse IgG2a antibody directed against human CD3e. For the amplification of the cH1–cH3 domains a primer (S IgG2aCH1 + HD69 OH) hybridizing to the 5' end of mouse IgG2a was designed. This primer harbored a stretch of 20 nucleotides complementary to the 3' end of the HD69 vH. The second primer (AS IgG2a *Xba*I) bound to the 3' end of mouse IgG2a sequence including a stop codon and a *Xba*I restriction endonuclease (RE) site. For the amplification of the mouse cκ sequence a primer (S IgGκ + HD69vκ) was used, which bound to the 5' end of the mouse cκ sequence and harbored a 20-nucleotide overhang hybridizing to the adecatumumab vL 3' region. The anti-sense primer (AS mIgG cκ *Xho*I) hybridized to the 3' end of mouse cκ encoding a stop codon and a *Xho*I RE site. The vH of adecatumumab was amplified from the expression vector pEF-DHFR HC HD69 using the primer S IgG leader hybridizing to the 5' IgG signal peptide and harboring an *Eco*RI RE site and the primer AS HD69vH + IgG2aOH binding to the 3' end of vH HD69 and a having a 20-nucleotide sequence overhang complementary to the 5' mouse IgG2a cH1 sequence. The adecatumumab vL was accordingly amplified with the primers S IgG leader and AS HD69 vL + cκ hybridizing to the 3' end of HD69 vL and containing on overhang binding to the 5' end of mouse cκ. Finally, heavy and light chain sequences were generated by assembling the corresponding PCR fragments by means of overlapping PCR. For the heavy and light chain, the primer combinations S IgG leader/AS IgG2a *Xba*I and S IgG leader/AS IgG cκ *Xho*I were used, respectively. The complete sequence of the mu-adeccatumumab HC was then subcloned into the vector pPCR-Script-Cam, the mu-adeccatumumab LC sequence was subcloned into pPCR-Script-Amp. The correct sequence was verified by automated DNA sequencing. Finally, the HD69 chimeric heavy chain was cloned into the expression vector pEF-DHFR, which was digested with *Eco*RI and *Xba*I. The light chain digested with *Eco*RI and *Xho*I was inserted into pEF-ADA, which was cut with *Eco*RI/*Sal*I. Mu-adeccatumumab was produced in CHO dhfr-cells transfected with the expression vectors pEF-DHFR-HD69 HC and pEF-ADA-HD69 LC and mu-adeccatumumab purified from cell culture supernatants in a one step process using a Protein G column and Äkta FPLC System (Amersham Biosciences, Little Chalfont, UK).

The human IgG1 kappa control antibody (I-5154) was obtained from Sigma-Aldrich (Taufkirchen, Germany) and served as isotype control for adeccatumumab. The murine IgG2a antibody Orthoclone

OKT3 (Janssen-Cilag, Neuss, Germany) served as an isotype control for mu-adeccatumumab.

Binding comparison of adeccatumumab and mu-adeccatumumab

Kinetic binding experiments with adeccatumumab and mu-adeccatumumab were performed using surface plasmon resonance on the BIAcore™ 2000 (BIAcore AB, Uppsala, Sweden) with a flow rate of 5 µl/min and HBS-EP (0.01 M HEPES, pH 7.4, 0.15 M NaCl, 3 mM EDTA, 0.005% surfactant P20) as running buffer, at 25°C. The extracellular domain of the EpCAM antigen (residues 17–265) was immobilized on a CM5 sensor chip with different densities for each flow cell.

Binding kinetics of the antibodies were measured by injecting 10 µl of protein solution at concentrations ranging from 2 to 0.07 µM and monitoring the dissociation for 100 s. The data were fitted using BIAevaluation™ software determining the rate constant for dissociation and association kinetics. From the rate constants the equilibrium binding constant K_D was calculated.

For the competition binding experiments, the binding of a single concentration of one antibody (ligand) was measured in the presence of various concentrations of the competitor antibody. In order to reach equilibrium binding, B16/EpCAM 3E3 cells (100,000/well) were incubated for 18 h at room temperature in 150 µl of FACS buffer (PBS, 1% FCS, 0.05% NaN_3) containing the respective ligand and competitor antibody. For detection of the binding of the ligand antibody, a FITC-labeled detection antibody specific for human or mouse antibodies was used (anti-human IgG-FITC, ICN 67217; anti-mouse IgG-FITC, Sigma F-6257). Assay data were analyzed with Prism software (GraphPad Software Inc., San Diego, CA, USA). After non-linear regression of the competitive binding curves the K_i value for the competitor could be calculated knowing the K_D value from a parallel saturation binding experiment.

Bioactivity comparison of adeccatumumab and mu-adeccatumumab

For ADCC assays, murine NK cells were prepared by negative selection of C57BL/6 splenocytes using the murine NK cell isolation kit from BD Biosciences (San Jose, CA, USA) as described by the manufacturer. Isolated NK cells were cultured for 7–14 days in RPMI 1640/10% FCS supplemented with 1,700 U/ml Proleukin (Chiron GmbH, Munich, Germany) at a density of about 1×10^6 cells/ml. Every 2–3 days, cells were

counted and fresh medium added. After 7–14 days in culture, NK cell purity was between 90 and 100%. Stimulated murine NK cells were re-suspended in RPMI 1640/10% FCS at a concentration of 1.6×10^7 cells/ml and used as effector cells in ADCC assays. For the preparation of human effector cells, peripheral blood mononuclear cells (PBMC) were enriched by Ficoll-Hypaque gradient centrifugation [11], washed and re-suspended at 1.2×10^7 cells/ml.

EpCAM-positive Kato III cells were used as target cells and labeled with the fluorescent membrane dye PKH-26 (Sigma, Taufkirchen, Germany) according to the manufacturer's protocol in order to distinguish target from effector cells in subsequent FACS analysis. PKH-26 labeled target cells were adjusted to a density of 4×10^5 and 6×10^5 cells/ml for assays with murine and human effector cells, respectively. Equal volumes of target and effector cell suspensions were mixed resulting in an effector-to-target (E:T) ratio of approximately 50:1 and 20:1 for murine and human effector cells, respectively, and 50 μ l added/well of a 96-well U-bottom microtiter plate (Greiner, Solingen, Germany). Fourfold serial dilutions of adecatumumab and tenfold serial dilutions of mu-adecatumumab were prepared and 50 μ l added/well resulting in a concentration range of 50,000–0.05 ng/ml for adecatumumab and 50,000–0.2 ng/ml for mu-adecatumumab. ADCC reactions were incubated for 10 and 4 h at 37°C for assays with murine and human effector cells, respectively. Propidium iodide (PI) was added to a final concentration of 1 μ g/ml and 5×10^4 cells analyzed by flow cytometry using a FACSCalibur instrument (Becton Dickinson, Heidelberg, Germany). Dose-response curves were computed by non-linear regression analysis using a four-parameter fit model provided with the GraphPad Prism software (GraphPad Software). All experiments were performed in triplicates.

Quantification of cytotoxicity was based on the number of dead target cells in relation to the total number of target cells in each test sample. The specific cytotoxicity was calculated by the formula: (dead target cells (sample)/total target cells (sample)) \times 100.

Animal studies

In vivo experiments were performed in female 6–10 week old immunocompetent C57BL/6 mice bred at the Institute of Immunology (Munich University, Germany). The mice were maintained under sterile and standardized environmental conditions ($20 \pm 1^\circ\text{C}$ room temperature, $50 \pm 10\%$ relative humidity, and 12-h light/dark rhythm) and received autoclaved food and bedding (ssniff, Soest, Germany) as well as drinking

water ad libitum. All experiments were performed according to the German Animal Protection Law with permission from the responsible local authorities.

Statistical analysis of the mean number of lung tumor colonies of the corresponding treatment groups versus the vehicle control group was performed using the Student's *t*-test.

Pharmacokinetic analysis

To generate a pharmacokinetic profile of adecatumumab and mu-adecatumumab, 20 female C57BL/6 mice were intravenously injected with 300 μ g of the respective antibody and animals allocated to four different groups of 5 mice each. Different groups were alternately bled at different time points after injection (pre-dose, 0.5, 1, 2, 4 and 10 h, 1, 2, 4, 7, 9, 11, 14, 17, 21, 24 and 28 days) and serum concentrations quantified by specific ELISAs.

ELISA plates (NUNC, Wiesbaden, Germany) were coated with 100 μ l (5 μ g/ml) of rat anti-adecatumumab antibody (Micromet AG, Munich, Germany). Plates were incubated overnight at 4°C and blocked with PBS/1% bovine serum albumin for 60 min at 25°C. Test samples were diluted in PBS/10% mouse plasma pool, 100 μ l added/well and incubated for 60 min at 25°C. For adecatumumab quantification, plates were incubated with 100 μ l (0.15 μ g/ml) of chicken anti-adecatumumab antibody conjugated with biotin (Micromet AG) at a final concentration of 2 μ g/ml for 60 min at 25°C followed by incubation for 60 min at 25°C with 100 μ l streptavidin conjugated with alkaline phosphatase (Dako, Hamburg, Germany) at a final concentration of 0.5 μ g/ml. For mu-adecatumumab quantification, plates were incubated with 100 μ l of goat anti-mouse antibody conjugated with alkaline phosphatase (Sigma, Taufkirchen, Germany) for 60 min at 25°C. Finally, plates were incubated with 100 μ l of substrate (1 mg/ml of *p*-NPP dissolved in 0.2 M TRIS buffer; Sigma, Taufkirchen, Germany) for 20 min at 25°C and the absorbance (405 nm) read on Power WaveX select (Bio-Tek instruments, Bad Friedrichshall, Germany). Twofold serial dilutions of each test sample were analyzed in duplicates and OD values that were within the linear range of the standard curve were used to calculate the concentration of adecatumumab and mu-adecatumumab.

Pharmacokinetic calculations of adecatumumab and mu-adecatumumab were performed by the pharmacokinetic software package WinNonlin Professional 4.1 (Pharsight Corporation, Mountain View, CA, USA; 2003). Parameters were determined by non-compartmental analysis (NCA). The NCA was based on model 201 (intravenous bolus injection).

Tumor model

B16/EpCAM cells (1×10^5) were intravenously injected into C57BL/6 mice and animals treated three times a week with the indicated dose levels of adecatumumab, mu-adecatumumab or human IgG1 control antibody starting 1 h after B16/EpCAM inoculation. Mice were sacrificed and dissected on day 26 after B16/EpCAM cell injection. Lungs were filled with tissue teck (Vogel GmbH, Giessen, Germany) and analyzed macroscopically for the number of tumor colonies. To monitor exposure to the respective antibodies three animals per group were alternately bled before and 30 min after the 3rd, 6th, 9th, 11th infusion as well as at the end of the study.

Results

Generation of mu-adecatumumab

The murine IgG2a version of adecatumumab (mu-adecatumumab) was generated by combining the vL and vH regions of adecatumumab (formerly HD69) [15] with the mouse constant κ light and constant CH1-CH3 heavy region sequences, respectively. The mouse constant domains were amplified from mRNA isolated from the human CD3 ϵ -specific hybridoma OKT3. By this means, mu-adecatumumab retained the variable regions of adecatumumab required for human EpCAM binding and acquired the Fc portion of murine IgG2a. Expression vectors encoding heavy and light chains of mu-adecatumumab were stably transfected into CHO dhfr negative cells and secreted mu-adecatumumab was purified from cell culture supernatants by Protein G affinity chromatography. SDS/PAGE and Western blot analysis indicated a purity >95% for mu-adecatumumab. The concentration of the antibody in CHO cell culture supernatant was approximately 11 mg/l.

Adecatumumab and mu-adecatumumab show comparable EpCAM binding affinity and specificity

Plasmon resonance spectroscopy and binding competition analysis demonstrated that mu-adecatumumab retained binding affinity and specificity comparable to that of the parental human IgG1 antibody adecatumumab. Binding curves to recombinant EpCAM coated on BIAcore sensor chips were recorded at four concentrations of adecatumumab and mu-adecatumumab in five independent experiments. The equilibrium dissociation constant (K_D) for EpCAM binding was determined with 66.6 ± 33.6 and 90.9 ± 36.4 nM

for adecatumumab and mu-adecatumumab, respectively. Differences in K_D values were not statistically different indicating that affinity for EpCAM was retained in mu-adecatumumab. To determine whether mu-adecatumumab had retained the epitope specificity of adecatumumab, EpCAM-expressing B16/EpCAM 3E3 murine melanoma cells were incubated with a non-saturating concentration of mu-adecatumumab (4 $\mu\text{g/ml}$). In competition binding analyses, increasing concentrations of adecatumumab or a human IgG1 isotype control antibody were tested for displacement of the bound antibody. As determined by flow cytometry, adecatumumab effectively competed with mu-adecatumumab for binding to B16/EpCAM 3E3 cells while the isotype control antibody had no effect (Fig. 1).

Adecatumumab and mu-adecatumumab show strong species-specific differences in ADCC

We studied the cytotoxic potency of adecatumumab and mu-adecatumumab in ADCC assays using human and murine effector cells. The human gastric carcinoma cell line KATO III with approximately 1.3×10^6 EpCAM binding sites per cell was employed as target. Adecatumumab showed a much higher ADCC activity than mu-adecatumumab when unstimulated human PBMC were used as effector cells (Fig. 2a). Half-maximal lysis (EC_{50}) was seen at a concentration of 169.6 ng/ml for adecatumumab versus 2,110 ng/ml for mu-adecatumumab, resulting in a 12.4-fold potency difference. None of the antibodies exerted ADCC

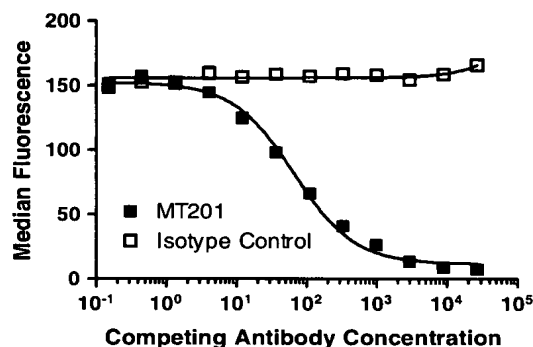


Fig. 1 Competition by adecatumumab of mu-adecatumumab binding to B16/EpCAM 3E3 cells. B16/EpCAM 3E3 murine melanoma cells were incubated with 4 $\mu\text{g/ml}$ of mu-adecatumumab followed by binding competition with increasing concentrations of either human adecatumumab (dark square) or human IgG1 isotype control antibody (open square). Mu-adecatumumab bound to B16/EpCAM 3E3 cells was determined by flow cytometry using a fluorescently labeled anti-mouse IgG antibody, and data analyzed with Prism software (GraphPad Software Inc.)

activity when tested in assays with unstimulated mouse splenocytes or NK cells isolated thereof (data not shown), which is consistent with published work [12]. However, when NK cells pre-stimulated with IL-2 were used at an E:T ratio of 50:1, adecatumumab showed a dose-dependent ADCC activity. Mu-adecatumumab was found to be more efficacious with murine NK cells than adecatumumab (Fig. 2b). The murine version of adecatumumab induced half-maximal target cell lysis at a concentration of 38.1 ng/ml and human adecatumumab at 1,664 ng/ml, resulting in 43.7-fold higher potency for mu-adecatumumab with

murine cells. Human IgG1 and murine IgG2a isotype control antibodies did not elicit specific ADCC activity under either experimental condition underscoring target specificity of the antibodies.

Pharmacokinetic properties of adecatumumab and mu-adecatumumab in mice

Single administration of 300 μ g adecatumumab and mu-adecatumumab resulted in maximum serum concentrations (C_{max}) of 119.2 and 204 μ g/ml, respectively, 30 min after i.v. bolus injection into C57BL/6 mice. Serum concentrations of the antibodies were well detectable until the end of the 28-day study period (Fig. 3). Serum concentration versus time profiles for both adecatumumab and mu-adecatumumab exhibited a bi-exponential curve progression with an early distribution phase between 0 and 10 h and a terminal elimination phase. Despite curve progression looking similar for both antibodies, mu-adecatumumab doses resulted in constantly higher serum concentration compared to adecatumumab, which was also reflected by higher exposure (AUC_{last}) values of 519.8 days \cdot μ g/ml for mu-adecatumumab versus 335.9 days \cdot μ g/ml for adecatumumab, respectively. The volume of distribution (V_z) and the clearance (CL) were calculated with 5.28 ml and 0.56 ml/day for mu-adecatumumab, and with 7.78 ml and 0.86 ml/day for adecatumumab. Both, the volume of distribution and the clearance were higher for adecatumumab compared to mu-adecatumumab. The elimination rate constants resulted in similar distribution half-lives ($T_{1/2\alpha}$) of 0.27 and 0.31 days and terminal elimination half-lives ($T_{1/2\beta}$)

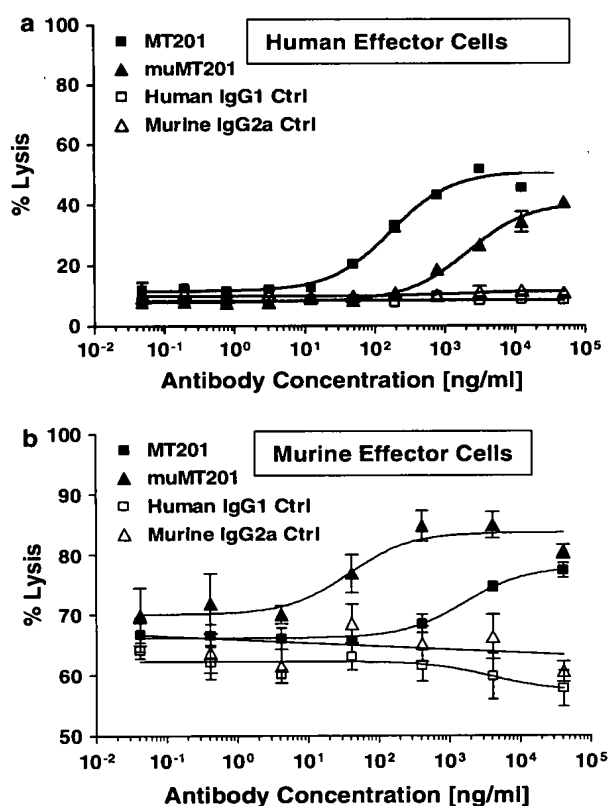


Fig. 2 ADCC of mu-adecatumumab and adecatumumab with human and murine effector cells. **a** Kato III cells and non-stimulated human PBMC were co-incubated at a ratio of 1:20 in the presence of indicated adecatumumab (filled squares) and mu-adecatumumab (filled triangles) concentrations. Human IgG1 (open squares) and mouse IgG2a (open triangles) isotype control antibodies served as negative controls. ADCC activity was measured after 4 h. Target cell lysis was determined by PI uptake using flow cytometry. **b** Kato III cells and IL-2 pre-stimulated murine NK cells were co-incubated at a ratio of 1:50 in the presence of indicated adecatumumab (filled squares) and mu-adecatumumab (filled triangles) concentrations. Human IgG1 (open squares) and mouse IgG2a (open triangles) isotype control antibodies were used as negative controls. ADCC activity was measured after 10 h. Error bars show standard deviations of triplicate wells

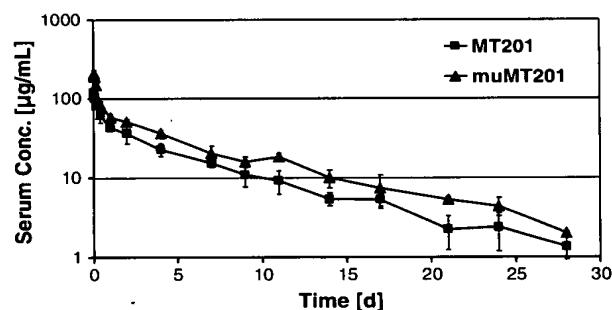


Fig. 3 Pharmacokinetics of adecatumumab and mu-adecatumumab following i.v. bolus injection in C57BL/6 mice. Twenty female C57BL/6 mice were intravenously injected with 300 μ g of adecatumumab or mu-adecatumumab and animals allocated to four different groups of five mice each. Different groups were alternately bled at different time points after injection (pre-dose, 0.5, 1, 2, 4 and 10 h, 1, 2, 4, 7, 9, 11, 14, 17, 21, 24 and 28 days) and serum concentrations of the respective antibodies quantified by specific ELISAs. Error bars show standard deviations from five different animals per group

of 6.21 and 6.57 days for adecatumumab and mu-adecatumumab, respectively.

Establishment of a syngeneic lung metastasis model in C57BL/6 mice

The *in vivo* efficacy of adecatumumab and mu-adecatumumab was compared side-by-side in an immunocompetent C57BL/6 mouse model. We established a tumor model with B16 mouse melanoma cells in which, following intravenous injection, tumor cell colonies are formed in the lungs. In order to render B16F10 cells amenable for immunotherapy with human EpCAM-specific antibodies, cells were stably transfected with an expression vector encoding human EpCAM. Subclone B16/EpCAM 3E3 was selected and its EpCAM expression determined by saturation binding. Approximately 2.0×10^6 EpCAM binding sites were measured, a number which is comparable to the 1.3×10^6 EpCAM sites expressed on KATO III human gastric carcinoma cells. The high-level of EpCAM expression on B16/EpCAM cell was found to be stable for at least 6 weeks in cell culture even in the absence of selection pressure (data not shown).

For establishment of the animal model, syngeneic B16/EpCAM cells were intravenously injected at different numbers into C57BL/6 mice and the number of tumor colonies in lung tissue counted at different time points after inoculation. Conditions under which 1×10^5 injected B16/EpCAM cells resulted in an average of 80–100 tumor colonies between 21 and 28 days after injection were chosen for the following efficacy studies.

Superior anti-tumor activity of mu-adecatumumab in immunocompetent mice

The single-dose pharmacokinetic profiles of adecatumumab and mu-adecatumumab were used for modeling a dosing regimen that would result in serum trough levels at or above 30 $\mu\text{g/ml}$. This concentration corresponds to the targeted trough levels for adecatumumab in two ongoing clinical phase II studies. Based on PK modeling, a loading dose of 600 $\mu\text{g/mouse}$ followed by maintenance doses of 250 $\mu\text{g/mouse}$ three times per week were selected for adecatumumab and for the human IgG control antibody. For mu-adecatumumab, a loading dose of 300 $\mu\text{g/mouse}$ and maintenance doses of 125 $\mu\text{g/mouse}$ three times per week were administered. Following intravenous inoculation with 1×10^5 B16/EpCAM, ten animals per group were treated with the antibodies and serum levels of adecatumumab (Fig. 4a) and mu-adecatumumab (Fig. 4b)

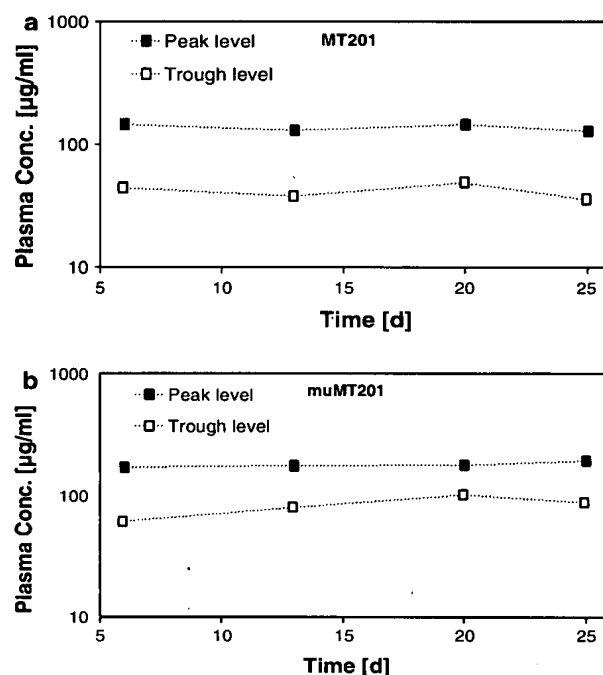


Fig. 4 Adecatumumab and mu-adecatumumab peak to trough levels following repetitive intravenous treatment of C57BL/6 mice. Ten C57BL/6 mice were intravenously injected with adecatumumab, mu-adecatumumab and human IgG isotype control three times a week for four consecutive weeks. A single loading dose of 600 $\mu\text{g/mouse}$ followed by maintenance doses of 250 $\mu\text{g/mouse}$ were selected for adecatumumab and for the human IgG control antibody. For mu-adecatumumab, a loading dose of 300 $\mu\text{g/mouse}$ and maintenance doses of 125 $\mu\text{g/mouse}$ were administered. For monitoring peak (filled squares) and trough plasma concentrations of adecatumumab and mu-adecatumumab (open squares), three animals per group were alternatingly bleed before and 30 min after the 3rd, 6th, 9th, 11th infusion as well as at the end of the study. Antibody concentrations were determined by specific ELISAs

determined after the 3rd, 6th, 9th and 11th administration. Adecatumumab injections resulted in mean peak to trough plasma concentrations of 136–41 $\mu\text{g/ml}$, which were close to the expected plasma concentrations of 150–30 $\mu\text{g/ml}$ during the course of the study. Mean peak to trough concentration of mu-adecatumumab were determined with 172–82 $\mu\text{g/ml}$. Although plasma concentrations of mu-adecatumumab were somewhat higher than for adecatumumab, the overall exposure with both antibodies was considered to be in an effective and comparable range.

Macroscopic inspection of mouse lungs showed that both, the human and murine version of the anti-EpCAM antibody, led to a strong reduction of tumor growth compared to the isotype control (Fig. 5a, b). While lungs from mice treated with mu-adecatumumab

had very few detectable tumors (Fig. 5a, bottom panels), small tumors were still visible on lungs from mice treated with human adecatumumab (Fig 5a, middle panels). Although the size of tumor colonies in human adecatumumab-treated mice was smaller than tumor size in lungs of animals treated with the human isotype control antibody (Fig. 5a), the number of colonies was only slightly reduced after adecatumumab treatment without reaching statistical significance (Fig. 5b). In contrast, treatment with mu-adecatumumab induced a highly significant reduction in the number of lung tumor colonies by > 85% ($P < 0.0001$), and the few remaining tumor colonies were of very small size (Fig. 5a, b).

Discussion

This study shows that the species origin of the Fc portion of a monoclonal antibody can greatly influence

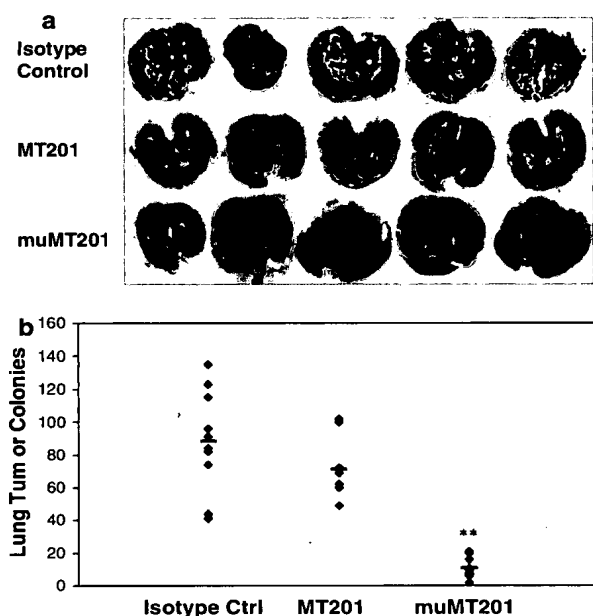


Fig. 5 The effect of mu-adecatumumab and adecatumumab on lung tumor colony formation in immunocompetent mice. B16/EpCAM cells (1×10^5) were intravenously injected into C57BL/6 mice and animals treated three times a week with the indicated doses of adecatumumab, mu-adecatumumab or human IgG1 control antibody starting 1 h after intravenous B16/EpCAM cell injection. **a** Lungs were filled with tissue teck and digital photographs taken. **b** The number of lung tumor colonies was determined macroscopically. While symbols indicate the number of lung colonies for one single mouse, the black bar indicates means of each group. Asterisks indicate statistical differences between treatment and isotype control group (** $P \leq 0.01$ as determined with Student's *t*-test)

anti-tumor activity in a mouse model. The increased anti-tumor activity of murine Fc γ 2a versus human Fc γ 1 in a fully immunocompetent mouse model appears to be primarily based on enhanced ADCC. This is evident from ADCC assays where the version of adecatumumab with a murine Fc γ 2a portion was much more cytotoxic against cancer cells than the human IgG1 version when murine effector cells were used. CDC is unlikely to significantly contribute to the species dependency of anti-tumor activity. Human adecatumumab and murine edrecolomab, two antibodies binding with similar affinity to human EpCAM, showed identical CDC with human complement [11]. Moreover, knock-out of the common γ signaling chain of Fc γ R did almost completely neutralize the anti-tumor activities of trastuzumab and rituximab in a mouse xenotransplant model, suggesting a small contribution by the remaining CDC potential in the mouse [3]. Lastly, CDC is known to be ineffective with tumor cells overexpressing complement resistance factors such as CD59 and CD55, which is frequently seen with tumor cell lines [5, 8]. This is especially true, as B16 cells could not be killed by in vitro CDC assays (data not shown).

In mouse models, monotherapy with humanized IgG1 antibodies rarely shows strong anti-tumor activity. While inhibition of tumor take or retardation of tumor outgrowth can be achieved, regression of established tumors is very difficult to observe. Certain monoclonal IgG1 antibodies are thought to have additional anti-tumor activity through inhibition of growth factor signaling or direct induction of apoptosis. Examples are anti-EGFR and anti-HER-2 antibodies [7, 16]. If their ADCC activity is suboptimal in mice due to a human Fc γ 1 domain, the overall cytotoxic activity of such antibodies may be underestimated. At the same time, the contribution of signal inhibition to overall anti-tumor activity will be overrated. This has to be considered when judging the potential of a therapeutic antibody candidate. One possibility to achieve more reliable information about the effector mechanisms and potency of therapeutic antibody candidates would be to investigate analogous murine versions in mouse models. An alternative approach could be the development and use of genetic mouse models in which the genes encoding murine Fc γ Rs are replaced by the respective human genes. Given there are three genes for Fc γ Rs, generation of such knock-in/knock-out mice will be a major endeavor. The use of functionally equivalent murine Fc domains is much simpler and will moreover allow the use of different mouse strains and models. A yet different approach to assess contribution of immuno-

logical mechanisms to an antibody's cytotoxic activity is the use of F(ab)₂ fragments. In theory, F(ab)₂ fragments, which still bind target in a bivalent fashion, can inhibit tumor growth only by signaling effects but not through immunological effector mechanisms all of which are thought to reside in the Fc portion of the antibody.

Adecatumumab was shown to lyse tumor cells via ADCC and CDC, while no pro-apoptotic or anti-proliferative signaling activity has yet been demonstrated for this human antibody [11]. Adecatumumab was shown to significantly inhibit in nude mice for several weeks outgrowth of tumors derived from the subcutaneously inoculated human colon cancer cell line HT-29 [11]. Because HT-29 cells can be lysed by adecatumumab via ADCC, but not via CDC, only the former can account for anti-tumor activity in nude mice. Here, we found that human adecatumumab did not significantly reduce the number of lung metastases compared to an IgG1 isotype control in a syngeneic mouse model using B16/EpCAM melanoma cells but could substantially reduce the size of visible lung metastases. This shows that human adecatumumab clearly had anti-tumor activity in mice but was rather retarding tumor growth than preventing tumor formation, analogous to results from the HT-29 subcutaneous xenograft model [11]. In contrast, mu-adeccatumumab showed a very pronounced inhibition of lung metastases formation. We therefore postulate that the in vivo anti-tumor activity of adecatumumab was thus far greatly underestimated in nude mouse models. The approach of exchanging human Fcγ1 with murine Fcγ2 taken here for adecatumumab should be applicable to all other human IgG1 therapies. In the case of antibodies with signaling activity, F(ab)₂ fragments should be tested in addition in mouse models.

How predictive is the efficacy seen with a mouse antibody in mice for an equivalent human antibody in humans? Certainly, fast-growing tumors established in mice from cell lines may only be distantly related to the natural, more slowly growing tumors in man, which display a higher degree of genetic heterogeneity of tumor cells, and may be different with respect to tissue morphology and stromal architecture. While issues of tumor penetration may be comparable in mouse and man, it may be harder for an antibody to control by ADCC a rapidly growing tumor in mice than a slowly growing tumor in man. Moreover, our present in vitro experiments indicate that murine immune cells are much less effective as human immune cells in ADCC, as they required for activity prolonged IL-2 stimulation, longer incubation periods and higher E:T ratios.

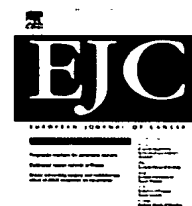
References

1. Blumenthal RD, Osorio L, Hayes MK, Horak ID, Hansen HJ, Goldenberg DM (2005) Carcinoembryonic antigen antibody inhibits lung metastasis and augments chemotherapy in a human colonic carcinoma xenograft. *Cancer Immunol Immunother* 54:315–327
2. Cartron G, Dacheux L, Salles G, Solal-Celigny P, Bardos P, Colombat P, Watier H (2002) Therapeutic activity of humanized anti-CD20 monoclonal antibody and polymorphism in IgG Fc receptor FcγRIIIa gene. *Blood* 99:754–758
3. Clynes RA, Towers TL, Presta LG, Ravetch JV (2000) Inhibitory Fc receptors modulate in vivo cytotoxicity against tumor targets. *Nat Med* 6:443–446
4. Dall'Ozzo S, Andres C, Bardos P, Watier H, Thibault G (2003) Rapid single-step FCGR3A genotyping based on SYBR Green I fluorescence in real-time multiplex allele-specific PCR. *J Immunol Methods* 277:185–192
5. Golay J, Zaffaroni L, Vaccari T, Lazzari M, Borleri GM, Bernasconi S, Tedesco F, Rambaldi A, Introna M (2000) Biologic response of B lymphoma cells to anti-CD20 monoclonal antibody rituximab in vitro: CD55 and CD59 regulate complement-mediated cell lysis. *Blood* 95:3900–3908
6. Golay J, Gramigna R, Facchinetti V, Capello D, Gaidano G, Introna M (2002) Acquired immunodeficiency syndrome-associated lymphomas are efficiently lysed through complement-dependent cytotoxicity and antibody-dependent cellular cytotoxicity by rituximab. *Br J Haematol* 119:923–929
7. Goldberg RM (2005) Cetuximab. *Nat Rev Drug Discov (Suppl.)*:S10–S11
8. Juhl H, Helmig F, Baltzer K, Kalthoff H, Henne-Bruns D, Kremer B (1997) Frequent expression of complement resistance factors CD46, CD55, and CD59 on gastrointestinal cancer cells limits the therapeutic potential of monoclonal antibody 17-1A. *J Surg Oncol* 64:222–230
9. Maloney DG, Smith B, Rose A (2002) Rituximab: mechanism of action and resistance. *Semin Oncol* 29:2–9
10. Mellstedt H (2003) Monoclonal antibodies in human cancer. *Drugs Today (Barc)* 39(Suppl. C):1–16
11. Naundorf S, Preithner S, Mayer P, Lippold S, Wolf A, Hanakam F, Fichtner I, Kufer P, Raum T, Riethmüller G, Baeuerle PA, Dreier T (2002) In vitro and in vivo activity of MT201, a fully human monoclonal antibody for pancreatic carcinoma treatment. *Int J Cancer* 100:101–110
12. Niwa R, Shoji-Hosaka E, Sakurada M, Shinkawa T, Uchida K, Nakamura K, Matsushima K, Ueda R, Hanai N, Shitara K (2004) Defucosylated chimeric anti-CC chemokine receptor 4 IgG1 with enhanced antibody-dependent cellular cytotoxicity shows potent therapeutic activity to T-cell leukemia and lymphoma. *Cancer Res* 64:2127–2133
13. Prang N, Preithner S, Brischwein K, Goster P, Woppel A, Müller J, Steiger C, Peters M, Baeuerle PA, da Silva AJ (2005) Cellular and complement-dependent cytotoxicity of Ep-CAM-specific monoclonal antibody MT201 against breast cancer cell lines. *Br J Cancer* 92:342–349
14. Preithner S, Elm S, Lippold S, Locher M, Wolf A, Silva AJ, Baeuerle PA, Prang NS (2006) High concentrations of therapeutic IgG1 antibodies are needed to compensate for inhibition of antibody-dependent cellular cytotoxicity by excess endogenous immunoglobulin G. *Mol Immunol* 43(8):1183–1193
15. Raum T, Gruber R, Riethmüller G, Kufer P (2001) Anti-self antibodies selected from a human IgD heavy chain repertoire: a novel approach to generate therapeutic human antibodies against tumor-associated differentiation antigens. *Cancer Immunol Immunother* 50:141–150

16. Sliwkowski MX, Lofgren JA, Lewis GD, Hotaling TE, Fendly BM, Fox JA (1999) Nonclinical studies addressing the mechanism of action of trastuzumab (Herceptin). *Semin Oncol* 26:60–70
17. Surfus JE, Hank JA, Oosterwijk E, Welt S, Lindstrom MJ, Albertini MR, Schiller JH, Sondel PM (1996) Anti-renal-cell carcinoma chimeric antibody G250 facilitates antibody-dependent cellular cytotoxicity with in vitro and in vivo interleukin-2-activated effectors. *J Immunother Emphasis Tumor Immunol* 19:184–191
18. Takai T (2002) Roles of Fc receptors in autoimmunity. *Nat Rev Immunol* 2:580–592
19. Weng WK, Levy R (2003) Two immunoglobulin G fragment C receptor polymorphisms independently predict response to rituximab in patients with follicular lymphoma. *J Clin Oncol* 21:3940–3947



ELSEVIER

available at www.sciencedirect.comjournal homepage: www.ejconline.com

A phase I study with adecatumumab, a human antibody directed against epithelial cell adhesion molecule, in hormone refractory prostate cancer patients

Ralf Oberneder^{a,d}, Dorothea Weckermann^{b,d}, Beatrice Ebner^c, Cornelia Quadt^c,
Petra Kirchinger^c, Tobias Raum^c, Mathias Locher^c, Nadja Prang^c,
Patrick A. Baeuerle^{c,*}, Eugen Leo^c

^aUrologische Klinik München-Planegg, Germingerstr. 32, Planegg, Germany

^bZentralklinikum Augsburg, Urologische Klinik, Stenglinstr.2, Augsburg, Germany

^cMicromet AG, Research and Development Department, Staffelseestr.2, 81477 Munich, Germany

ARTICLE INFO

Article history:

Received 20 March 2006

Received in revised form

16 May 2006

Accepted 18 May 2006

Available online 23 August 2006

Keywords:

Monoclonal antibody

Adecatumumab

EpCAM

Hormone refractory prostate cancer

Phase I study

ABSTRACT

Aim of the study: Adecatumumab (also known as MT201) is a human recombinant IgG1 monoclonal antibody binding with low affinity to epithelial cell adhesion molecule (EpCAM). To explore safety, pharmacokinetics and pharmacodynamics of adecatumumab, a phase I trial in patients with hormone refractory prostate cancer (HRPC) was performed. **Methods:** Twenty patients were treated with two adecatumumab infusions on days 0 and 14 in cohorts with doses of ten up to 262 mg/m².

Results: Adecatumumab was well tolerated at all doses tested, and no maximum tolerated dose reached. Most adverse events were mild or moderate with pyrexia and nausea being most frequent. The highest dose of adecatumumab induced shortly after infusion robust and transient increases of TNF-alpha serum levels. At all doses, significant transient declines of peripheral natural killer cells were observed shortly after antibody infusions. Adecatumumab had a serum half-life of 15 days, and immune responses to the antibody were not detected.

Conclusions: A benign safety profile, long serum half-life and low immunogenicity do warrant further exploration of adecatumumab for treatment of EpCAM-expressing neoplasia.

© 2006 Elsevier Ltd. All rights reserved.

1. Introduction

EpCAM is a surface glycoprotein expressed on many carcinomas of different origin, including prostate, breast and gastrointestinal cancers.¹ Its presumed biological function is to serve as a homotypic, calcium-independent cell adhesion

molecule.² More recent studies have shown that overexpression of EpCAM confers an oncogenic phenotype to quiescent cells, and is required for the invasive, migratory and proliferative potential of certain tumour cells.^{3,4} EpCAM may also contribute to immune evasion of tumour cells. When ectopically expressed or transferred to dendritic cells by tumour cell

* Corresponding author. Tel.: +49 89 895277 601; fax: +49 89 895277 205.

E-mail address: patrick.baeuerle@micromet.de (P.A. Baeuerle).

^d These two authors equally contributed to the study.

0959-8049/\$ - see front matter © 2006 Elsevier Ltd. All rights reserved.
doi:10.1016/j.ejca.2006.05.029

debris, EpCAM strongly impairs MHC class II-dependent antigen presentation.⁵ Using tissue microarray technology, 3900 samples from 134 histologically different tumour types and subtypes were analysed for EpCAM expression.⁶ Particularly high and frequent expression was found in patients with prostate cancer, consistent with three other immunohistochemical studies.⁷⁻⁹

Because of its overexpression on a wide variety of epithelial tumour cells, many immunotherapeutic approaches have employed EpCAM as target antigen. These include murine¹⁰ and humanised monoclonal antibodies,^{11,12} immunotoxins,¹³ and vaccine-based approaches.¹⁴ Most clinical experience to date has been gathered with the low-affinity murine anti-EpCAM antibody edrecolomab (Panorex®).¹⁰ Major limitations of this murine antibody are its short serum half-life in man, its high immunogenicity and its low effectiveness with immune effector cells of human origin. The latter results in considerably reduced antibody-dependent cellular cytotoxicity (ADCC) with human immune effector cells when compared to humanised or human anti-EpCAM antibodies.¹⁵ Nevertheless, clinical activity was reported for edrecolomab in Dukes C colorectal cancer patients in two out of three phase III trials.^{16,17} Moreover, edrecolomab was well tolerated. This is in contrast to two humanised anti-EpCAM antibodies, ING-1 and 3622W94, both of which caused acute pancreatitis as a dose limiting toxicity in phase I studies.^{11,12} It is not known whether this acute organ toxicity was due to their higher binding affinity for EpCAM, their human IgG1 format, recognition of a different epitope on EpCAM, or combinations thereof.

Adecatumumab (also known as MT201) is a human, recombinant monoclonal IgG1 antibody binding to EpCAM with rather low affinity.^{15,18} Being fully human, adecatumumab is expected to be less immunogenic than murine, chimeric or humanised antibodies, potentially translating into a lower frequency of neutralising antibody responses in patients. The human nature of adecatumumab is also expected to result in a half-life as observed with other human IgG1, and in optimal compatibility with human immune effector mechanisms. Adecatumumab has demonstrated cytotoxic activity against tumour cell lines of multiple origins including breast, prostate, ovarian, gastric and colon cancers *in vitro*,^{15,19,20} in an animal model,¹⁵ and *ex vivo* with human ovarian cancer samples.¹⁹ The prime mechanisms of action of adecatumumab are antibody-dependent cellular cytotoxicity (ADCC) and complement-dependent cytotoxicity (CDC).

This is the first phase I study performed with adecatumumab for assessment of safety and tolerability in patients with HRPC and to determine pharmacokinetic (PK) and pharmacodynamic (PD) properties of the antibody.

2. Patients and methods

2.1. Description of study drug

Adecatumumab is a human monoclonal antibody of the IgG1 isotype binding with low affinity to EpCAM.¹⁵ The variable domains of the antibody were derived from human B cell repertoires ensuring closeness to human germline and lowest possible immunogenicity.¹⁸ For clinical use, ade-

catumumab was recombinantly produced by a contract manufacturer in CHO cells. The antibody is formulated in phosphate-buffered saline at 10 mg/mL antibody and can be stored at 4–8 °C for more than 1 year. Preclinical data have shown that adecatumumab eliminated prostate cancer cell lines 22RV1 and LNCAP by ADCC, while PC3 and DU145 had to low an EpCAM level to show susceptibility to ADCC by adecatumumab. The antibody was well tolerated in cynomolgus monkeys treated for 3 months with multiple doses up to 180 mg/kg.

2.2. Trial design and selection of starting dose

The starting dose of 10 mg/m² was selected based on toxicology data from two other humanised anti-EpCAM IgG1 antibodies called ING-1 and 3622W94. Both of these high-affinity humanised antibodies had an MTD of 30 mg total dose, i.e. approximately 17 mg/m².^{11,12} Given that adecatumumab is of the same immunoglobulin isotype as ING-1 and 3622W94, we considered it reasonable to start dosing of adecatumumab below the MTD of the two clinically tested antibodies. A standard 3+3 design was used to escalate by increasing the adecatumumab dose with each cohort by 100%, and in the case of the occurrence of CTC grade 1 or 2 toxicities, by 60%. Cohort 1 had only two patients. Because of the limited amount of available antibody, adecatumumab doses had to be restricted to two biweekly administrations and a maximum of 262 mg/m² (6–7 mg/kg). Continuation of the study with newly produced material was not a possibility because the production process for adecatumumab for phase I material had been terminated in favour of development of a new cell line and fermentation process. Nevertheless, maintenance of trough levels for 4 weeks and reaching an antibody dose as used by other IgG1 cancer therapies was considered sufficient for an initial safety assessment of adecatumumab in man.

2.3. Study design and patient selection

This was an open-label, non-randomised, multi-center, dose-escalation phase I study in which adecatumumab was administered intravenously to patients with advanced HRPC. The study objectives were to assess safety, pharmacokinetics, pharmacodynamics and the maximum tolerated dose (MTD) of adecatumumab in patients with HRPC given as two single intravenous (i.v.) infusions at a 2-week interval.

Patients aged over 18 with histologically confirmed relapsed HRPC were enrolled in two centers (Augsburg and Munich; Germany). Relapse was confirmed by a continuous increase of PSA during two consecutive measurements at least 2 weeks apart. Patients with previous monoclonal antibody treatment, a high tumour burden, Eastern Cooperative Oncology Group (ECOG) status >2, chemo- or radiotherapy within 3 months, CNS metastases, poor life expectancy, other severe diseases, or liver, renal or bone marrow dysfunction were excluded. Hormonal therapy at entry had to be left unchanged during the study.

Each patient received two i.v. infusions of adecatumumab over 30 min separated by 2 weeks provided that there was no dose limiting toxicity during or after the first infusion. A total

of 20 patients were treated in seven dose cohorts. Two patients were treated with the lowest dose of 10 mg/m² and three patients each at doses of 20, 40, 64, 102, 164 and 262 mg/m².

The study was conducted in accordance with the Declaration of Helsinki, and Good Clinical Practice. All patients gave their voluntary informed consent and signed a consent document that had been approved by the institutional review boards of both participating centres.

2.4. Safety measurements

Adverse events (AEs) and vital signs were recorded every other day until study day 23, and weekly thereafter. During infusion, vital signs and oxygen saturation were recorded every 5 min, and at longer intervals thereafter. Physical examination, clinical laboratory values, ECG, oxygen saturation and vital signs were recorded before the start of the study and weekly during the treatment and follow up periods. Adverse drug reactions (ADRs) that occurred after the start of the study treatment were graded by the investigator according to NCI Common Toxicity Criteria (CTC, version 2.0). The frequency of grade 3 or 4 toxicities (i.e. ADRs or AEs considered at least possibly related to the study drug by the investigator) was evaluated for each cohort with the aim to determine a maximum tolerated dose (MTD). MTD was defined as one dose level below the dose level that caused, in at least two out of three patients, a grade 3 or 4 toxicity. This toxicity was defined as dose limiting.

2.5. Cell culture

Chronic myeloid leukaemia cell line K562 was used for determination of natural killer (NK) cell activity and derived from the American Type Culture Collections (Manassas, VA, USA). Cells were cultured at 37 °C in a 5% CO₂ incubator in Iscove's modified Dulbecco's medium with 4 mM L-glutamine adjusted to contain 1.5 g/L sodium bicarbonate supplemented with 10% fetal bovine serum (Invitrogen GmbH, Karlsruhe, Germany).

2.6. Pharmacodynamic measurements

Cytokine levels for gamma-interferon (IFN- γ), tumour necrosis factor alpha (TNF- α), and interleukin 1 beta (IL-1 β) were measured at baseline and frequently throughout the study using the Immulite system, an automated solid phase ELISA (enzyme linked immunoabsorbent assay) assay (DPC Biermann GmbH, Bad Nauheim, Germany). Interleukin 2 (IL-2) concentrations were measured using a standard ELISA (Beckman-Coulter GmbH, Krefeld, Germany). Prostaglandin E₂ (PGE₂) concentrations were determined using a validated commercial ELISA assay (Assay Designs Inc., Ann Arbor, MD, USA).

2.7. Pharmacokinetic measurements

Adecatumumab serum concentration was measured at pre-dose and frequently during the treatment and observation period in i.v. collected blood samples. Time points of blood

sample collection are depicted in Fig. 1. To determine adecatumumab concentrations, an ELISA-based assay has been developed and validated at Micromet. Monoclonal rat anti-adecatumumab antibody HD4A4 7B1 (Micromet AG, Germany) was coated at a final concentration of 1 mg/mL to a 96-well microtitre plate overnight at 2–8 °C. A blocking step was performed using PBS buffer with 1% BSA. Quality control samples, calibration standards and patient samples were diluted 1:20 and 1:50 in phosphate buffered saline (PBS) containing 5% and 2% human serum, respectively. Samples were incubated for 1–2 h at 25 ± 2 °C following washing using an ELISA plate washer (Tecan GmbH, Crailsheim, Germany). Next, a final concentration of 5 µg/mL biotinylated chicken polyclonal anti-adecatumumab solution (Davids Biotechnologie, Regensburg, Germany) containing 1% bovine serum albumin (BSA) was incubated for 1 h at 25 °C. After washing, 0.5 µg/mL streptavidin alkaline phosphatase (AP) solution with 1% BSA was added and incubated for 30 min at 25 °C. pNPP was then used as substrate for AP. Colour intensity of the antibody staining reaction was measured in a Power Wave plate reader with a 405 nm filter (Bio-Tek Instruments GmbH, Bad Friedrichshall, Germany). For evaluation of unknown adecatumumab concentrations in patient samples, KC4 software (Bio-Tek Instruments GmbH, Bad Friedrichshall, Germany) was used. The lower limit of quantification of the assay was 200 ng/ml serum.

2.8. Immunogenicity measurements

Human antibody responses against adecatumumab were determined using an ELISA-based assay. Adecatumumab (Micromet AG, Germany) was coated at a final concentration of 0.2 µg/mL to a 96-well microtitre plate overnight at 2–8 °C. Blocking was performed using PBS buffer with 1% BSA for 1 h at 25 °C. After washing, negative control serum from healthy donors, patient pre- and post-dose serum as well as serum spiked as positive control with serial dilutions of rat monoclonal anti-adecatumumab antibody HD4A4 7B1 (Micromet AG, Germany), were transferred to the microtitre plates and incubated for 1.5 h at 25 °C. Plates were washed using

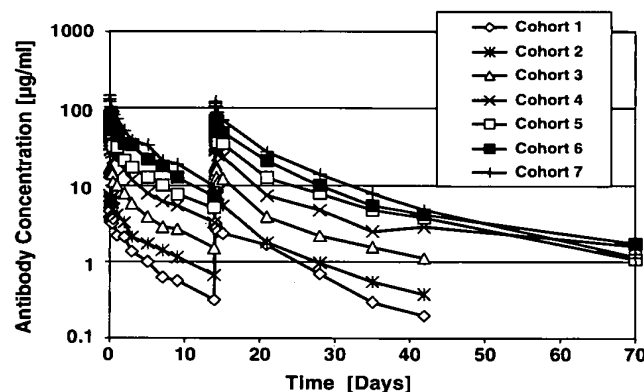


Fig. 1 – Serum concentration/time profiles of adecatumumab for all seven cohorts. Depicted is the arithmetic mean of each cohort.

an ELISA plate washer (Tecan GmbH, Crailsheim, Germany) followed by an incubation of biotinylated adecatumumab (Micromet AG, Germany) at a final concentration of 2 µg/mL in PBS containing 1% BSA for 1 h at 25 °C. Detection, staining and evaluation was carried out as described for the adecatumumab pharmacokinetic assay (see above). The assay sensitivity was adjusted to an upper limit of 95% negative and 5% false positive results to exclude false negative results, using samples from healthy donors as well as from a patient population ($n = 50$). Samples for immunogenicity evaluations were taken before and after treatment. The lower limit of quantitation of the assay was 100 ng/mL.

2.9. Determination of natural killer cell number and activity

Natural killer (NK) cell numbers were determined at baseline and at various time points after treatment using the Simultest IMK Lymphocyte Kit (Becton Dickinson GmbH, Heidelberg, Germany) following the manufacturer's recommendations. Antibody-labeled cells were analysed using a FACSCalibur flow cytometer (Becton Dickinson GmbH, Heidelberg, Germany). CD16/CD56 double-positive peripheral blood lymphocytes, i.e. NK cells, were determined as absolute numbers and as a percentage of total blood lymphocytes.

For determination of NK cell cytotoxic activity, peripheral blood mononuclear cells (PBMC) were prepared before and at various time points after treatment following conventional procedures. PBMC were washed with PBS buffer and resuspended in RPMI medium supplemented with 10% foetal calf serum (Invitrogen, Karlsruhe, Germany). K562 target cells lacking MHC class I and II molecules were labelled with 3,3'-diiododecylthiopyranine perchlorate (Sigma, Aldrich, Seelze, Germany), a fluorescent cell membrane dye allowing for flow cytometric separation of effector PBMC from target cells. Next, 5×10^6 PBMC were incubated with 1×10^5 labelled K562 cells at 37 °C over 2 h in RPMI medium in the absence or presence of 200 U/mL recombinant cytokine IL-2 (Sigma Aldrich, Seelze, Germany). Basal and IL-2 induced NK cell activity was monitored by uptake of propidium iodide (PI) dye (1 µg/mL) into nuclei of lysed K562 cells. Aliquots of 20,000 cells were analysed by flow cytometry using a FACSCalibur instrument. Cytotoxicity was quantitated as a percentage of K562 cell lysis.

2.10. Clinical and biochemical response measurements

Tumour lesions were assessed using standard imaging techniques such as computerised tomography (CT), magnetic resonance tomography (MRT), and standard X-ray before the start of study treatment and at day 42. Responses were re-evaluated by a reference radiologist. Tumour response was defined according to the Response Evaluation Criteria in Solid Tumours (RECIST).

PSA serum levels were determined immediately before the start of treatment (day 0) and in weekly intervals thereafter until week 6 (day 7, 14, 21, 28, 35, and 42) and at week 10 (day 70) using an Elecsys instrument and respective reagents (Roche Diagnostics, Penzberg, Germany) in a central laboratory. PSA measurements, before the start of the study, were

performed in local laboratories using various assay procedures, and were employed to verify PSA rise. PSA levels at baseline were compared to day 42 and, where available, day 70 values. A 50–79% decline below starting level qualified as 'partial PSA response', a decline of 80% or greater as complete PSA response. PSA doubling time and weekly PSA net production were also assessed.

2.11. Statistical analyses

A two-sided sign test was performed based on per protocol data to assess whether there were statistically significant differences in the number of peripheral NK cells before and 12 h after the first dose, or, independently, after the second dose of adecatumumab. Statistical analysis of TNF serum levels was performed on all patients' data by a two-sided Wilcoxon rank sum test to analyse whether there was a significant difference of relative changes of TNF levels between low (1–5) and high dose levels (6 and 7).

3. Results

3.1. Study population

Twenty patients with HRPC were enrolled between September 2001 and July 2002 (Table 1). All cohorts with the exception of cohort 5 contained patients from both centres. All patients had advanced disease and were extensively pretreated. The mean time from first diagnosis was 3.6 years (range: 0.7–11.1 years). Twelve patients had tumour stages T3 or T4, and in 11 patients (55%) the Gleason score was ≥ 7 . Sixteen patients had a radical prostatectomy and all but one patient received hormonal treatment before study inclusion. All but one patient with a T4N1 tumour stage had documented metastatic disease. Total PSA levels before adecatumumab treatment varied between 2.0 and 1400 ng/mL with a mean PSA serum concentration (\pm SD) of 156.82 (\pm 324.43) ng/mL. Four of the six patients in cohorts 6 and 7 had the highest PSA baseline levels in the study. While all 20 patients were evaluable for safety assessment, three patients had to be excluded

Table 1 – Patient characteristics

Baseline characteristics	Value
Patient number (N):	20
Age (years): mean \pm SD (range)	64.1 \pm 5.4 (56–74)
Prior therapy N (%)	
Chemotherapy	6 (30%)
Hormone therapy	19 (95%)
Orchiectomy	6 (30%)
Radiotherapy	15 (75%)
Prostatectomy	16 (80%)
PSA levels (ng/ml)	
<4	2 (10%)
4–9.9	4 (20%)
10–19.9	2 (10%)
20–99.9	7 (35%)
100–999.9	4 (20%)
>1000	1 (5%)

from the per protocol response analysis for concomitant hormonal treatment or chemotherapy.

3.2. Safety assessment

Adecatumumab was generally well tolerated at all doses administered. No patient discontinued the study medication due to an adverse event. The majority of adverse events (AEs) were of mild or moderate severity. Only six out of a total of 120 AEs were considered severe, of which none were classified as related to the study drug by the investigators. Among a total of 77 clinical AEs considered to be drug-related by the investigators (Table 2), pyrexia was the most frequent (45%) followed by nausea (25%), feeling cold, diarrhea and vomiting (15% each). Laboratory abnormalities considered as drug-related were lymphopenia (25%), elevation in lactate dehydrogenase and decrease in activated PTT (20% each), increase in transaminases and disorders of white blood cells (15%). There was a significant increase in the incidence of adverse events per patient in cohorts 6 and 7 versus cohorts 1 to 5 ($p = 0.0003$, and $p = 0.0001$ for the drug-related AE; two-sided Wilcoxon rank sum test), suggesting a relationship between the dose of adecatumumab and frequency of adverse events.

Only two patients experienced grade 3 toxicities with a possible relationship to the study medication (Table 2). One

was an elevation of glutamate transaminase (γ -GT) in cohort 3 and one a transient lymphocytopenia in cohort 7. No grade 4 toxicities according to CTC criteria were observed. In contrast to what has been observed with high-affinity humanised anti-EpCAM IgG1 antibodies^{11,12} adecatumumab did at no dose, and at no time point during treatment and follow-up period, cause acute pancreatitis. Neither a significant increase of serum amylase or lipase above baseline levels was observed. A total of four serious adverse events were reported in four patients. Only one SAE, i.e. prolonged hospitalisation due to fever in cohort 3, was considered possibly related to the study drug.

3.3. Immunogenicity

Sera of all 20 patients were analysed at baseline and at days 28, 35, and 42 for the presence of human antibodies against adecatumumab. Antibodies against adecatumumab were not detected at any of the time points. Likewise, there was no evidence for a neutralising response to adecatumumab from the pharmacokinetic analysis (see Fig. 1), as the serum half-life of adecatumumab was not significantly reduced in any of the 20 patients after the second infusion of the antibody.

3.4. Pharmacokinetics

The mean serum concentration and clearance profiles of adecatumumab from all seven cohorts are shown in Fig. 1. The main pharmacokinetic parameters of adecatumumab following the second intravenous administration of adecatumumab are summarised in Table 3. Dose-linearity for the parameters C_{max} , AUC_{0-7} , AUC_{last} and AUC_{inf} was evident. Clearance and volume of distribution showed no dose dependency and no major differences after the first and the second dose were apparent. Compartmental analysis was consistent with a three compartment model with half-lives of 0.565 days ($t_{1/2\alpha}$), 3.78 ($t_{1/2\beta}$) and 13.3 days ($t_{1/2\gamma}$). The half-life of the terminal phase is in accordance with the non-compartmental analysis, which showed an apparent terminal half-life of 14.74 ± 4.23 days. The apparent terminal half-life was determined to be approximately 7 days for single dose (calculated from day 7 to 14) and 15 days for multiple dose administration (calculated from days 28 to 42 or 35 to 70). The difference in half-life values between first and second dose was a consequence of the longer evaluation period after the second dose. The mean apparent terminal half-life for cohorts 4 to 7, as determined between days 35 and 70, was on average 17 days (see Table 3). After 70 days, the adecatumumab serum concentrations of all patients from cohort 4 to 7 had not yet reached the lower limit of assay quantification of 200 ng/mL. The $T_{1/2}$ values derived from such limited time courses may underrepresent the true value.

3.5. Pharmacodynamic effects

Serum levels of the inflammatory cytokines IFN- γ , TNF- α , IL-1 β , IL-2 as well as for PGE₂ and C-reactive protein (CRP) were determined at various time points after administration of adecatumumab. Natural killer (NK) cells were also analysed

Table 2 – Safety assessment of adecatumumab and summary of patients with possible drug-related CTC toxicities

Toxicities	Grade 1/2	Grade 3	Total N = 20
Clinical abnormalities	(Number of patients with toxicities)		
Fever	9	0	9 (45%)
Nausea	6	0	6 (30%)
Diarrhea	3	0	3 (15%)
Rigors, chills	3	0	3 (15%)
Abdominal pain or cramping	2	0	2 (10%)
Fatigue	2	0	2 (10%)
Hot flashes / flushes	2	0	2 (10%)
Sweating	2	0	2 (10%)
Vomiting	2	0	2 (10%)
Dyspnea	1	0	1 (5%)
Palpitation	1	0	1 (5%)
Salivary gland changes	1	0	1 (5%)
Laboratory abnormalities			
Hepatic other: LDH	4	0	4 (20%)
PTT	4	0	4 (20%)
γ -GT	2	1	3 (15%)
SGOT	3	0	3 (15%)
SGPT	3	0	3 (15%)
Alkaline phosphatase	1	0	1 (5%)
Hematology			
Lymphopenia	4	1	5 (25%)
Neutrophils/granulocytes	3	0	3 (15%)
Platelets	1	0	1 (5%)
Urine analysis			
Hematuria	1	0	1 (5%)
Proteinuria	1	0	1 (5%)

Table 3 – Multiple-dose pharmacokinetic parameters for adecatumumab

Multi dose	Dose (mg/m ²)	t _{1/2} (Day)	V _{ss} (L)	Cl _{ss} (L/day)	C _{max} (μg/mL)	AUC _{T(14-28)} (Day·μg/mL)	AUC _{inf} (Day·μg/mL)
Cohort 1	10	10.01	11.42	1.063	3.4	22.46	30.60
Cohort 2	20	10.78	10.62	1.168	8.9	36.6	50.94
Cohort 3	40	14.20	11.88	1.046	18.3	81.7	131.7
Cohort 4	64	16.95	11.92	0.941	34.7	158.7	288.3
Cohort 5	102	16.11	12.11	0.878	51.1	246.0	411.0
Cohort 6	164	22.37	12.78	0.956	74.6	365.8	601.2
Cohort 7	262	12.77	9.98	1.034	127.1	563.4	788.4
Mean		14.74	11.53	1.01			
SD		4.23	0.95	0.10			
CV		28.7	8.2	9.4			
Min		10.01	9.98	0.88			
Max		22.37	12.78	1.17			
Geo Mean		14.25	11.50	1.01			
Median		14.20	11.88	1.03			

Abbreviations used are: t_{1/2}, terminal half life; V_{ss}, steady-state volume of distribution; Cl_{ss}, steady-state clearance; C_{max}, maximum serum concentration; AUC_T, area under the curve up to the last measured time point; AUC_{inf}, area under the curve to infinity; SD, standard deviation; CV, coefficient of variation; Min, minimum; Max, maximum; GeoMean, geometric mean.

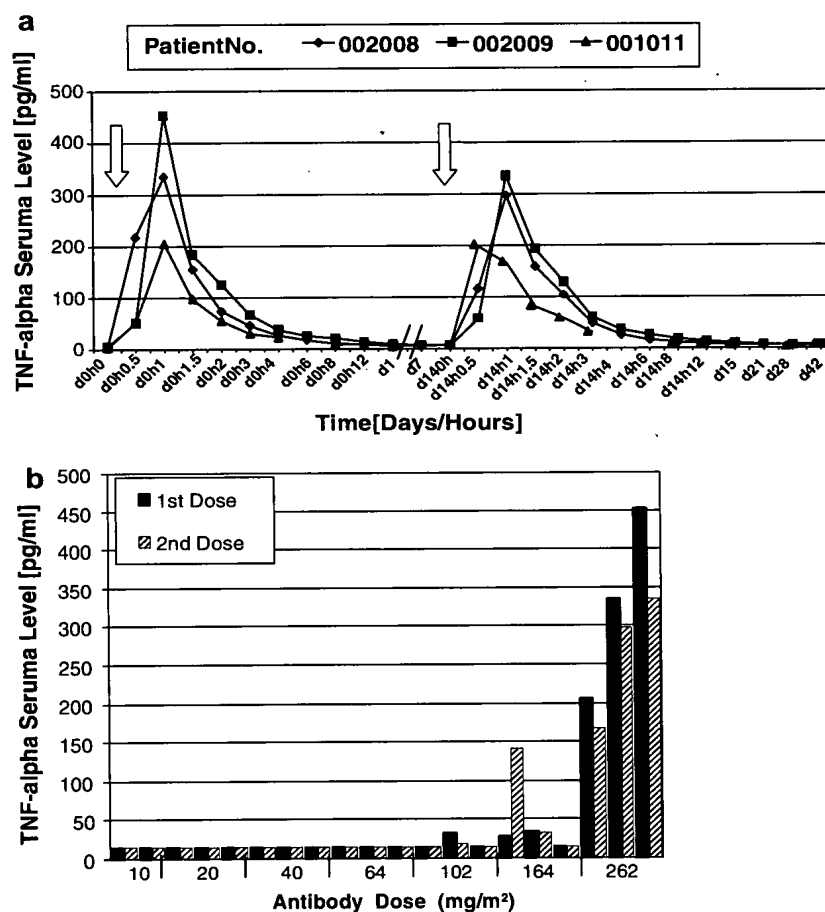


Fig. 2 – Response of TNF-alpha serum levels to adecatumumab infusion and dose. (a) TNF-alpha concentration/time profiles for all three patients of cohort 7 are shown. Patients were treated with two 1-h adecatumumab infusions at 262 mg/m², the beginning of which are shown on the X-axis in days (d) and hours (h). (b) TNF-alpha peak levels as reached by all 20 patients following first and second adecatumumab infusions.

in detail because they were shown to be key effector cells for ADCC as induced by adecatumumab and other human IgG1 antibody therapies.²¹ Here, the total and relative number, cytotoxic activity and activation state of peripheral NK cells were investigated in response to adecatumumab.

Transient increases in TNF- α serum concentrations above baseline were observed in cohorts 5, 6 and 7. All three patients in cohort 7 reached TNF- α peak levels between 206 and 453 pg/mL 1 h after the first adecatumumab infusion, which returned to baseline values or below after 8 h (Fig. 2a). All other patients in the study did not exceed serum levels of 35 pg/mL TNF- α after the first infusion of adecatumumab (Fig. 2b). When compared to the TNF- α response in cohorts 1-5, the transient TNF- α increase in cohorts 6 and 7 was significant ($p = 0.0002$ at +1 h; two-sided Wilcoxon rank sum test on all patient data). The TNF- α increase in response to adecatumumab was thus fast, transient, and dose dependent.

Transient increases after administration of adecatumumab were also observed for IFN- γ . Five patients from different cohorts had peaks of IFN- γ reaching 3-6.8 IU/mL (baseline <1 IU/mL) between 2 h and 1 day following the first antibody dose. No significant change in serum concentration was seen for IL-1 β . Serum levels of PGE₂ and IL-2 showed random peaks, and strong fluctuations were observed for CRP serum levels.

A time- but not dose-dependent correlation was seen between adecatumumab administrations and the absolute and relative number of peripheral NK cells. Fourteen of 17 patients (82%) in the per protocol analysis set showed a statistically significant decline in total NK cell number within 12 h post start of each adecatumumab infusion. Declines were statistically significant for the first ($p = 0.0127$) and second infusion ($p = 0.049$; two-sided sign tests). In the vast majority of cases, NK cell numbers had returned to baseline when measured 2 weeks after adecatumumab infusion (data not shown).

The basal and IL-2-stimulated cytotoxic activity of peripheral NK cells against MHC class I-negative K562 cells and the percentage and total number of peripheral NK cells expressing the early activation marker CD69 showed a wide variation during adecatumumab treatments (data not shown), but was not observed to correlate with dose or administration of adecatumumab.

3.6. Response assessment

A variety of PSA measurements were performed in this phase I study, including biochemical response, PSA-doubling time and determination of weekly PSA production. No biochemical response was observed. Although inhibitory effects on PSA doubling time and weekly PSA production were noted in retrospective analyses during adecatumumab treatment (data not shown), the low number of patients per cohort, the highly variable PSA starting values and the short duration of treatment altogether reduced the significance of such observations.

All 20 patients had baseline assessments and 19 had follow-up assessments of tumour lesions by CT scans. Of these, nine patients had measurable target lesions at baseline. Tumour response assessment on day 42 showed one partial response (PR), six stable and two progressive diseases. The partial response could not be confirmed 4 weeks later because the patient did not attend the scheduled visit.

4. Discussion

This is the first time a human anti-EpCAM monoclonal antibody of low binding affinity has been tested in man. Adecatumumab was generally well tolerated at all doses tested. The majority of reported AEs were mild or moderate, and reversible. Four adverse events were reported in four patients, of which only one was rated as possibly related to the study drug by the investigator; and no grade 4 adverse events were reported. The significant increase in the incidence of adverse events in cohorts 6 and 7 may have been related to the release of TNF- α at the highest dose levels. Patients with inflammatory liver disease might experience *de novo* expression of EpCAM on hepatocytes.²¹ In some patients with pre-existing liver enzyme elevations from inflammatory or other liver impairments, a further transient and mild increase in these laboratory parameters was observed upon infusion of adecatumumab, which could have been related to EpCAM neoexpression on hepatocytes.

The tolerability of adecatumumab at the highest antibody exposure in the present trial is favourable in comparison to two high-affinity antibodies called ING-1 and 3622W94. The latter have equilibrium dissociation constants in the low nano-molar range and have been reported to cause pancreatitis as a dose-limiting toxicity in patients with solid tumours.^{11,12} Both ING-1 and 3622W94 had an MTD of 1 mg/kg, which may not support sustained serum trough levels as reached by other currently approved IgG1 cancer therapies. Based on the experience with high-affinity anti-EpCAM IgG1 antibodies, a very careful dose escalation was therefore performed in the present study, and serum concentrations of pancreatic lipase and amylase were closely monitored. No significant changes of these enzymes occurred during this study with serum antibody levels expected to be sufficient to saturate accessible EpCAM on target tissues.¹⁵ Of note, the two high-affinity mAbs ING-1 and 3622W94 induced acute pancreatitis during antibody infusion, while adecatumumab did not even affect basal serum levels of pancreatic enzymes. No maximum tolerated dose was reached yet with adecatumumab but this is not uncommon for monoclonal antibody therapies. Antibody side effects are mostly target antigen-dependent and will be maximal once all accessible target is bound by the antibody. From the current study, it would appear that with respect to safety adecatumumab is more related to the murine IgG2a antibody edrecolomab than to humanised antibodies ING-1 or 3622W94, suggesting that high-affinity EpCAM binding or recognition of a different epitope rather than presence of a human IgG1 Fc γ portion may have been responsible for the low tolerability of ING-1 and 3622W94. The safety profile of adecatumumab over longer periods of time remains to be established.

Adecatumumab had a serum half-life after repeated injection of approximately 15 days, which permits infrequent dosing of the antibody and facilitates long-term dosing, as is possible with other currently approved antibody therapies. No antibody responses directed against the human monoclonal antibody were found during the course of the study. This may be explained by the fact that the variable heavy and light chain domains of adecatumumab are 95% identical to human

germ line sequences due to their origin from human B cell repertoires.¹⁸ Yet, larger studies with prolonged dosing are required to precisely determine the frequency of a HAHA response to adecatumumab.

With two doses of 262 mg/m² given every other week, serum levels were achieved for adecatumumab as appear necessary for several other therapeutic IgG1 antibodies used in oncology, including anti-CD20 mAb rituximab (375 mg/m², weekly), anti-EGFR mAb cetuximab (400/250 mg/m², weekly) and anti-HER-2 mAb trastuzumab (140/70 mg/m², weekly). The need for high antibody doses in man is in contrast to the relatively high in vitro cytotoxic efficacy of most therapeutic IgG1 antibodies. This may be due to a number of factors. One is that part of the efficacy of IgG1 can be mediated by ADCC, which employs effector cells, such as NK cells, bearing the low-affinity Fc γ receptor (FcR) type III (CD16).²¹⁻²³ It is thus the affinity of IgG1 for CD16 and not for the target antigen, which is rate-limiting for ADCC. The low affinity Fc γ R/IgG1 interaction is further reduced by excess serum IgG, which can very effectively compete for binding of therapeutic IgG1 to CD16.^{15,24} High antibody concentrations may also be needed for CDC, which in vitro assays requires antibody concentrations at or in excess of 10 μ g/mL.¹⁵ High antibody titres may furthermore facilitate target tissue penetration by creating a steeper concentration gradient, compensate for antibody loss by internalisation or binding to soluble antigen, and compensate for a reduced affinity of antibodies to certain Fc γ receptors with frequent polymorphisms.^{22,23} For ongoing phase II studies in prostate and breast cancer, the present phase I study helped to define 2 mg/kg and 6 mg/kg as dose levels for efficacy testing, which approximately correspond to dose levels of cohorts 6 and 7.

Because there is no established PD marker in blood for cytotoxic IgG1 activity, a number of pharmacodynamic (PD) parameters were explored in this phase I study. Pre-clinical experiments have shown a key role of NK cell-mediated ADCC of adecatumumab against human cancer cell lines,²⁴ which is why we have focused on determining the number, activity and activation state of peripheral NK cells and inflammatory cytokines produced by NK and other immune cells. While there was an obvious redistribution of peripheral NK cells in response to adecatumumab infusions this was seen with all antibody doses and does therefore not provide a dose response parameter. Most obvious was a dose-dependent increase of TNF- α serum levels in response to adecatumumab, while other cytokines and mediators tested did not show a significant antibody dose-dependent response. Presently, it is unclear which immune cell types produced TNF- α in all three patients of cohort 7 and much less pronounced in patients of cohort 6. By selecting doses of 2 and 6 mg/kg for phase II studies, two doses will be tested for efficacy, which are different in their capacity to induce TNF- α in patients. This may allow further exploration as to whether a TNF- α serum response at these dose levels has potential as a PD marker for adecatumumab.

Conflict of interest statement

None declared.

REFERENCES

- Balzar M, Winter MJ, de Boer CJ, Litvinov SV. The biology of the 17-1A antigen (Ep-CAM). *J Mol Med* 1999;77:699-712.
- Balzar M, Briaire-de Bruijn IH, Rees-Bakker HA, et al. Epidermal growth factor-like repeats mediate lateral and reciprocal interactions of Ep-CAM molecules in homophilic adhesions. *Mol Cell Biol* 2001;21:2570-80.
- Osta WA, Chen Y, Mikhitarian K, et al. EpCAM is overexpressed in breast cancer and is a potential target for breast cancer gene therapy. *Cancer Res* 2004;64:5818-24.
- Muenz M, Kieu C, Mack B, Schmitt B, Zeidler R, Gires O. The carcinoma-associated antigen EpCAM upregulates c-myc and induces cell proliferation. *Oncogene* 2004;23:5748-58.
- Gutzmer R, Li W, Sutterwala A, et al. A tumor-associated glycoprotein that blocks MHC class II-dependent antigen presentation by dendritic cells. *J Immunol* 2004;173:1023-32.
- Went PT, Lugli A, Meier S, et al. Frequent EpCam protein expression in human carcinomas. *Hum Pathol* 2004;35:122-8.
- Poczatek RB, Myers RB, Manne U, et al. Ep-CAM levels in prostatic adenocarcinoma and prostatic intraepithelial neoplasia. *J Urol* 1999;162:1462-6.
- Zellweger T, Ninck C, Bloch M, et al. Expression patterns of epithelial therapeutic targets in prostate cancer. *Int J Cancer* 2005;113:619-28.
- Went M, Vasei L, Bubendorf L, et al. Frequent high-level expression of immunotherapeutic target Ep-CAM in colon, stomach, prostate and lung cancers. *Brit J Cancer* 2006;94:128-35.
- Veronese ML, O'Dwyer PJ. Monoclonal antibodies in the treatment of colorectal cancer. *Eur J Cancer* 2004;40:1292-301.
- de Bono JS, Tolcher AW, Forero A, et al. ING-1, a monoclonal antibody targeting Ep-CAM in patients with advanced adenocarcinomas. *Clin Cancer Res* 2004;10:7555-65.
- Saleh MN, Posey JA, Khazaeli MB, et al. Phase I trial testing multiple doses of humanized monoclonal antibody (Mab) 3622W94. *ASCO Annual Meeting* 1998; abstract no. 1680.
- Di Paolo C, Willuda J, Kubetzko S, et al. A recombinant immunotoxin derived from a humanized epithelial cell adhesion molecule-specific single-chain antibody fragment has potent and selective antitumor activity. *Clin Cancer Res* 2003;9:2837-48.
- Loibner H, Himmler G, Putz T, et al. Reduction of Ep-CAM positive cells in peripheral blood of patients with epithelial cancers following vaccination with the cancer vaccine IGN101. *ASCO Annual Meeting* 2002; abstract no. 1899.
- Naundorf S, Preithner S, Mayer P, et al. In vitro and in vivo activity of MT201, a fully human monoclonal antibody for pancreatic carcinoma treatment. *Int J Cancer* 2002;100:101-10.
- Riethmüller G, Holz E, Schlimok G, et al. Monoclonal antibody therapy for resected duodenal C colorectal cancer: seven-year outcome of a multicenter randomized trial. *J Clin Oncol* 1998;16:1788-94.
- Fields AL, Keller AM, Schwartzberg L, et al. Edrecolomab (17-1A antibody) (EDR) in combination with 5-fluorouracil (FU) based chemotherapy in the adjuvant treatment of stage III colon cancer: results of a randomised north american phase III study. *ASCO Annual Meeting* 2002; abstract no. 508.
- Raum T, Gruber R, Riethmüller G, Kufer P. Anti-self antibodies selected from a human IgD heavy chain repertoire: a novel approach to generate therapeutic human antibodies against tumor-associated differentiation antigens. *Cancer Immunol Immunother* 2001;150:141-50.

19. Xiang W, Wimberger P, Dreier T, et al. Cytotoxic activity of novel human monoclonal antibody MT201 against primary ovarian tumor cells. *J Cancer Res Clin Oncol* 2003;129:341-8.
20. Prang N, Preithner S, Naundorf S, et al. Cellular and complement-dependent cytotoxicity of Ep-CAM-specific monoclonal antibody MT201 against breast cancer cell lines. *Brit J Canc* 2005;92:342-9.
21. de Boer CJ, van Krieken JH, Janssen-van Rhijn CM, Litvinov SV. Expression of Ep-CAM in normal, regenerating, metaplastic and neoplastic liver. *J Pathol* 1999;188:201-6.
22. Cartron G, Dacheux L, Salles G, et al. Therapeutic activity of humanized anti-CD20 monoclonal antibody and polymorphism in IgG Fc receptor FcγRIII gene. *Blood* 2002;99:754-8.
23. Weng WK, Levy R. Two immunoglobulin G fragment C receptor polymorphisms independently predict response to rituximab in patients with follicular lymphoma. *J Clin Oncol* 2003;21:3940-7.
24. Preithner S, Elm S, Lippold S, et al. High concentrations of therapeutic antibodies are needed to compensate for inhibition of antibody-dependent cellular cytotoxicity by excess immunoglobulin G. *Mol Immunol* 2006;43:1183-93.